Effect of Binder Drop Placement Strategy on Surface Finish of Fine Ceramic Parts by 3D Printing

by

Vedran Knezevic

B.S. Physics
North Carolina Central University, 1996

Submitted to the Department of Mechanical Engineering in
Partial Fulfillment of the Requirements for the Degree of

MASTER OF SCIENCE IN MECHANICAL ENGINEERING

at the

MASSACHUSETTS INSTITUTE OF TECHNOLOGY

JUNE 1998

Signature of Author_____
Department of Mechanical Engineering
May 26, 1998

Certified by_____
Emanuel M. Sachs
Professor of Mechanical Engineering
Laboratory for Manufacturing and Productivity
Thesis Supervisor

Accepted by_____
Ain A. Sonin
Chairman of Graduate Committee

Effect of Binder Drop Placement Strategy on Surface Finish of Fine Ceramic Parts by 3D Printing

by

Vedran Knezevic

Submitted to the Department of Mechanical Engineering on May 26, 1998
In Partial Fulfillment of the Requirements for the Degree of Master of Science in Mechanical Engineering

ABSTRACT

The interaction of droplets with powder is the key set of phenomena that determine many aspects of Three Dimensional Printing (3DP) including dimensional control and surface finish of the printed part. In the creation of structural ceramic parts by 3D printing, fine powders on the order of 1 μm in size must be used. These powders are deposited as slurry and then dried to form a fairly hard cohesive powder bed. The purpose of this work is to understand the interaction of droplets with such cohesive powder beds, the integration of droplets with previously printed droplets, and to explore print styles which improve the dimensional control and surface finish.

Single drop primitives were printed and removed from the powder bed and found to resemble discs with a flat top and a rounded bottom with a typical diameter of 180 μm and a thickness of 40 μm. A number of different time domains are defined based on the interaction of droplets with cohesive powder beds. Critical times in defining these domains are: 1) the amount of time it takes for a droplet to splat and spread on the powder bed, 2) the amount of time it takes for the droplet to absorb into a powder bed, and 3) the amount of time it takes for an absorbed droplet to dry. Based on these time domains, doublets composed of two printhead droplets spaced 40 and 80 μm apart were printed at different interarrival times. At short interarrival times, the doublet appeared to be roughly equivalent to a single drop primitive but slightly larger. As the interarrival time increased the doublet became increasingly oblong.

When printing continuous line segments high rate printing requires that droplets be placed as rapidly as possible. Line segments with varying drop deposition styles were investigated. In one style, droplets are deposited one after the other at high rate such that droplets are arriving before the previous droplets are absorbed into the powder bed. Such line segments show evidence of binder rearrangement due to capillary effects on the surface of the powder bed. Two fundamental alternative styles were investigated where droplets are printed far enough apart that they interact with the powder bed and not with liquid on the surface of the powder bed. In the most successful of these styles, a line segment is created in either 2 or 4 passes of the printhead and droplets are always deposited in a symmetrical configuration with respect to previously deposited droplets. For example, in a first pass, droplets are deposited 200 microns apart and in a second pass droplets are once again deposited 200 microns apart but at a position intermediate to the droplets deposited on the previous pass. Such line segments showed straighter edges and narrower widths than those printed with single pass high frequency printing.

Thesis Supervisor: Emanuel M. Sachs
Title: Professor of Mechanical Engineering

Acknowledgments

I would like to thank a number of people for providing me with help, guidance and support during the course of this work:

Ely Sachs, for being a good advisor and a great teacher, and for giving me a chance to work on the 3DP project;

David Brancazio, our resident electronics and LabVIEW expert, all-around great guy, without whose help in writing all the different VIs, I would still be printing lines on the Alpha Machine;

Jim Serdy, the person whose dedication and commitment are an inspiration to all of us, and who has the most incredible stockpile of useful gadgets this side of Lab Supplies;

Michael Cima, for his help with a number of problems and questions that I was coming up against every Friday at ceramics meetings;

Laura Zaganjori, for her help with administrative things, quick jokes, keen insight into literature, movies and any number of subjects;

Lenny Rigione, the man whose patience and willingness to help is nothing short of legendary, who will never again hear me say the dreaded words: "Lenny, you have a minute? I have a few questions about this SEM...";

Guys in building 12: Jason Grau, for his help and insight into slurries, making powder bed and other fun things in material science, and Ben Wu – DOD guru extraordinaire;

Fred Cote, for everything that he has taught me about machining, for making those experiences easy, fun, and, above all, quick, for which I am immensely grateful, and for being a good friend;

Finally, I wish to thank all of the people whom I have had the privilege of knowing during my stay at 3DP, for sharing the good times and many laughs: Akan, Ako, Jeannie, Adam, Drew, Mike, Jerome, Edo, Costas, Bjorn, Xiaorong, and Pat.

I wish all of you the best of fortunes in all of your endeavors.

TABLE OF CONTENTS

LIST OF FIGURES

List of Tables

Chapter 1: Introduction

1.1 The Three Dimensional Printing Process

Three Dimensional Printing (3DP) is a rapid prototyping technology developed at MIT that manufactures parts directly from a CAD model. Like other solid free form technologies, it is an additive process, where smaller particles are joined together in a specific manner into a large part. Rapid prototyping is important because it decreases product development cycle and eliminates the need for product – specific tooling.

3DP process begins with creating a CAD model. The final model is sliced into thin layers by a separate software package. Each layer represents a cross-section of the original model. Layers are then printed sequentially to produce the final part.

One layer in 3DP process is printed by first spreading a thin layer of powder of the same thickness as one CAD layer over the surface of the powder bed. A printhead then travels across the powder bed depositing the binder, which is an additive that will bind the powder particles together, in a process similar to ink – jet printing. The distribution of the binder in the layer corresponds to the CAD slice that is being currently printed. After the printing is done, the piston supporting the powder bed is lowered by one layer thickness, a new layer of powder is spread and the process is repeated until the part is completed. Figure 1.1 represents the schematic of the process.

After the printing is completed, the unbound powder is removed leaving the green part with the desired geometry. A number of post – processing steps such as firing, sintering and infiltration with another material may follow to achieve full density and improve other material properties.

3DP is an additive manufacturing process, which makes it possible to print many different geometries and shapes that can not be fabricated with traditional manufacturing technologies.

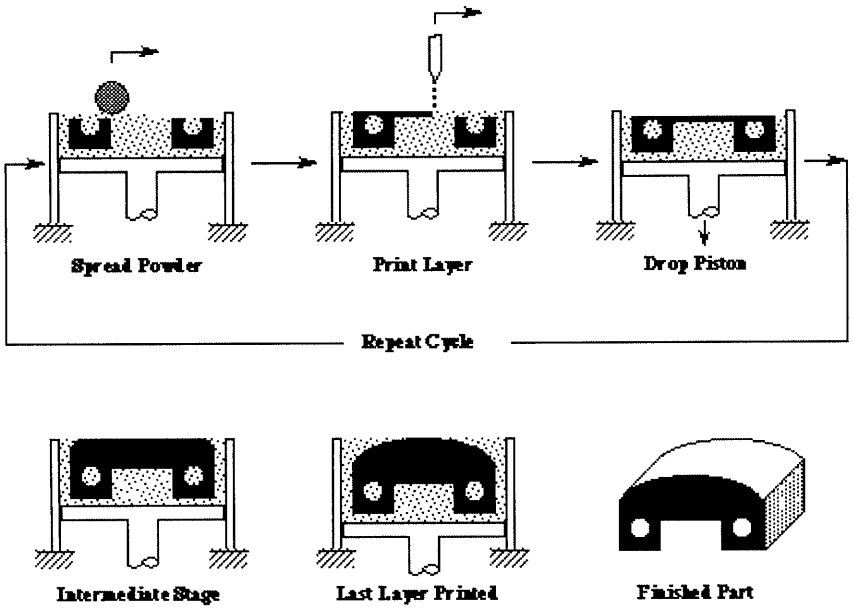

Figure 1.1: 3DP Process

This prototyping offers additional advantages in comparison to other existing prototyping technologies. The loose powder supports overhangs, undercuts, and internal cavities so that very complex parts can be printed. Additional flexibility is provided in the kind of materials that can be used for production. As long as a material can be obtained in the powder form, it can be used to print 3DP parts. A viable binder must be dispensed by the printhead to bind the powder particles so that the part can be removed from the powder bed. Furthermore, because different materials can be dispensed either via different printheads or different nozzles on the same printhead, 3DP can control the local material composition. This capability would allow designers to vary the material properties within a single part. Moreover, proper placement of droplets can be utilized to control the surface texture of printed parts.

3D printing has many possible applications. This includes printing of direct metal parts (Figure 1.2), injection molding tooling, casting shells, and structural ceramics (Figure 1.3).

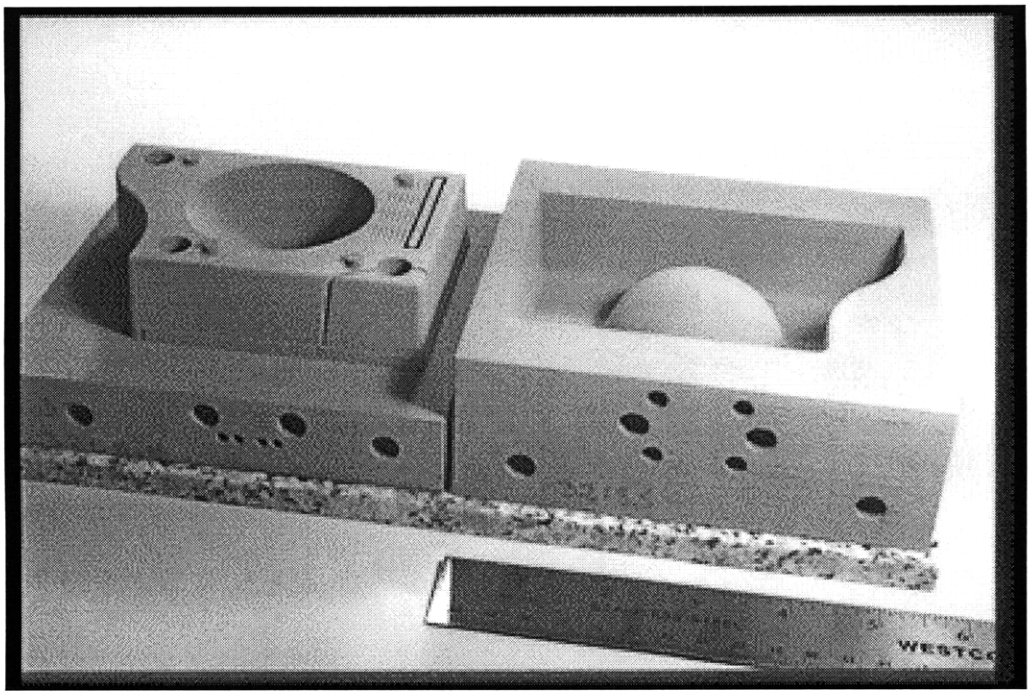

Figure 1.2: 3DP direct metal parts

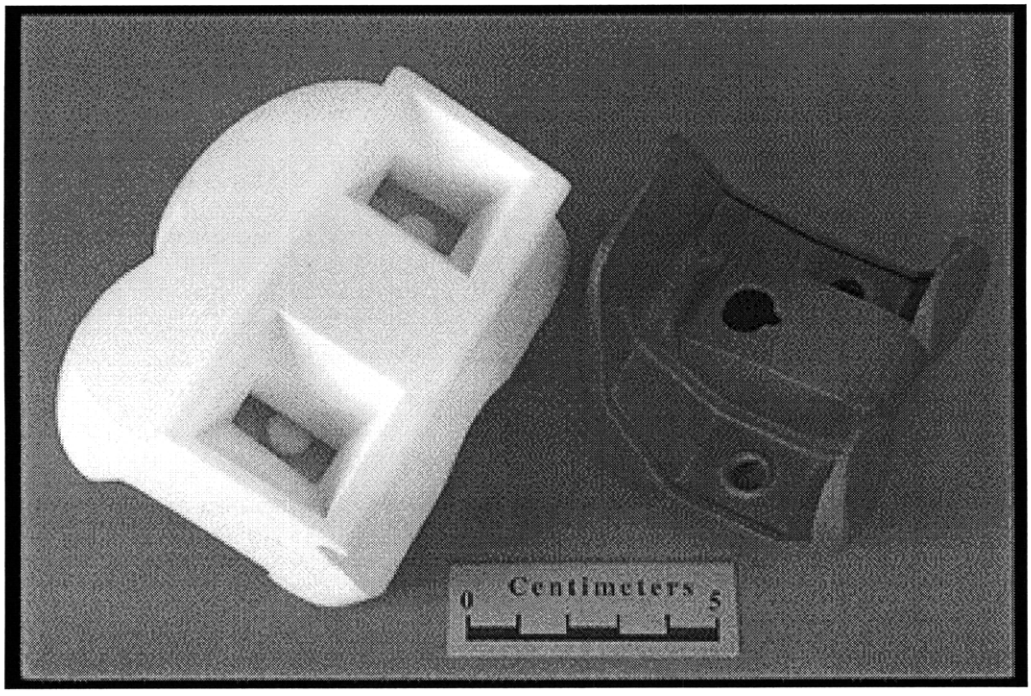

Figure 1.3: 3DP ceramics casting shell for knee implants

1.2 Motivation

Production of structural ceramic parts of high performance and reliability requires the use of fine ceramics powders. Decrease in the powder size also increases fracture strength. These powders can not be spread in uniform layers by using the counter-rotating rod that rolls over the surface of the powder bed, a standard 3DP method of layer deposition, because of their poor flowability. The powder has to be dispersed in a form the slurry and deposited into layer by slipcasting, tapecasting or ink-jet printing. These methods of slurry deposition generate a non-compliant powder bed whose surface does not deform upon the impact of binder droplets.

There is a significant difference between loose and rigid powder beds when it comes to binder absorption. The process of droplet penetration in non – compliant powder beds takes place in two phases: the droplet splats on the surface of the powder and then it is absorbed. In loose powder beds, the two processes of bringing the moving droplet to rest and comingling it with the powder take place in the same time frame. As the result of these phenomena, printed lines are wide but rather flat in rigid powder beds, and some negative effects can occur as well: pooling and splashing.

Previous studies of binder infiltration in rigid powder bed indicated that increasing the time between droplet arrivals should improve the surface finish of printed features. The drawback is that in order to come as close to this condition the build rate becomes very low and the cycle time for printing a 3DP part increases tremendously. The objective of this thesis is twofold:

1) Understand drop – drop interactions in rigid powder beds

2) Develop drop placement strategies that produce high quality fine ceramics parts while retaining high build rate.

1.3 Organization of the Thesis

There are six chapters in this thesis. Chapter 2 describes the material system of fine alumina ceramic powder beds and binders used in this research. It also discusses the process of generating powder beds that are suitable for printing through slipcasting and tapecasting. Chapter 3 presents the experimental setup, which consists of the Drop-on-Demand printhead and powder beds. Various protocols that ensure repeatable results are also depicted. The review of previous work, the motivation for experiments and the description of different print styles are given in Chapter 4. Chapter 5 contains the results of various experiments such as primitives, drop pairs, line segments, and line width, along with the controls and other data. Conclusions and suggestions for further work comprise Chapter 6.

Chapter 2: Material System

2.1 Alumina Powder

In structural ceramics, it is very advantageous to use powders of small particle size (0.5 – 1.0 μm). This enables production of parts with high green density, which makes sintering processes easier. Another advantage is that the surface finish of manufactured parts is limited by the size of the powder used in the build. Theoretically, the roughness of the powder size is what limits the finish of the part: the smaller the powder, the smaller the surface roughness of the part. Furthermore, use of smaller powders means that parts can be printed with smaller layer thickness which would go toward eliminating or at least reducing the slicing defects such as stair-stepping [Arthur, 1996].

The use of fine powders presents a problem in terms of spreading a layer of uniform thickness into which to print the binder. Powders of large particle size (bigger than 10 μm) have been used in the 3DP process by spreading layers using a counter-rotating rod that may be vibrating to improve flowability. However, when a small particle size powder is used, the counter-rotating bar no longer represents viable means for deposition of uniform layers. The reason is that the small particles have poor flowability and tend to stick together forming larger, irregularly shaped agglomerates. Furthermore, the powder tends to stick to the spreader bar, rendering the spreading impossible. Therefore, another method of deposition for fine powder was required.

One method that produces good results in 3DP alumina based material systems is the slurry-based process. This method entails dispersing alumina powder in a solvent, usually water, with nitric acid concentration between 0.05M and 0.10M in form of an electrostatically-stabilized slurry. Two alumina powders of grades APA (99.95% pure) and HPA (99.99% pure) from Ceralox (Ceralox, Tucson, AZ) with mean particle diameters of 0.5 μm and 1.0 μm were used for this study. The powder also contained MgO and trace amounts of sodium, silicon, and iron. The solids fraction loading of alumina in slurry was 0.30 and 0.35. Polyethylene glycol (PEG) with molecular weight of 400 was added to slurry to improve the dispersion of powder beds in the part removal

stage of the fabrication process. Furthermore, in addition to using deionized water as a solvent for slurry, a mixture of water and methanol in ratio of 3 : 2 was used as well. Detailed instruction on preparing well dispersed slurries, correct amounts of ingredients, and the sequence of actions required can be found in [Caradonna, 1996.]. For this research, it has been found that the best results for redispersion of powder beds and subsequent retrieval of printed features are obtained when the slurry is milled with the alumina milling media for no longer than 24 hours, which is much shorter than Caradonna quoted. The lifetime of the slurry is up to 5 days and the experiments have to be planned accordingly. After this time, the slurry begins to flocculate which causes problems in slurry deposition and redispersion.

2.2 Deposition of Alumina Slurries

Two different methods were used to create alumina slurry powder beds for binder printing: slipcasting and tapecasting.

2.2.1 Slipcasting

This research focused on investigation of single primitives, segments of lines, and complete lines of binder deposited into alumina powder beds, and the impact of different print styles and other variables on the shape of the printed features. Slipcasting provided the fastest and least cumbersome method of production of uniform powder beds. The drawback is that only one layer, which is essentially a thick powder bed, can be deposited at one time. The thickness control is also rather crude, certainly worse than it is possible to achieve in tapecasting. Furthermore, properties of the slipcast cake are influenced and determined by different properties of the plaster upon which it is slipcast. This can sometime provide for differences among powder beds and, if the plaster is not of good condition, rendering redispersion impossible.

Slipcasting is a widely utilized process used to produce complex shapes in a multitude of ceramic-based materials. There are many application such as chinaware, crucibles, medical devices (bone implants) etc. It entails pouring the slurry onto a

permeable mold, usually gypsum. The liquid from the slurry infiltrates into the mold due to capillary pressure and leaves behind a densely packed layer of particles.

The gypsum plaster was wetted with deionized water before pouring the slurry into the mold. The resulting slipcast powder bed is used for binder printing.

Porous silicate discs, another kind of substrates, were also used for slipcasting. In this instance, it has been found that the surface finish of the slipcast powder beds improves if the entire slurry is not allowed to slipcast. Therefore, after some period of time, usually a few hours, the remaining slip is drained from the mold, leaving a layer of desired thickness on the substrate. The best results for redispersion and analysis are obtained when the powder bed is of small thickness. The desire for small thickness is balanced with the increasing fragility as the thickness decreases. The optimal thickness is 1-2 millimeters. The powder beds made this way have a packing fraction density of 58.5% and mean pore size of about 0.1 μm (Figure 2.1) as measured by mercury porosimetry.

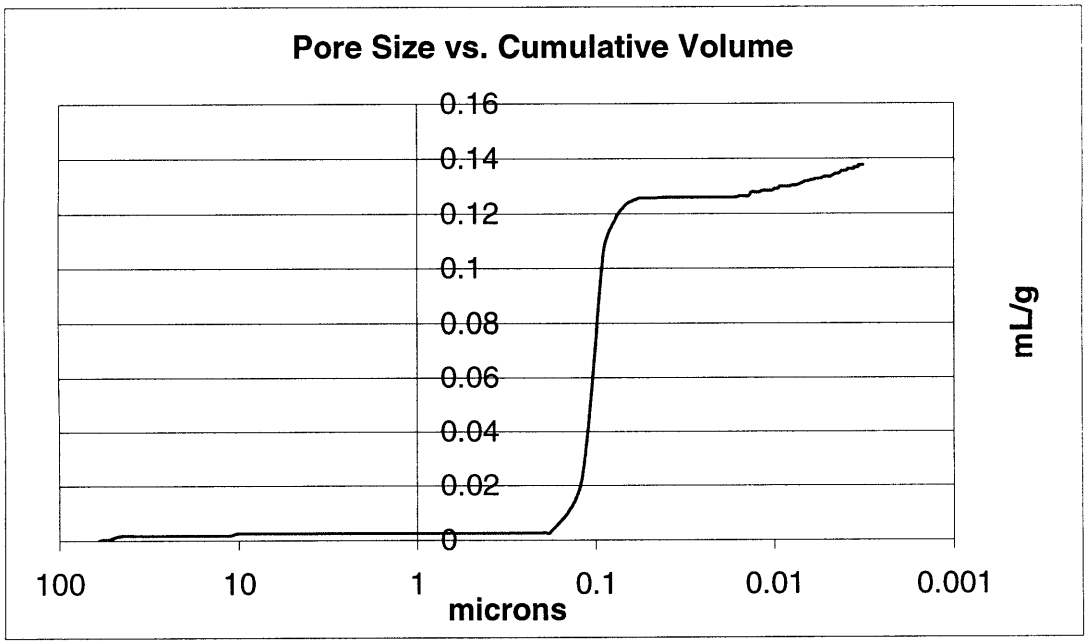

Figure 2.1: Pore Size vs. Cumulative Volume for slipcast 35 v/o HPA 1.0 μm alumina slurry obtained by mercury porosimetry

Duramax 3007 was also used as a dispersant for alumina material system. Alumina powder was dispersed in water using Duramax in different weight percentages: 1.8 and 7.2. Powder beds of good surface finish were slipcast in both cases. PAA could not have been used as a binder for these powder beds. First of all, the infiltration time for macroscopic droplets (volume = 15 μL) of PAA was on the order of minutes. Redispersion was also attempted after the binder has finally infiltrated. When the powder bed was placed in water, the region that contained PAA promptly disintegrated. Therefore, a new binder is required if this material system is pursued further.

2.2.2 Tapecasting

Tapecasting consists of spreading thin layers of slurry on top of a plaster by the means of a doctor blade. After spreading one layer, the powder bed is dried to prevent cracking, and the new layer is deposited. The advantage is that if the blade is controlled well, it is possible to deposit layers of high quality surface finish whose thickness can be as small as few microns. The desired thickness would be controlled over the entire build because the thickness of each layer can be set accurately. The schematic of the tapecasting setup is shown on Figure 2.2.

The first issue to resolve is how to deliver the slurry to the blade. One approach that has been tried in the past [Caradonna] is to pour a pool of slurry on one end of the porous plaster and then to spread it in a layer. This resulted in a nonuniform layer thickness because the control of the entire apparatus was not adequate. Too much slurry would be poured at the start, the slurry would flow under the blade, and the amount deposited per unit area of the plaster would be different. The respective casting rates for different parts were not equal, and the layer thickness was not uniform. Although the tapecast powder beds had optical surface finish, they were not adequate for 3DP production, and bars of PAA binder printed using a drop – on – demand (DOD) cartridge did not have sufficient strength to be removed [Caradonna].

A different, better setup was necessary. The following simple apparatus was designed and assembled on the Proto Machine, the first generation 3DP machine. The advantage of using this setup was that most of the components were already in place. It

was very easy to control the layer thickness by placing and securing the plaster, which is used as a substrate for tapecasting, onto a piston that can be moved vertically in steps of 8.2 μm. The piston is moved by using a computer program and a controller.

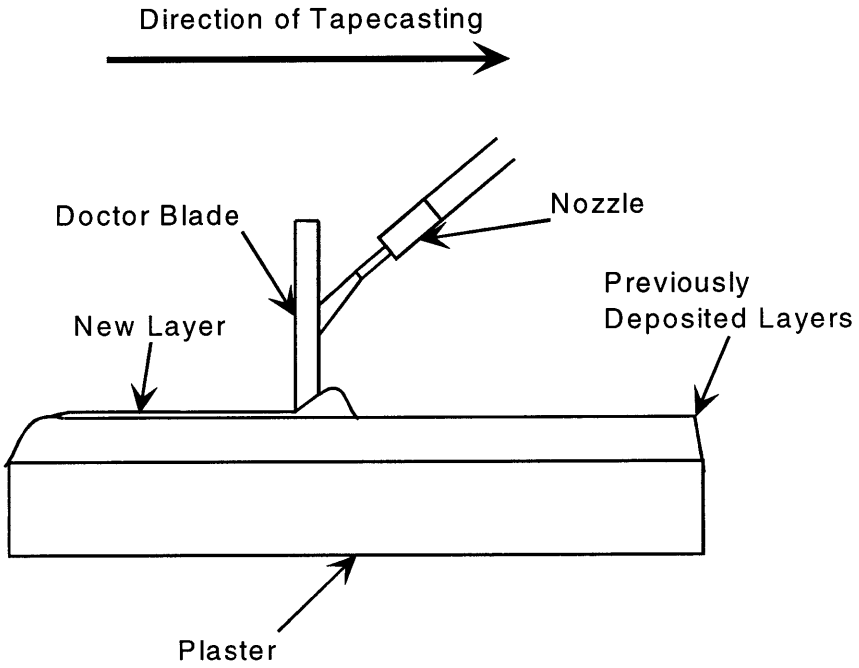

Figure 2.2: A schematic of tapecasting basics

Alumina slurry was delivered via gravity feed from a Nalgene™ bottle that was placed about 6 ½ feet above the tapecasting setup. Tapecasting, in the scope of this research, was never meant to be investigated as the means of depositing slurry for the efficient build of 3DP parts. Concentration was placed on proofs of concepts which could advance understanding of binder – powder bed interaction during binder deposition. Therefore, gravity feed, an easier solution to implement, was used in place of a more reliable approach: pressure vessel. The flowrate of the slurry was ~0.14 cc/sec and could be easily adjusted by a combination of three different variables: different diameter tubing for delivering the slurry, a different size nozzle, and by varying the height of the bottle containing the slurry above the plaster. The rate of the slurry deposition was carefully controlled because the negative side effects of having too much of it were well known. Furthermore, the nozzle was manually moved from one end of the blade to the other so

that an equal quantity of slurry was maintained across the entire width of the plaster. There is no predetermined number of strokes that have to be performed because that depends on the flowrate of the slurry. The goal is to have the thinnest possible pool of slurry spread across the entire width of the doctor blade. The flowrate was usually about 0.14 cc/sec, so the nozzle was moved approximately three times from one end of the blade to the other per each layer. The slurry was turned off after the blade rastered across about ¾ of the plaster length. The already deposited pool of slurry on the plaster was enough to finish tapecasting the layer.

Spreading of the slurry was accomplished by attaching a thin metal blade to the carriage on a recirculating ball linear slide from Thomson Industries. It is extremely important that the blade is perfectly parallel with the plaster, so during the machining of the parts, generous clearances were made for all the drilled holes, which allowed for easy attachment of the blade. The blade was moved manually across the plaster slowly due to the small flowrate, which probably caused some detrimental effects such as ripples and bubbles.

After spreading each layer, the powder bed was dried using a quartz heat lamp from Right Touch Inc. The lamp (120 V, 4.2 A, 60 Hz, 500 W Max.) was used in combination with a Variac autotransformer from General Radio Company (Concord, MA). The Variac setting goes from 0 to 140 volts output for 120 volts input. The setting was kept at 30, and the lamp was on for only 40 sec in order to lightly warm the powder bed. The temperature of the powder bed was simultaneously monitored with the use if a thermocouple, and did not exceed 40°C. The distance between the lamp, which is situated near the top of the lampholder, and the powder bed was about 4 inches.

An alternative two – blade approach was also used (Figure 2.3) in addition to the original single – blade setup. The slurry is deposited in between two blades, which deposits only the necessary amount of slurry onto the plaster. The spacing between blades is very narrow, about 1 mm, and the angle very small, to ensure that a pool of slurry would build up between the blades and would overflow as close to the edges as possible, thus creating a powder bed with large surface area.

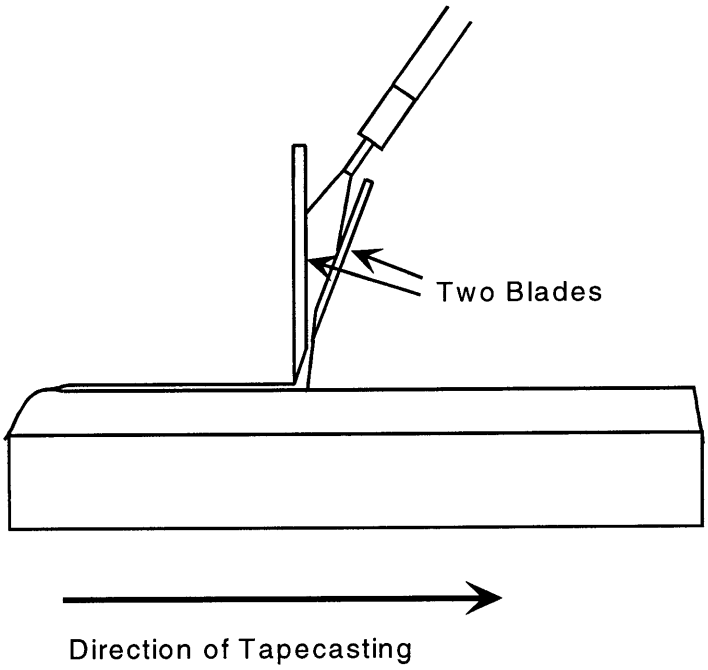

Figure 2.3: Two – blade tapecasting setup

This method was better than the original in its ability to control the flow of the slurry on the powder bed and to prevent the flow of the slurry under the blade, which causes nonuniform layers thickness [Caradonna].

Powder beds of up to 30 layers, and different layer and overall thickness were tapecast with these two basic setups. Individual layer thickness was varied from 41 to 65 μm/layer. Despite the less than perfect control of the printing conditions, powder beds possessed optical surface finish with no or very little bubbling on the surface. Bubbles usually occurred in the first few layers, but would vanish in subsequent layers. The same problem that was mentioned earlier [Caradonna], of having the edge of the powder bed be taller than the middle part due to differential casting rate still persisted. It is certainly a problem if a large build is attempted, but was not an issue in this work.

In addition to using gypsum plaster, slipcast alumina powder beds were also used as substrates for tapecasting a single, thick layer of slurry. The reason for switching to this method was to avoid heating the powder beds, which is a part of the tapecasting

procedure. If the powder beds are not dried during tapecasting, they will crack. If they are dried, then there exists the possibility that PEG_{400}, a slurry ingredient necessary for redispersion, will be boiled off and render the powder beds non – redispersable. But if only one layer of slurry is tapecast, it can be allowed to dry on its own, it will not crack, and PEG will still be in the powder bed. The layer had to be rather thick, more than 100 μm, to ensure that regardless of the binder printed, it would have enough space for binder infiltration.

Tapecasting was a success in that powder beds of sufficient thickness for binder printing were made. They were also uniform in their thickness, except at the edges. The density of powder beds created by tapecasting was 63% and the mean pore size was about 0.12 μm (Figure 2.4).

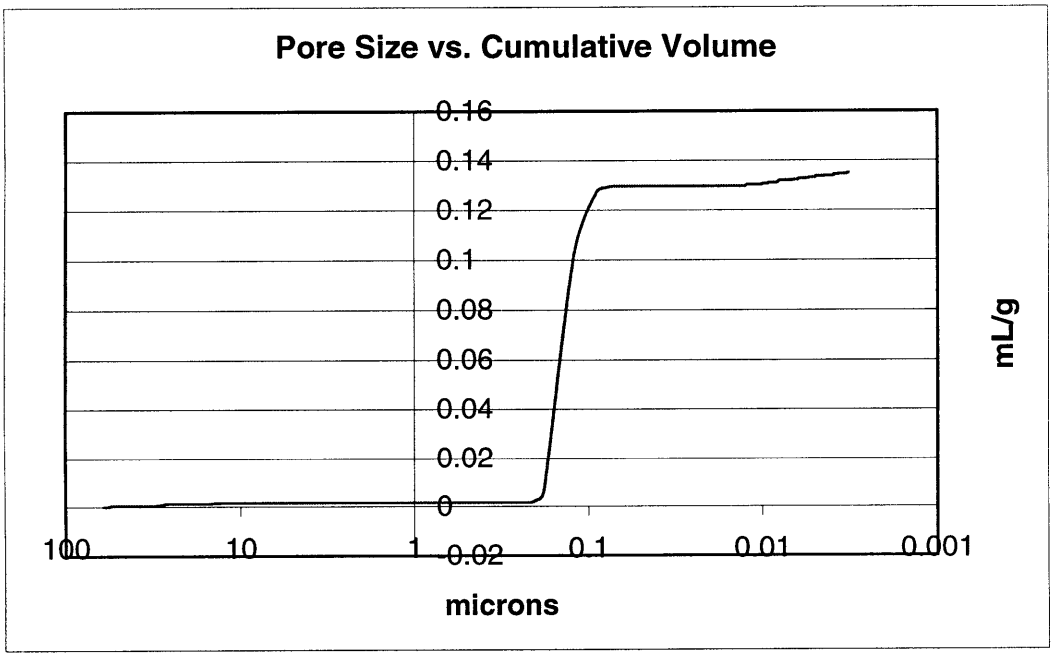

Figure 2.4: Pore Size vs. Cumulative Volume for tapecast 35 v/o HPA 1.0 μm alumina measured by mercury porosimetry

This tapecasting approach would certainly benefit from a more controlled experimental setup, required to eliminate the problems such as ripples, bubbling etc. But, it worked well for the intended purposes of this work.

2.3 Binder

The binder used in this research, developed by [Khanuja], is an aqueous polyacrylic acid (PAA) solution with a molecular weight of 5000. PAA is a hydrophilic polymer whose carboxyl group reacts with alumina powder to produce alumina carboxylate. This reaction makes PAA insoluble in water, which enables removal of printed parts. PAA was used as 10 and 20 weight % solutions. PAA was supplied as a 50 weight % solution in water, which has to be accounted for when preparing binder solution. For example, to prepare 100 cc of 20 weight % PAA one has to mix 40 cc of the 50 weight % PAA solution with 60 cc of deionized water. PAA has a very faint yellow color so in order to visualize and evaluate printed features a dye is required. The dye of choice was amaranth, a red dye.

PAA is a good system to investigate the binder – powder bed interactions, but it was not used for building parts because of its low strength.

Joncryl^{TM} (S.C. Johnson Polymer) was also used as a binder material. It is a styrene – acrylic copolymer that thermally crosslinks, and forms strong solids. The advantage of Joncryl binders is higher strength of printed parts.

Chapter 3: Experimental Setup

Results of this work could have been easily affected by many different factors. Special care was paid in each step of the experimental process in order to standardize all the procedures and have as little difference in experimental conditions from one day to the next as possible. The entire process can be divided in several different phases:

1) Preparing the slurry

2) Generating powder beds

3) Printing

4) Redispersion and removal of lines

Every step will be discussed on individual basis in this chapter.

3.1 DOD System

The printhead is the most important part of the printing procedure and merits special attention.

3.1.1 Overview

There are two main choices for print style in 3DP. They are Continuous Jet Printing (CJ) and Drop on Demand (DOD) Printing.

CJ is a print technology developed by the 3DP research group. It works on the principle of the thermodynamic instability of a fluid jet. A cylindrical stream of fluid has larger surface energy than a collection of spheres of the same total volume as the stream. The stream, when excited by vibrational energy such as a piezoelectric source, will break up and form droplets. These droplets then pass between two conductive parallel plates, so called "charging cell", where droplets gain amount of charge which is determined by applying a known amount of voltage across the plates. The direction of droplets can be adjusted by passing them between a second set of plates that form an electric field. The droplets will be deflected proportionally to the accumulated charge, and will be printed into the powder bed some distance from the center or will be caught in a separate fluid

catcher. Typical values for 3DP jets are flow rate of 1 cc/min and droplet frequency of 45 kHz.

Drop – on – demand (DOD) is a standard technology utilized in off-the-shelf ink jet printers. Most of these printers fire drops through one of two ways: a resistive heating element, so called bubble jet technology, or a piezoelectric element. DOD creates only one drop at a time and can be used over a wide range of frequencies.

Most of the work was done by using cartridges commonly employed in Hewlett Packard DeskJet Printers, which operate on principle of a resistive heating element. Such a thermal ink jet printhead ejects ink droplets by utilizing the conservation of momentum of collapsing bubbles in a layer of liquid ink. The printhead has an ink-containing chamber with an array of individually accessible heating elements (Figure 3.1).

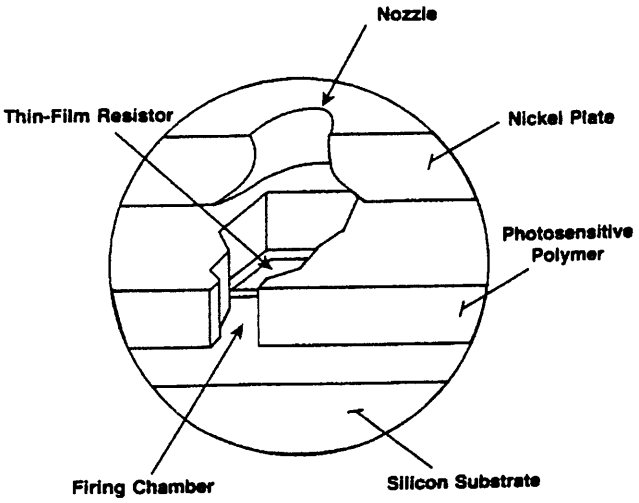

Figure 3.1: Cross section of an ink-jet nozzle

Selectively addressed heating elements momentarily produce vapor bubbles in the ink. When the bubbles collapse radially inward towards their respective heating elements, an oppositively directed force is generated which is large enough to overcome the surface tension of the ink and propel a droplet of ink toward paper, or in the case of 3DP, powder bed (Figure 3.2). After the droplet leaves and the bubble collapses, capillary force draws ink to refill the nozzle.

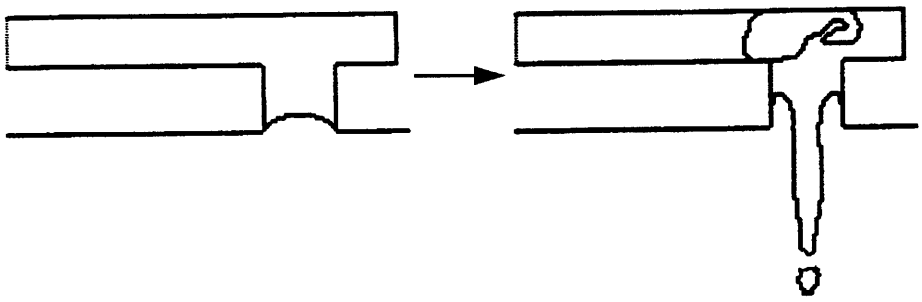

Figure 3.2: Droplet generation in HP DOD printhead

HP DOD printhead was designed to print at the frequency of up to 3600 Hz. It is possible to have it print at a wide range of frequencies ranging from as low as 40 Hz to as high as 5000 Hz. This allowed us to study the influence of varying the frequency during printing on the final shape of printed features.

However, a bubble jet printhead is not perfect. One of the problems is occurrence of satellite droplets. They are generated at the same time as the main droplet and can be readily observed in powder beds. This was not of big importance for this study because satellite droplets almost always fall away from the site where the main droplet impacts. Since nothing wider than single lines has been printed, satellite droplets were acceptable. A far worse problem were resistors which were used to fire droplets. Their performance degrades over time and necessitates a frequent change of nozzles.

We decided to use DOD system as opposed to CJ because that gave us much more of control over many different printing styles, variable frequencies and other printing parameters. One of the main objectives was to test a hypothesis that low frequency printing would improve surface finish of printed parts. There are two ways to accomplish this, as described in section 4.2. One is to make a single, low frequency pass along the fast axis. The drawbacks of this approach are very slow build rates and inherent difficulties associated with low frequency printing, such as nozzles being clogged by the binder material. A hypothesis is that a better approach would be to print droplets which

are not touching each other in the first pass, and in subsequent passes advance the printhead along the fast axis and fill in the blanks to create a complete line. This is further explained in Chapter 4.

The latter style was hard to implement with CJ printing. The reason is Alpha Machine electronics and the manner in which 3DP parts are built. When the .3dp file is encoded in machine instructions, jet voltages are written in the memory and used to direct the droplets from all eight jets on the printhead. The movement of the printhead along the fast axis makes encoder pulses trigger the reading of deflection voltages from the memory. In the current setup it is not possible to synchronize the encoder and piezo frequencies, which causes some uncertainty as to where droplets will land.

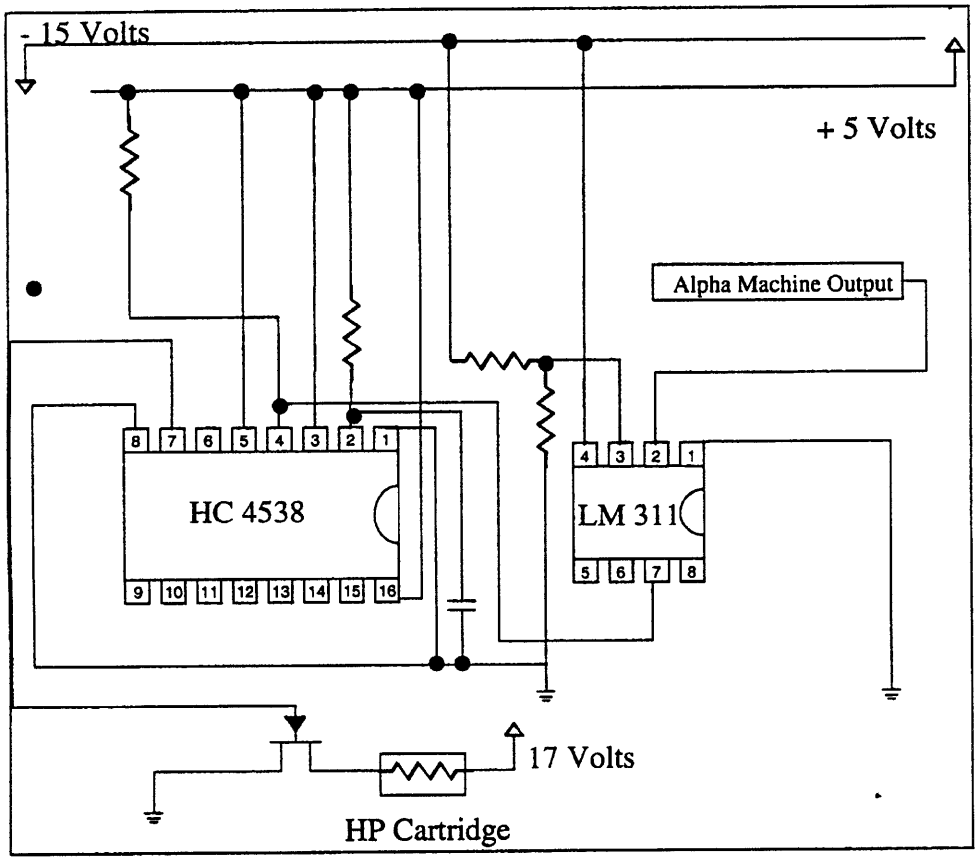

Figure 3.3: HP DOD drive circuit to use with the Alpha Machine (from [Baker])

This problem can be avoided by using DOD printhead. The deflection signal coming from the Alpha Machine is used in combination with an electric circuit (Figure 3.3) which was built by another researcher [Baker].

With the use of the circuit and the DOD printhead it was then possible to achieve good control over droplet landings regardless of different printing conditions.

An additional benefit in using DOD printhead, rather than CJ printhead, is the smaller droplet size, which is 50 μm and 85 μm in diameter, respectively.

HP cartridges used in this research were filled with black ink. The ink had to be emptied and cartridges thoroughly cleaned. A small 5 or 10 cc syringe filled with deionized water was used to flush the cartridges five or six times, until not a trace of ink remained. Only then was a binder solution added by using a clean 5 cc syringe. It was also found that if too much of the PAA binder solution is placed in the cartridge, the printhead would not discharge distinct droplets. Rather, all the droplets would combine into a big drop that would hang off the nozzle orifice. Therefore, it is advantageous to print with a small quantity of binder.

PAA would also clog the nozzles if there was a period of time where the printing frequency was low or the printhead was idle. Such are the cases when single low frequency lines were printed or a new powder bed was being placed on the build piston. It was necessary to clean the nozzles by wiping them with a damp paper towel.

3.1.2 Testing the DOD printhead

In order to analyze effects that different printing variables have upon surface finish, it was necessary to measure in a quantitative way the accuracy to which the DOD printhead can deposit the droplets in a predetermined manner. A set of experiments was designed to test and analyze this. The experimental setup is described in Table 1.

The conditions were set with the following goals in mind: test a range of frequencies, from low (60 Hz) through medium (850 Hz) to high (2500 Hz), and examine whether the number of passes in which droplets are deposited in one line makes a difference to the accuracy. The printhead was filled with the original HP black ink to minimize the possible interference of binders. To better visualize the droplet impact

positions, a piece of emulsion coated glass was used as a printing medium. The distance from the printhead to the glass was 400 μm. Figure 4 explains the meaning of variables found in Table 3.1. A much more detailed description of different print styles as well as the manner in which variables are labeled can be found in section 4.2.

Sample	FA velocity (m/s)	Initial Spacing (μm)	Center-center Spacing (μm)	Line Spacing (μm)	Frequency (Hz)	Number of Lines	Passes/Line
1	0.012	200	200	200	60	15	1
2	0.17	200	200	200	850	15	1
3	0.5	200	200	200	2500	15	1
4	0.34	400	200	200	850	15	2

Table 3.1: Printing Conditions for Droplet Landing Study

It is worth noting that variable "initial spacing" refers to the spacing between consecutive droplets deposited in the first pass along a line. Consulting Figure 3.4, it is clear that in the case where there is only one pass per line, initial spacing and center – center spacing are equal. In the case where there is more than one pass per line, initial spacing is equal to the number of passes in that line multiplied by the center – center spacing.

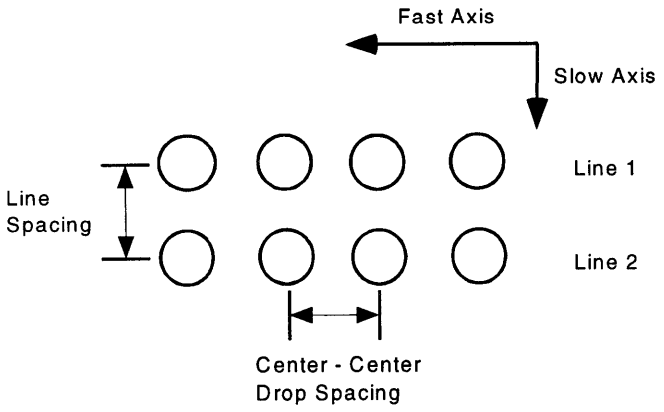

Figure 3.4: Illustration of some printing variables

Measurements of droplet position were performed on the CMM machine by displaying droplets' images onto a TV monitor via a CCD camera, which was fastened to the CMM, and an optical lens. The lens was attached to a 2X adapter, which increased overall magnification. The field of view was about 0.75mm * 0.5mm so it was very easy to visually determine the coordinates of the droplets' centers. With this setup it was possible to resolve coordinates with repeatability of 3 μm. For each sample, X and Y coordinates of 30 drops in 12 lines were measured for a total of 360 coordinate pairs. This sample was large enough that statistical analysis could be performed.

Two separate calculations were made for each sample: one for the accuracy of droplet placement along the fast axis, and one for the accuracy along the slow axis. The averages and standard deviations were calculated. The results are displayed in Table 3.2. The standard deviation is the standard deviation of the population and is calculated using the following equation:

$$\sigma = \sqrt{\frac{N\sum x^2 - \left(\sum x\right)^2}{N^2}} \qquad \text{(Equation 3.1)}$$

Sample	FA velocity (m/s)	Frequency (Hz)	Passes Per Line	Center – Center Spacing (μm)	Line Spacing (μm)
1	0.012	60	1	199.85 +/- 4.88	199.20 +/- 2.22
2	0.17	850	1	199.95 +/- 4.61	199.19 +/- 0.74
3	0.5	2500	1	199.77 +/- 6.38	199.25 +/- 3.00
4	0.34	850	2	200.03 +/- 5.24	199.15 +/- 2.52

Table 3.2: Results of Droplet Landing Measurement Study

The results indicate that the line spacing is unaffected by the change in frequency and other printing variables, which was expected. There is a small change in the accuracy of placement in the fast axis, which decreases slightly as the fast axis velocity increases. The change is very small, only 2 microns, which indicates that as long as the fast axis

velocity is limited to less than 0.5 m/s it will not play a significant role in surface finish of printed parts.

The number of passes in a given line does not influence the accuracy of droplet placement, as can be observed from the results for the sample 4. The deviation is due to the increase in velocity, and is not caused by a change in print style.

3.2 Powder and Slurry Control

The printhead is only one of the factors that has to be controlled during printing. Strict control has to be observed from the very start, which includes powder and slurry issues.

There is not much control that can be exerted over the kind of powder that is used in experiments. This is provided by the manufacturer. It was only possible to limit this study to two different kinds of alumina powder: APA 0.5 μm and HPA 1.0 μm, both manufactured by the same company, Ceralox.

During the slurry mixing step the situation improves tremendously because it is possible to devise schemes which would minimize and perhaps even limit variation in slurries. First of all, all the slurries are supposed to be prepared in the same manner, which consists of always using the same amounts of ingredients and performing the mixing steps in the same time intervals, as is described in Chapter, 2 and references.

Furthermore, tests can be conducted with slurry before powder beds are made either through slipcasting or tapecasting. They are:

1) Settling Rate
2) pH measurement
3) Viscosity measurement
4) Zeta potential – it measures the charge on particles in the slurry. The bigger the charge is, the better is the slurry dispersed. This potential is pH dependent and varies with time.

The first two tests were deemed as sufficiently quick means of establishing validity of a batch of slurry. However, viscosity measurements were also performed once

for the 35 v/o HPA 1.0 μm alumina slurry. The results, shown in Figure 3.5, are in good agreement with the results obtained by other researchers ([Caradonna], [Grau, oral communication]).

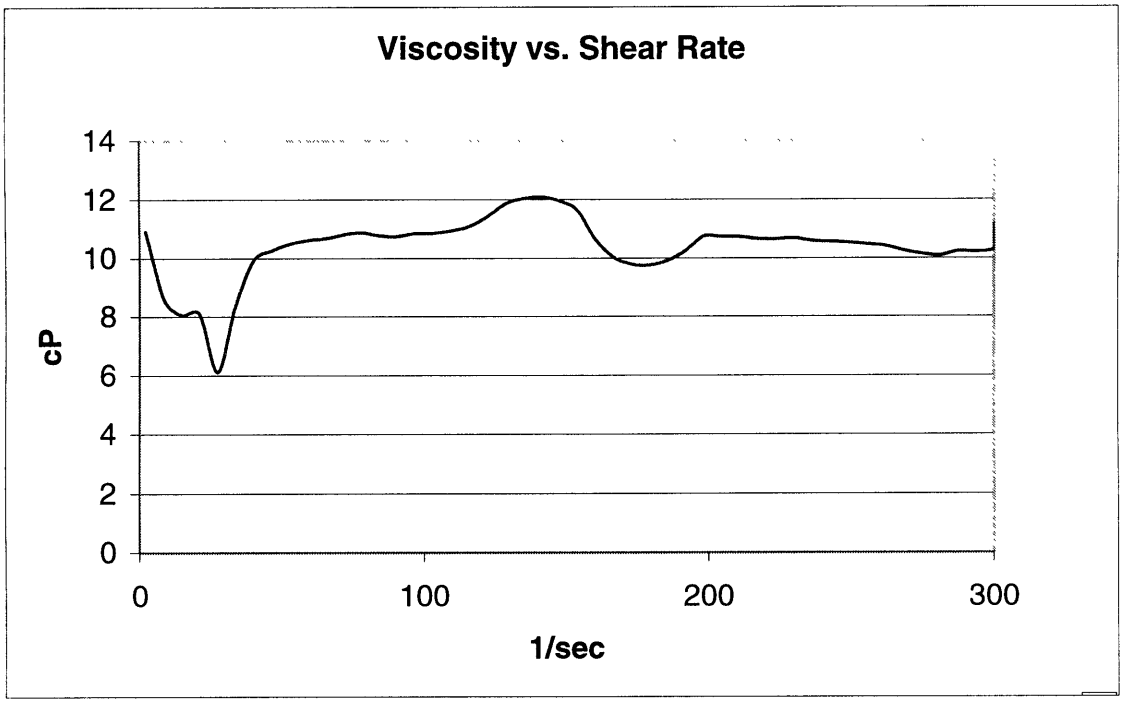

Figure 3.5: Viscosity results for 35 v/o HPA 1.0 μm alumina slurry

Unlike viscosity measurements, settling rate and pH measurement were performed much more frequently.

The settling rate test is very useful because it relates the speed with which solid agglomerates settle to their size, through the use of Stoke's formula. Stoke's law (Equation 3.2) associates the settling velocity (v) of a spherical particle in a fluid to the particle diameter (D), the particle density (ρ_p), the fluid density (ρ_l), the fluid viscosity (μ_l) and the acceleration (a) to which the particle is subjected.

$$v = \frac{D^2(\rho_p - \rho_l)a}{18\mu_l} \qquad \text{(Equation 3.2)}$$

The Stoke's diameter obtained in this way indicates the average particle diameter in the dispersion.

The Stoke's law is intended primarily for use with a single particle in a fluid. In the case of highly loaded dispersions, such as the slurries described here, a modification to the original Stoke's formula is required to account for interactions among particles, which inhibit the settling rate. Richardson and Zeki have proposed the following extension (equation 3.3) of the original:

$$v = \frac{D^2(\rho_p - \rho_l)(1-f)^{\nu}a}{18\mu_l} \qquad \text{(Equation 3.3)}$$

The additional variables are the solid volume fraction of the suspension (f) and a constant (ν) that varies with the particle size:ν = 5.25 for sub-micron particles, and 4.65 for large particles.

Alumina slurries have a very long settling time and it was not practical to wait for the solids to settle due solely to gravity. The IEC DPR – 6000 centrifuge provided a solution to the problem at hand. An even number of samples of 10 cc of the slurry was loaded in the machine and centrifuged for 30 minutes at 750 RPM. The settling distance was measured with a ruler and, at that time, the particle diameter was calculated. The Stoke's formula gave the about 0.3 μm while the Richardson – Zeki's extension determined the diameter of about 0.6 μm. The acceleration was calculated by using the following equation:

$$a = 4\pi^2 f^2 r \qquad \text{(Equation 3.4)}$$

where f is the frequency of the centrifuge, and r is the radius of the rotation and is easily measured with a ruler. The frequency is read off in the units of RPMs from a small digital

indicator located on the centrifuge. The frequency must be converted into Hertz if equation3.4 is to hold true. Some typical values are the frequency of 750RPM (12.5 Hz), the radius of 0.16 m, and the calculated acceleration of 990 m/s^2.

The pH of each sample was measured after the centrifuge part was finished, using pH indicator strips. The measured pH was always about 4, which is the correct value (Grau, oral communication).

Additional particle size measurements were performed using the Horiba CAPA – 700 Particle Analyzer. The particle size result for 1.0 μm slurry was the average of 0.48 μm with the standard deviation of 0.26 μm.

The conclusion is that neither of these methods managed to measure the particle size perfectly. However, they did provide the means for standardization of this leg of the experimental process.

3.3 Powder Bed Control

Properties of powder beds can also be qualitatively and quantitatively assessed after slipcasting or tapecasting.

The first step is to visually evaluate whether or not the surface finish of the powder beds is of acceptable quality. Some of the defects that would automatically exclude the powder bed from further use are extensive bubbling on the surface and the surface that is not smooth.

The next step is to determine if the powder bed is redisperseable. Deionized water is used as a solvent. There have been instances where binder was printed into a powder bed only to discover that it could not be redispersed. Therefore, this is one of the most valuable tests in terms of possible time saving.

The final test for powder beds is the droplet infiltration time measurement. A drop of deionized water is placed on the surface of a powder bed and the time required for the droplet to completely infiltrate is carefully measured. The water always contained amaranth to facilitate observation. It is extremely important that the volume of drops does not change from one measurement to the next. A small pipette that repeatedly dispenses drops of 15 μL volume was used for all the measurements. A stopwatch was used to

measure the infiltration times. Tests were performed on slipcast and tapecast powder beds alike. The infiltration time for slipcast powder beds was between 7 and 10 seconds, while this figure rose to 50 – 60 seconds for tapecast powder beds. These tests were performed whenever new powder beds were made to determine the infiltration times and see if those times are similar.

3.4 Control During Printing

Standardization is required and possible during this leg of the experimental process as well, and can be accomplished by several methods, which are described in this section.

A dye is necessary to assess the quality of the printing performed and to measure the size of printed regions while still in the powder bed. Furthermore, it is also valuable to compare the shape of a printed region in powder bed with its shape once it is removed from a redispersed powder bed. Amaranth proved to be a satisfactory choice for a dye. Keeping the amount of amaranth in a binder constant is useful for systematization, and was always about 0.4 weight %.

If the surface of the powder bed is not perfectly level, than there is no way to predict where the droplet will land and what kind of shape it will assume. Hence, it absolutely necessary that only powder beds of sufficient flatness are used. Furthermore, the accuracy of droplet deposition depends on the distance between the printhead and powder beds: the bigger the distance, the less accurate the landings are. If more than one piece of powder bed is used at the same time for binder printing, they have to have as similar thickness as possible and the printhead always has to be kept at a constant distance. The average distance was always about 400 μm. The printhead – paper distance in HP DeskJet printers is at least 180 μm.

To illustrate the importance of the printhead – paper distance, consider Figure 3.6. These three images represent a 200 * 200 μm grid of black ink droplets on high quality ink – jet paper printed via the HP DOD setup. The grid in 3.6a was printed at the printhead - paper distance of 1 mm, 3.6b at 2 mm, and 3.6c at 3 mm. The fast axis

velocity was 1.0 m/s. The images clearly state the importance of having the printhead at the same distance, which is not supposed to be too far away from the powder bed.

Finally, in many instances the powder beds had to be heated so that different conditions of binder deposition could be investigated (a more detailed explanation is in Chapter 4). The same heat lamp that was used in tapecasting was used for this purpose in addition to a thermocouple that was utilized to monitor the temperature of the powder bed. The temperature of powder beds was always kept low, at about 30-32°C, to prevent PEG from boiling off, which would render the powder beds non-redispersable.

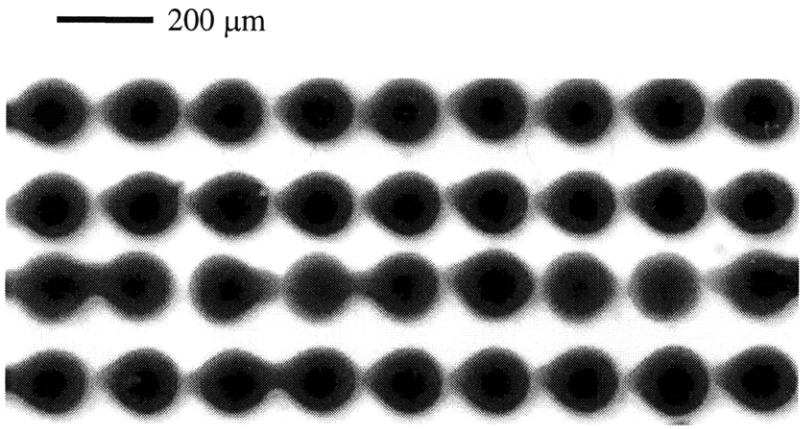

Figure 3.6 a: 200*200 μm grid printed at 1 mm distance

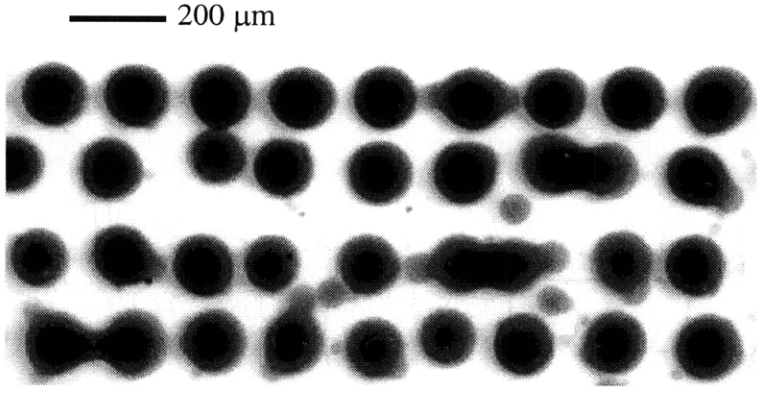

Figure 3.6 b: 200*200 μm grid printed at 2 mm distance

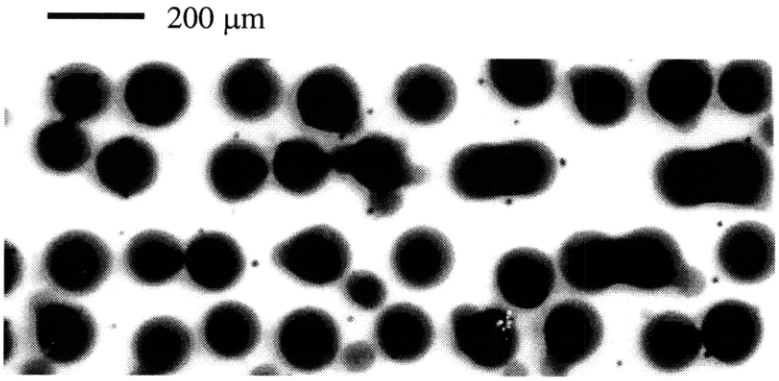

Figure 3.6 c: 200*200 μm grid printed at 3 mm distance

3.5 Redispersion and Removal of Printed Features

Removal of printed parts from the powder bed is accomplished by immersing the powder bed in a solution, usually deionized water. The water is allowed to wick in and is slowly added until the part is completely saturated. If the precautions for preparation of slurry and powder beds are followed, than the removal is very easy and requires neither ultrasonication nor the use of a shaker table. An acidic solution with pH of 3 was also used for redispersion but there was no difference between these two cases.

It was possible to remove and mount on SEM stubs intact line segments that ranged in length from 1 mm to 1.8 mm.

Chapter 4: Motivation

There have been previous attempts in the 3DP group to understand the formation of the primitive features and investigate the effect of printing parameters on surface finish of fine ceramic parts. This chapter briefly reviews conclusions of these studies and explains the motivation behind this research. The strategies for testing the hypothesis are also described.

4.1 Review of Previous Work

[Arthur] had studied the effects of printing variables on the surface finish of printed lines. She concluded that the frequency at which binder drops are printed and the infiltration time play a very important role in minimizing detrimental effects.

Splashing might occur when a droplet impacts a surface with high velocity, about 10m/s, which is the velocity of a DOD drop after being discharged by the printhead. The satellite droplets, which break off from the main drop, splatter in the powder bed and may cause the formation of an uneven primitive and damage the surface finish of the printed part. The chances of splashing occurrence increase if the surface is covered with a thin film of liquid. In this case the drops do not have enough time to infiltrate into the powder bed, and splashing may happen at even lower impact velocities.

If the printing frequency is high, in addition to increased chances of splashing, there is also a possibility of droplet coalescence. The droplets are not deposited as distinct primitives but merge together to create a large drop. This drop grows in size until the printhead traverses a distance greater than the drop's diameter, essentially outrunning the drop. The final effect is that separated regions of binder are placed in the powder bed rather than one continuous line. This phenomenon might mask the influence of different printing conditions and make it harder to assess their influence.

The conclusion is that sufficient time must be allowed between droplets, so each drop can be absorbed into the powder bed independently. This will minimize the chances that splashing and line breakup will occur.

[Arthur] also investigated the effect of binder dose and impact velocity on line width. She found that lines printed at constant jet velocity showed increasing width as the binder dose increased. The work on impact velocity yielded the results on splashing and binder pooling. These effects sometime obscured the effects of jet velocity on the impacted droplet size. However, there was a general increasing trend in the width of single lines with increasing jet velocity.

4.2 Different Time Domains in Droplet Infiltration

The process of line formation by binder droplets in a powder bed can be divided into six separate time domains. They differ from each other according to the stage at which the first droplet is found when the next one strikes.

When a binder droplet impacts the surface of a powder bed, it forms a spherical cap, which after a short period of shaking comes to rest. The droplet is then absorbed into the powder bed; a process driven by capillary forces. The next droplet can impact the powder bed containing the previous droplet at any moment during the binder infiltration. So with the respect to the stage of infiltration of the first drop, the droplet interaction can be divided into the following segments:

1) The first droplet is on the surface of the powder bed, still shaking. This lasts about 1 millisecond so if the printhead frequency is at 1 kHz or higher, the next droplet will hit the previous one at this stage (Figure 4.1).

   [Fan] investigated droplet – powder interaction in loose powder beds. He found that when an impact is into dry powder it takes approximately 1 ms for everything to come to rest. An analogy can then be drawn between this instance and compact powder beds.

2) The first droplet is still on the surface but has stopped shaking. It is not absorbed into the powder bed.

   It is known from previous work [Arthur] that it takes about 30-60 ms for an HP DOD droplet to be absorbed into a fine alumina ceramics powder bed, the time being

dependant on the surface roughness of the given powder bed. Therefore it can be assumed that if the printhead frequency is a few hundred Hertz e.g. 500 Hz, which is equal to the time interval of 2ms, the droplet collision can be classified under this category (Figure 4.2).

3) The first droplet is on the surface and is only partly absorbed when the next one hits (Figure 4.3). This event takes place a few tens of milliseconds after the first droplet impacts. If the printhead is driven at the lowest possible frequency, about 40 Hz, then this instance can be replicated.

4) The first droplet is fully absorbed. It is now migrating in the powder bed and is completely wet (Figure 4.4).

5) The droplet collision takes place when the first droplet is no longer migrating within the powder bed but is still wet (Figure 4.5).

6) The impact occurs when the first drop has stopped moving and is thoroughly dry (Figure 4.6).

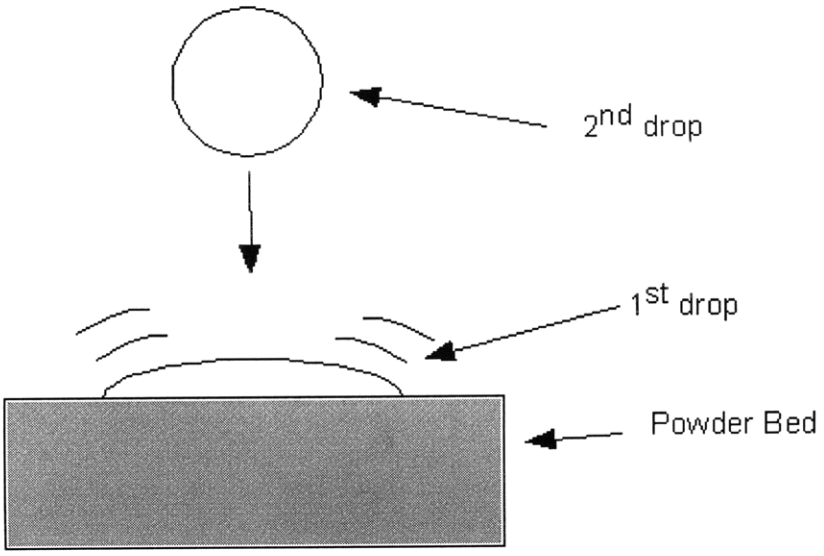

Figure 4.1: The droplet is on the surface of the powder bed, shaking.

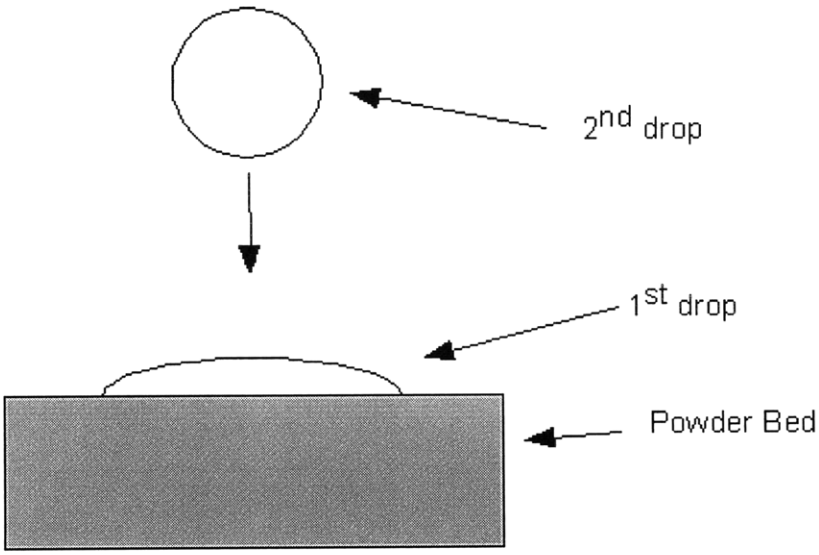

Figure 4.2: The droplet is on the surface. The infiltration has not begun.

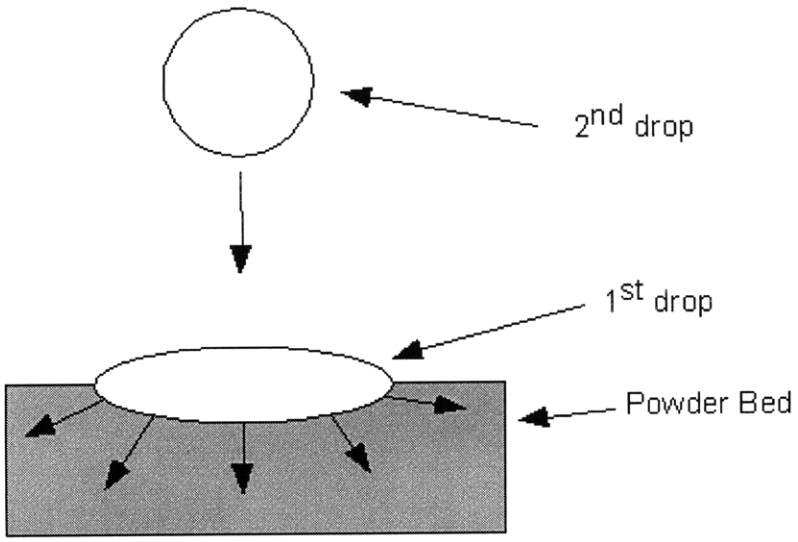

Figure 4.3: The droplet is partially absorbed.

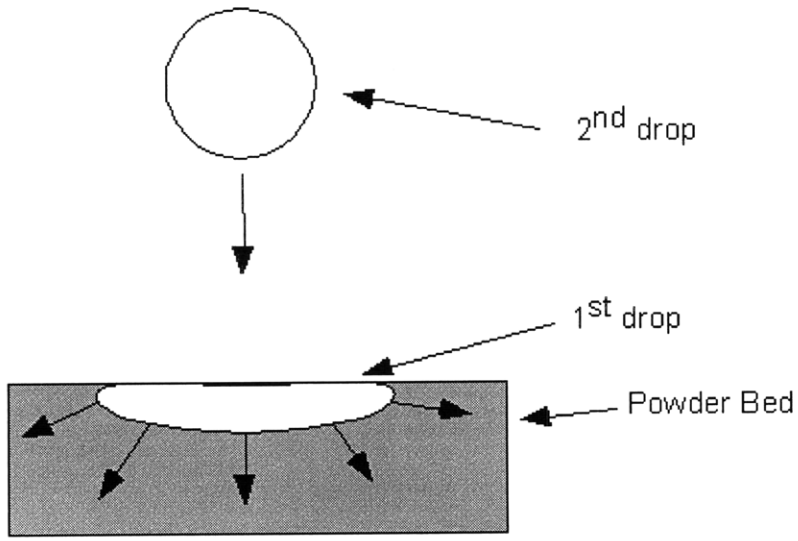

Figure 4.4: The droplet is fully absorbed, and is moving within the powder bed.

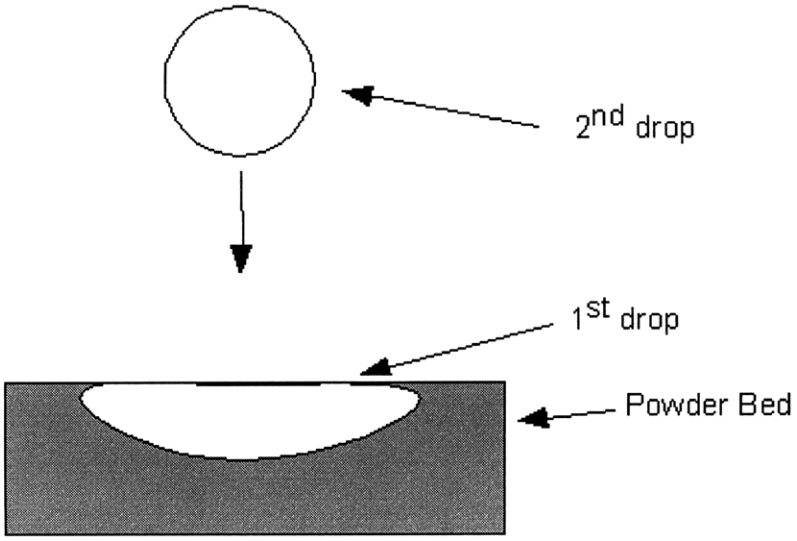

Figure 4.5: The droplet has stopped migrating but is still wet.

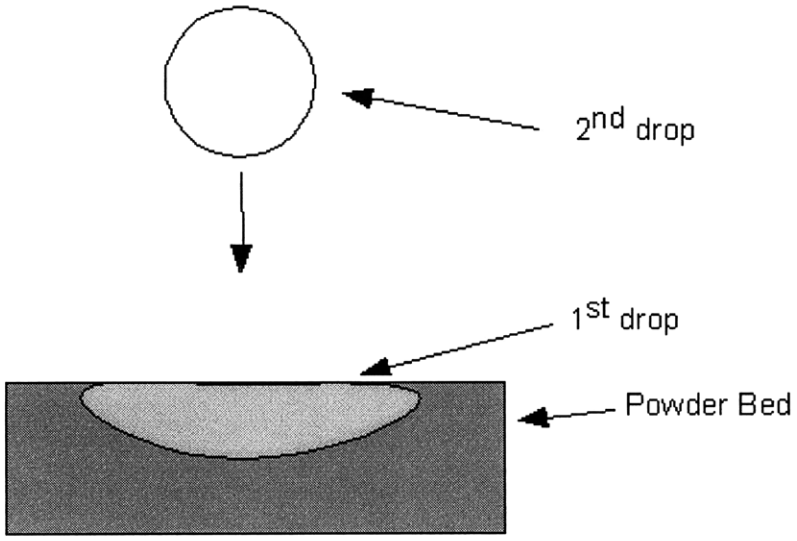

Figure 4.6: The droplet is dry.

There was no reliable method to estimate the time required for a droplet to stop migrating or dry. However, some large-scale experiments were done and the results can be scaled down to the size of a DOD droplet.

A drop of deionized water was deposited via pipette on a piece of slipcast powder bed. The mass of the powder bed was recorded before and after adding the water. A stopwatch was used to record the time required for the water to evaporate and the mass of the powder bed to return to normal. The recorded mass was 2.383g and 2.401g before and after adding the drop, respectively, so that the mass of the drop was 0.018 gram. The time interval required for drying was 40 minutes. The mass of a DOD droplet is 5×10^{-8}g, which is 360,000 times smaller than the macroscopic drop. Scaling the drying time down to the DOD level requires taking a look at mass transport and its possible limiting factors. It can be assumed that the limitations are due to transport from the surface of the powder into the atmosphere. This rate would be governed by the wetted surface, which can be assumed to scale as the volume$^{2/3}$. Thus, it can be expected that the drying time for a DOD drop to be 1 / 360,000$^{2/3}$ of that for the macroscopic drop, or 0.47 seconds. Alternatively, it can be assumed that the rate limit is the transport of the moisture through the powder bed to the surface. If it is assumed that this is a diffusion controlled process, it can be seen that the time required would go as the square of the depth of the penetration of the liquid. Since this depth would be expected to go as the volume to the powder of 1/3, the scaling relationship is back to the volume$^{2/3}$. Thus, the conclusion is that the approximate drying time for a DOD droplet is 0.5 seconds.

Another piece of powder bed was used as a control for this experiment. Its mass was measured every time that a measurement of the powder bed – water sample was taken to ensure that experimental conditions were unchanged.

The experiments had to be designed to investigate different time domains. An appropriate choice of frequencies was to print at 500 Hz, 50 Hz, 1 Hz, and to dry the powder bed while printing, thereby ensuring that the deposited droplets are completely dry. The lower operating limit of the printhead is 40 Hz, so all the frequencies higher than that can be printed in a single pass across the powder bed. The frequency of 1 Hz had to be deposited in more than one pass of the printhead. The same applies when the powder bed is dried after each pass. While the choice of the appropriate printing conditions is

only approximate because some time intervals could not be measured accurately, these particular settings were sufficient to illuminate various effects of changeable frequency.

4.3 Description of Print Styles

Low frequency printing can be achieved by making one pass along a line at a very low fast axis speed. However, this is a far cry from being economical because the build rate for the part is very low. A viable alternative is depositing droplets in one pass so far apart that they are not touching each other. The blank spaces are filled in subsequent passes, the number of which has to be determined. This can be extended in three dimensions. In the first layer a checkerboard pattern of droplets would be printed. The following layer would have the same pattern except that printing coordinated would be offset by some amount. As the droplets absorb into the powder bed, they would connect with the droplets from the first layer and combine into a 3D structure.

With this short introduction, we can go into more details about print styles. The original hypothesis was that the arrival time between droplets is the factor that influences the quality of surface finish. If that time is increased, the surface finish should be improved.

There are several different print styles where droplet deposition satisfies the hypothesis. However, they are not identical and each one merits a separate explanation.

The first print style deposits just one drop per pass along each line (Figure 4.7), the so called multiple pass printing. There are N passes per each line where N denotes the number of individual drops comprising the given line. The drawback is that in a large part the number of passes quickly becomes significant and theoretical build rate is very low.

In this print style there are two kinds of binder droplets within one line: the drop in the first pass infiltrates into the binder-free powder bed. All the other drops in that line will have a binder region to one side and intact powder bed to the other side.

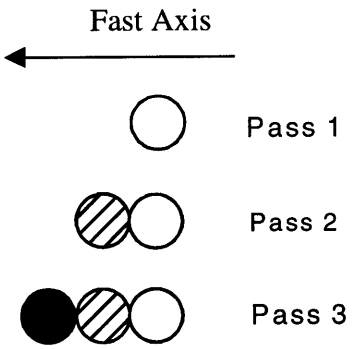

Figure 4.7: Multiple pass printing, case 1. Figure not drawn to full scale.

Figures 4.7 – 4.10 require a short explanation because they can be quite misleading if not interpreted correctly. The droplets are drawn in such a way that there is no overlap among them, regardless of the print style. This was done purely for the sake of simplicity. However, in reality the droplet diameter, which is 140 μm in a powder bed, is much larger than the center – center distance between drops. The latter quantity can vary from 20 μm to 100 μm. If the binder was printed to literally mimic the distances depicted on these pictures, it would be impossible to have lines of sufficient strength.

The alternative (Figure 4.8) that would improve the build rate while still being an acceptable way to test the hypothesis is to print more than just one drop per each pass. This initial distance between drops has to be larger than one-drop diameter. The final center to center distance between drops in the line is determined by offsetting the start location for printing in subsequent passes by a known amount. The only restriction is that the initial spacing must be an exact multiple of the center-center distance.

It is possible that there will be stitching defects in the surface finish at each site where two smaller segments combine into a larger line. These defects, if present, should exhibit a large degree of periodicity and should be separated by approximately the initial distance.

In this instance there will be three different categories of binder droplets in one line:

1) The ones in the first pass hit the intact powder bed (Pass 1 in Figure 4.8)

2) Droplets in all but the last pass have a region of powder bed saturated with binder on one side and a region of unused powder bed on the other side (Pass 2)
3) The drops in the final pass infiltrate into the part of powder bed that contains binder on all sides (Pass 3)

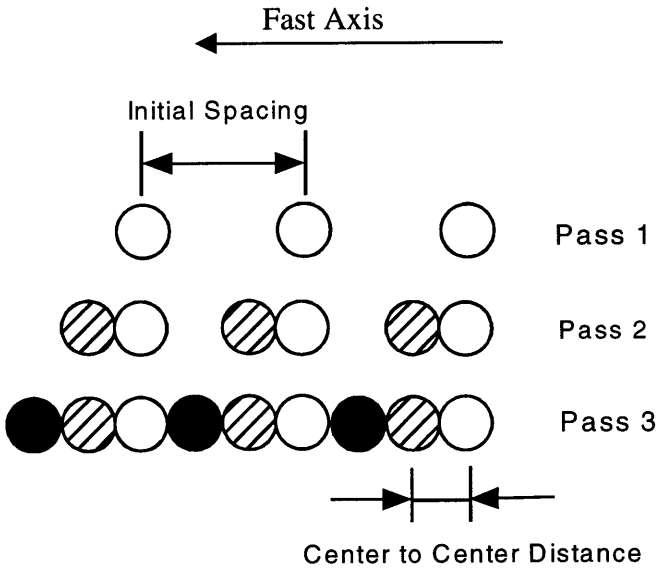

Figure 4.8: Multiple pass printing, case 2. Figure not drawn to full scale.

The aforementioned print styles do not deposit binder in a symmetrical manner. That is, most of the drops land in the region of powder bed where both sides of the droplet impact site are not equally saturated with binder. This might alter the infiltration process of binder and affect the surface finish. The following print styles address this problem.

The first approach of symmetrical printing is illustrated in Figure 4.9. The droplets in the first pass hit the intact powder bed. The droplets in the second pass, which is the final pass for the line, are printed in such a way that they land in the middle of the distance between adjacent drops from the first pass. Therefore, all the drops land "symmetrically" regardless of when they are deposited.

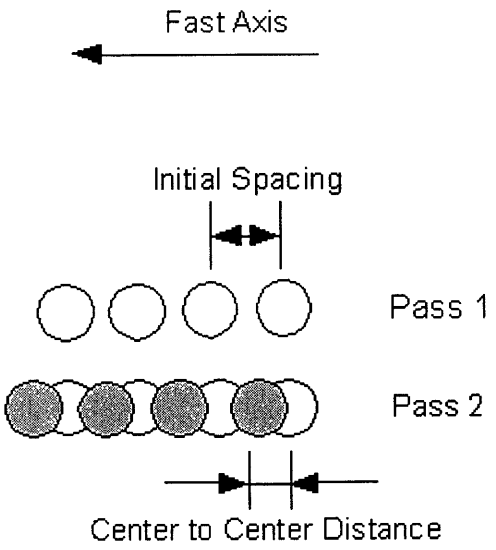

Figure 4.9: Symmetrical Printing, case 1. Figure not drawn to full scale.

The only drawback for this approach is the fact that the spacing within given pass must be bigger than one-drop diameter, which is approximately 180 μm. The following pass manages only to cut the center-center spacing to one half of the initial spacing. This is to say that the drops in the finished line will be 90 – 100 μm apart. At such a large spacing it is very likely that the overall shape of the line will not be straight but will follow the curvature of the individual drops.

Another solution for symmetrical printing is to have several passes in each line, each with a different offset. Figure 4.10 illustrates one such case where the drops in the first pass are spaced more than one-drop diameter. Pass 2 is offset with respect to the first one by ½ of the initial spacing. Pass 3 is offset by ¼ and pass 4 by ¾ of the initial spacing. The number of passes can be increased still, thereby decreasing the center-center distance.

This print style will also produce three different categories of drops:

1) The ones in the first pass will infiltrate into the unused powder bed

2) The drops from pass 2 will have symmetrical regions of binder on both sides

3) The drops in the final 2 passes will also be symmetrical yet different from the previous two categories.

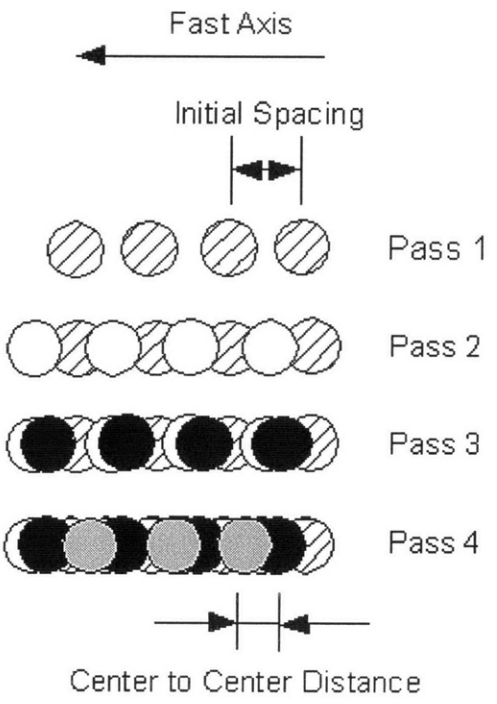

Figure 4.10: Symmetrical Printing, case 2. Figure not drawn to full scale.

All these print styles were explored and the results are presented in the following chapter.

Chapter 5: Results

A single 3DP part consists of smaller units (primitives, lines, and layers) which are stitched together to from a coherent system. Therefore, it makes sense to describe and analyze the part in terms of its basic building blocks.

5.1 Primitives

A primitive is a fundamental building block in the Three Dimensional Printing process. By definition, it consists of a single droplet of a binder and all the powder bed particles that the droplet binds together.

Primitives of 20 wt % PAA were printed into powder beds made of 30 v/o 1.0 μm alumina slurry using the HP DOD setup. Figures 5.1 through 5.3 show the results in slipcast powder beds. The primitives have a diameter of 140 μm in the powder bed as indicated by amaranth, while that increases to 180 μm when the powder beds are redispersed. Their thickness is about 40 μm (Figure 5.3).

Primitives printed into tapecast powder beds do not differ in shape, but they are slightly bigger: 170 μm diameter in the powder bed, and it is not known why that is so. It was not possible to redisperse these powder beds sufficiently well to acquire SEM

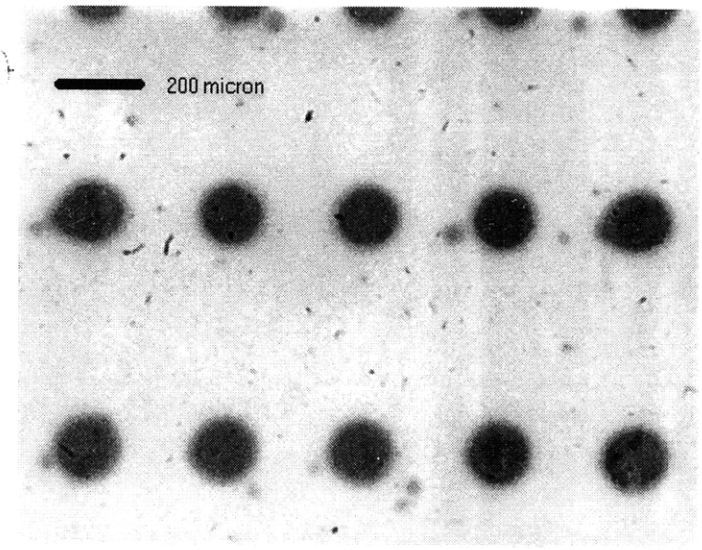

Figure 5.1: Primitives in a slipcast powder bed

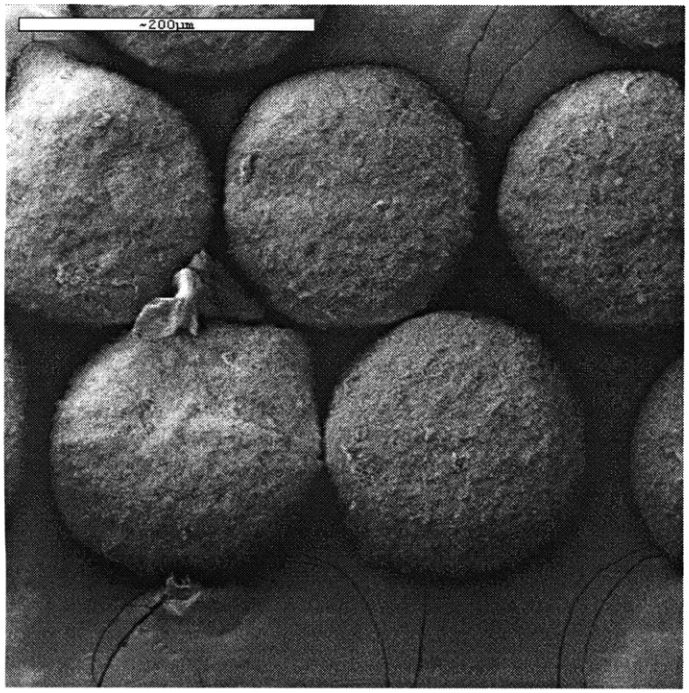

Figure 5.2: SEM of Primitives (bottom)

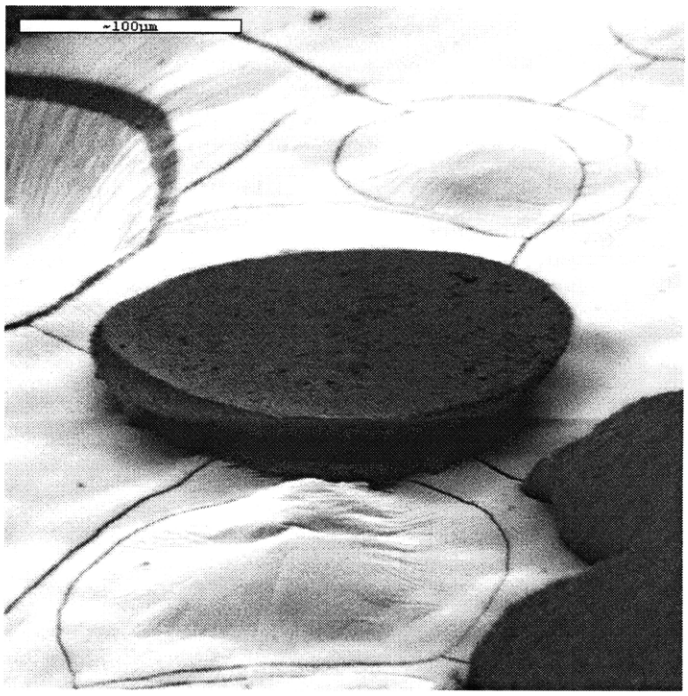

Figure 5.3: SEM of a Primitive Cross - Section (top)

pictures. Both approaches for tapecasting (30 tapecast layers vs. one layer tapecast on top of a slipcast powder bed) were tried, and it was still not possible to obtain single primitives. However, it was possible to remove single lines from tapecast powder beds.

Several guidelines have to be adopted for the sake of consistency and easier viewing of photos. Pictures of samples in the powder bed and the corresponding SEM pictures will be presented for each sample. Furthermore, a description of an SEM picture will state whether it depicts the top or the bottom of the sample. By definition, the top is that side of the where the binder droplet first impacted the powder bed.

5.2 Droplet Pairs

The next logical step to take after the primitives is to print a pair of drops that interact with each other under a variety of conditions. The goal is to simulate different time domains in droplet infiltration process, as described in section 4.2.

There were two main directions of investigating this problem. One was to print two drops always with the same frequency, but to vary the spacing. The goal was to see which spacing produces the best results in terms of the edge straightness.

A far more important aspect was the interaction of droplets printed under a variety of frequencies, but always at the same droplet spacing, in this case 40 μm. The frequency ranged from 10 kHz at one end of the spectrum all the way to the other extreme: printing a drop only after the first one is completely dry.

It should be noted that it is not always easy to draw conclusion from such small printed features as droplet pairs or line segments. It is possible to discern the same overall trends from one experiment to the next such as dependence of line width upon the print style used, and have the measurements that will be approximately alike. However, those measurements will not be completely equal due to variations in experimental conditions, which can not be entirely eliminated despite different testing mechanisms described in Chapter 3. One way of minimizing variations is to prints all the samples in a given experiment on the pieces of the same powder bed, or at the very least, on the pieces made of the same slurry. This guideline was always followed in the course of this study. Other recommendations outlined in Chapter 3 also apply.

5.2.1 Variation in Droplet Spacing

A series of samples was printed using the DOD setup. The frequency was held constant at 1000 Hz, while the droplet center – center spacing varied from 20 μm to 220 μm in the increments of 20 μm. The goal was to have a variety of settings varying from a high binder dose (droplets close by) to low binder dose (droplets so far apart that eventually one prints single primitives rather than pairs of drops). Only the frequency of 1000 Hz was used for this portion of the study.

As expected the pairs with low center – center spacing have a shape that very closely resembles single primitives (Figures 5.4 and 5.5). As the spacing increases, the printed region slowly elongates in the fast axis (Figures 5.6 through 5.8). Finally, the droplets completely separate and what is removed is a single primitive rather than a pair of droplets (Figures 5.9 and 5.10)

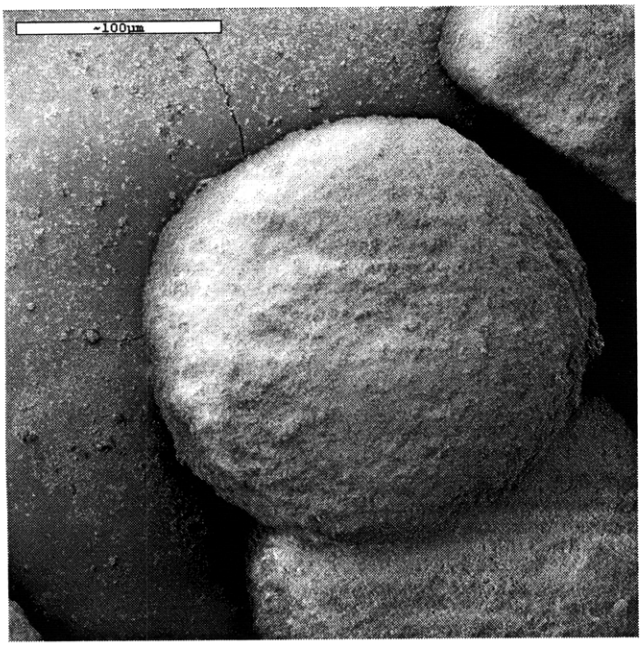

Figure 5.4: SEM of a Droplet Pair (20 µm spacing, bottom, 1000 Hz)

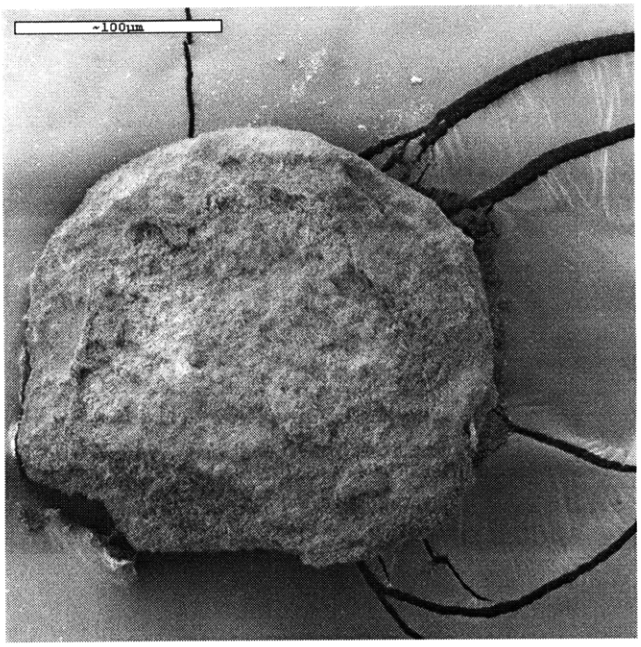

Figure 5.5: SEM of a Droplet Pair (60 µm spacing, bottom, 1000 Hz)

Figure 5.6: SEM of a Droplet Pair (100 µm spacing, bottom, 1000 Hz)

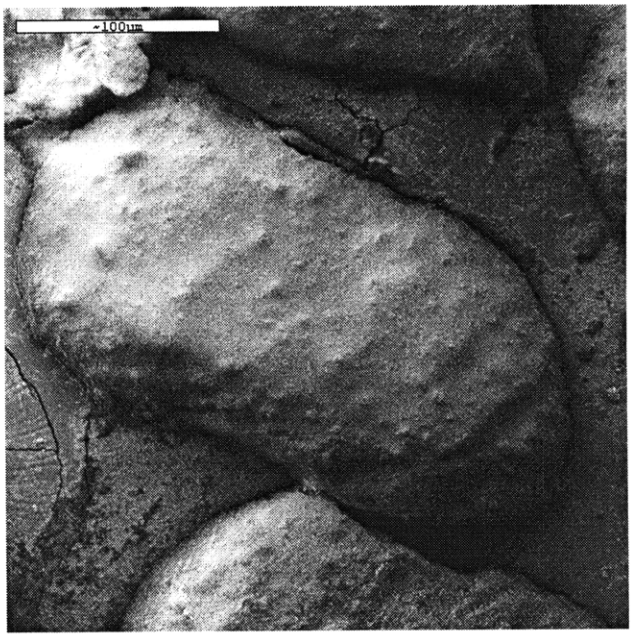

Figure 5.7: SEM of a Droplet Pair (140 µm spacing, bottom, 1000 Hz)

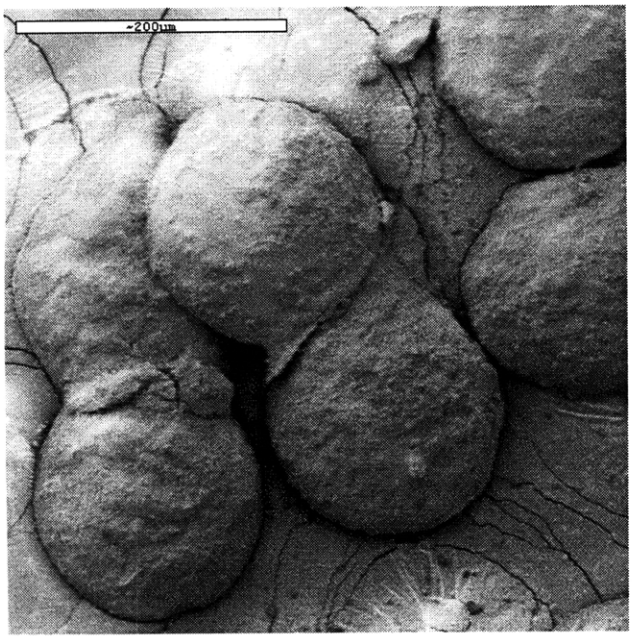

Figure 5.8: SEM of a Droplet Pair (180 µm spacing, bottom, 1000 Hz)

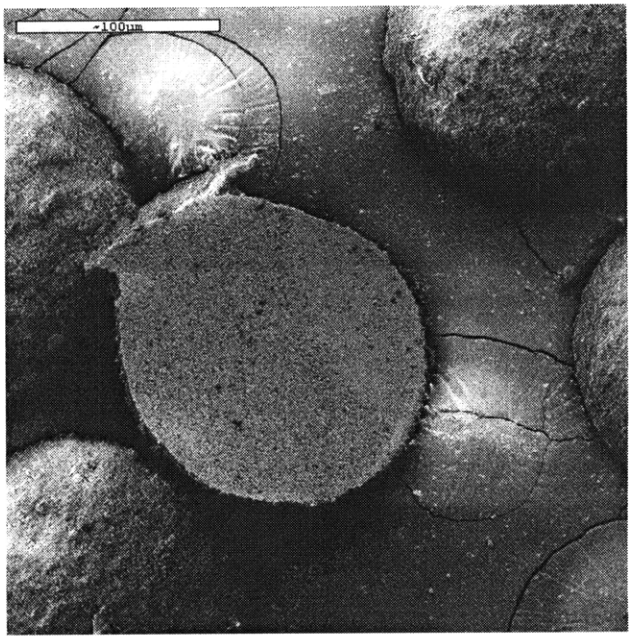

Figure 5.9: SEM of a Droplet Pair (200 µm spacing, top, 1000 Hz)

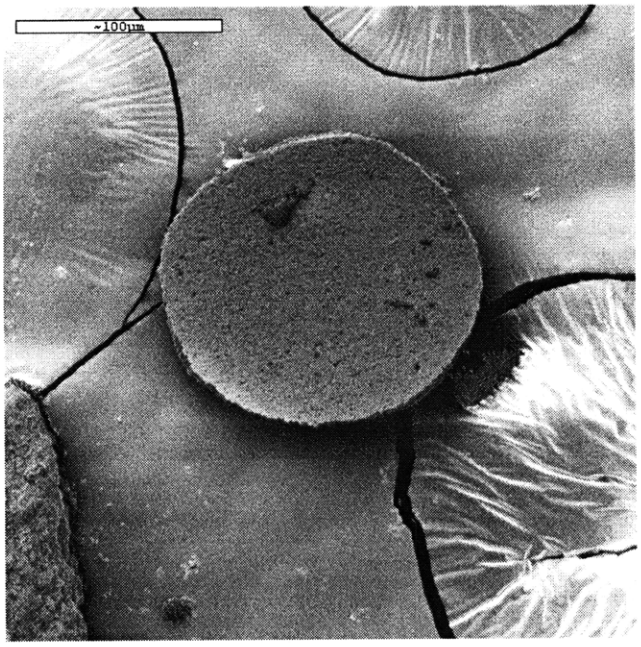

Figure 5.10: SEM of a Droplet Pair (220 µm spacing, top, 1000 Hz)

5.2.2 Variation in Frequency

The goal in this part of research was to simulate different time regimes as outlined in the section 4.2. The following settings at the droplet spacing of 40 and 80 μm were printed, unless otherwise noted:

1) Single pass at f = 5000 Hz (only 40 μm)

2) Single pass at f = 500 Hz

3) Single pass at f = 50 Hz

4) Multiple pass (2 passes/line) with effective frequency of 1 Hz: f_p=990Hz, v_p=0.495m/s

5) Multiple pass (2 passes/line) with drying between the passes: f_p=200 Hz, v_p = 0.1 m/s

It is not possible to have the printhead operate at the frequency of less than 40 Hz. In order to simulate printing at lower frequencies, several passes per each line have to be made and the binder deposited in such way. Whenever the printhead makes more that one pass per line, two different frequencies exist: the printhead frequency (f_p), and the effective frequency of droplets. The former is determined by the printhead speed (v_p) and the spacing between locations where the drops are fired. The latter depends solely on the time interval between the arrival times of two or more droplets that are impacting each other. For example, the effective frequency of 1 Hz can be achieved if the printhead rasters twice across the powder bed with the fast axis speed of 0.495 m/s. In each pass fired droplets do not touch each other. By the time the printhead makes the next pass across the powder bed, 1 second has passed so the effective frequency is 1 Hz. The speed of 0.495 m/s was used only for passes with 1 Hz effective frequency. All the other passes including the ones with drying were printed at smaller speed to avoid any possibility of droplets not aligning properly in the powder bed.

It was not possible to determine the time for a droplet to dry in the powder bed. The assumption was made that if the powder bed is dried after the printhead deposits the first droplet of the pair, and only then deposits the second droplet in the subsequent pass, then this time regime would be simulated. The issues raised in terms of drying were the same as in the tapecasting. The powder bed must not be heated too much to prevent evaporation of PEG_{400}. The same setup as in tapecasting (the Variac autotransformer and the heat lamp) was used here. The Variac setting was at 30, and the lamp was on for 30 seconds. The temperature of the heated powder bed never increased past 32°C, as

determined by the thermocouple. The powder bed then had to be allowed to cool down to the original temperature. It took 120 seconds to achieve that. This pause of 150 seconds was enough for PAA to clog up the printhead nozzles. The nozzles had to be cleaned with a damp paper towel without removing the printhead from the carriage.

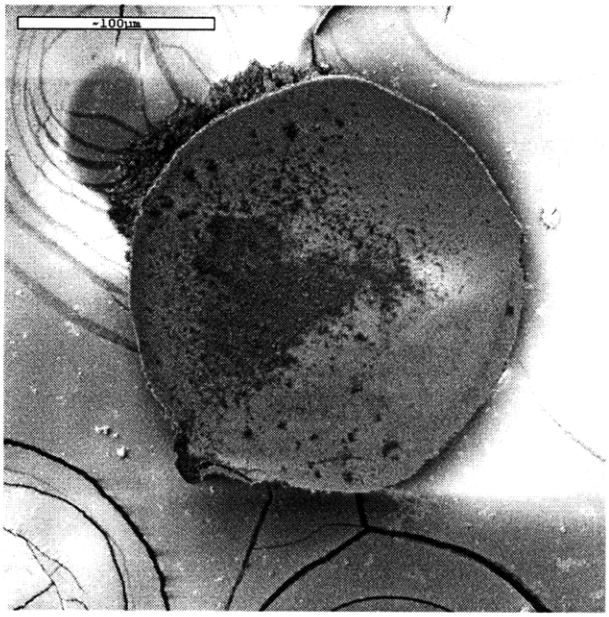

Figure 5.11: SEM of a Droplet Pair (40 µm spacing, 5000 Hz, top)

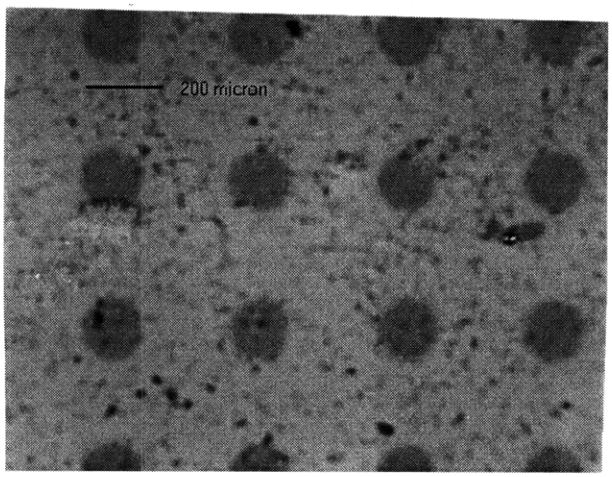

Figure 5.12: Droplet Pairs (40 μm spacing, 500 Hz, in powder bed)

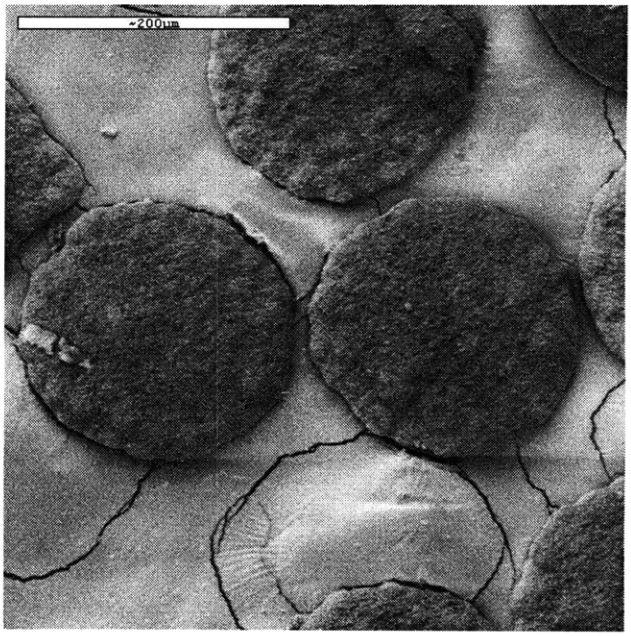

Figure 5.13: SEM of Droplet Pairs (40 μm spacing, 500 Hz, bottom)

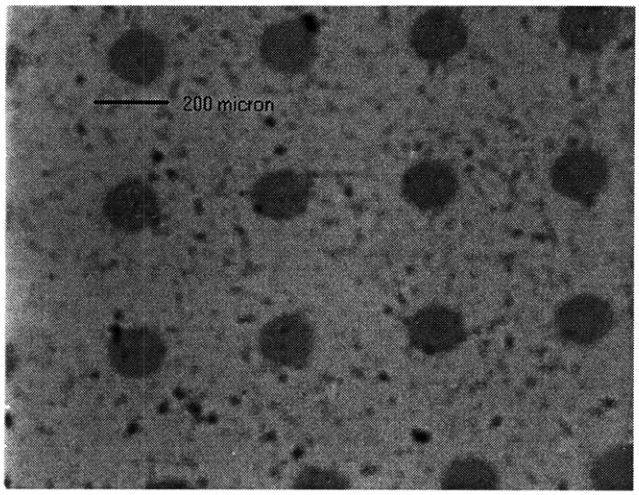

Figure 5.14: Droplet Pair (40 μm spacing, 50 Hz, in powder bed)

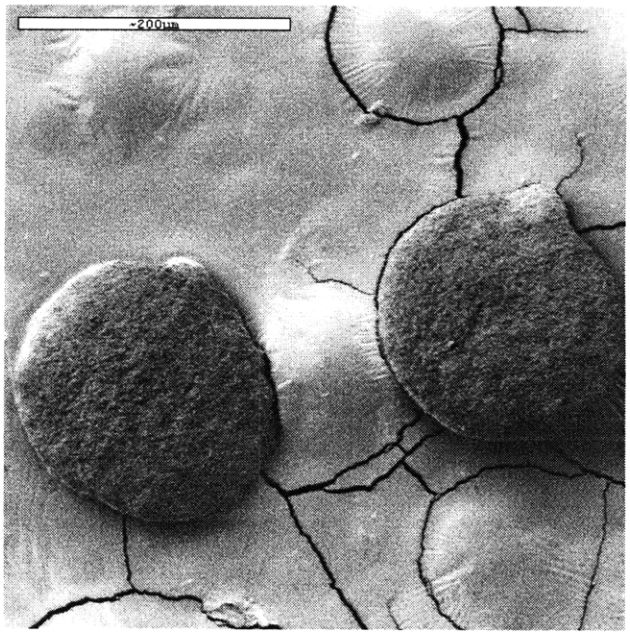

Figure 5.15: SEM of Droplet Pairs (40 μm spacing, 50 Hz, bottom)

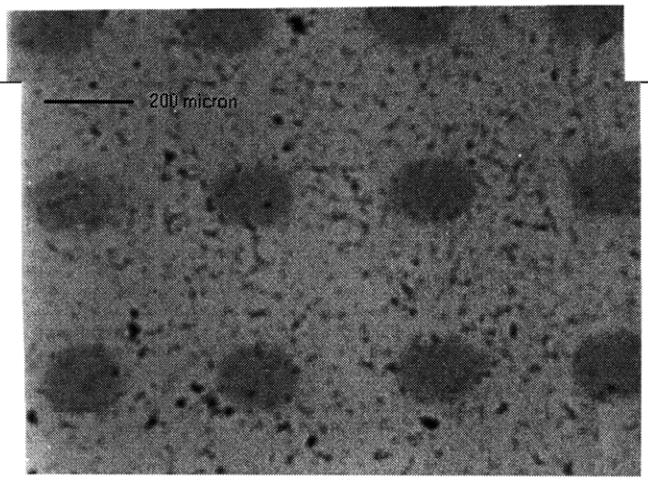

Figure 5.16: Droplet Pairs (40 μm spacing, 1 Hz, in powder bed)

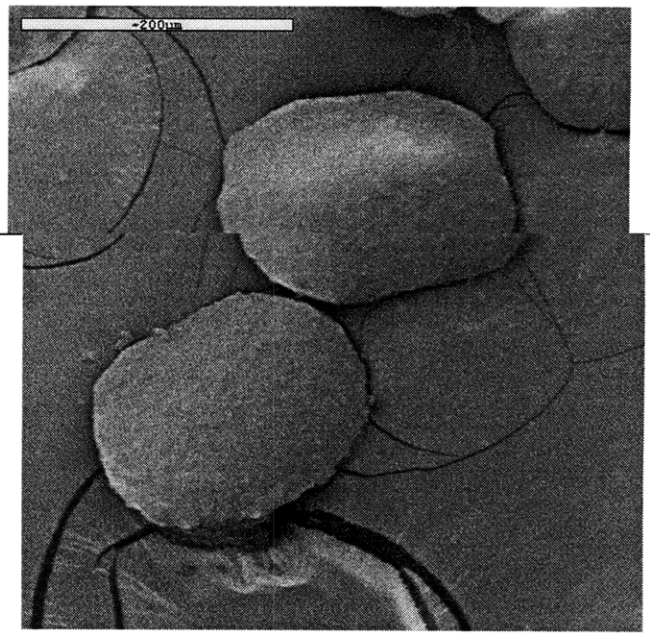

Figure 5.17: SEM of Droplet Pairs (40 μm spacing, 1 Hz, bottom)

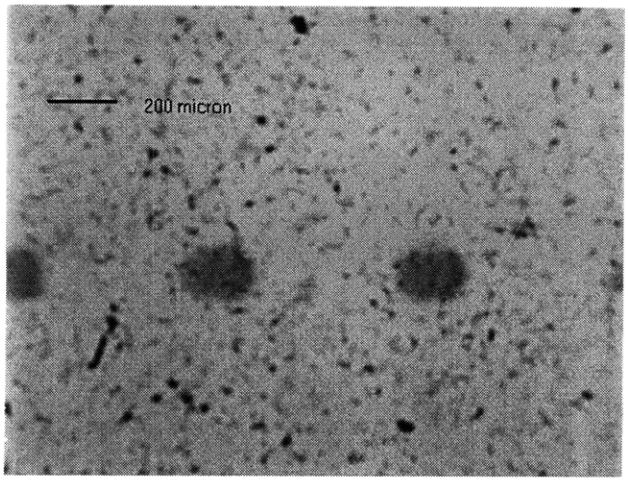

Figure 5.18: Droplet Pairs (40 μm spacing, drying between passes, in powder bed)

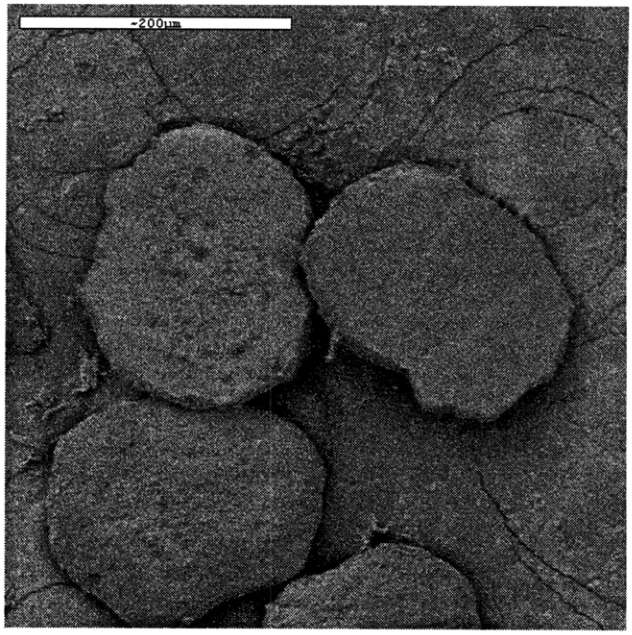

Figure 5.19: SEM of Droplet Pairs (40 μm spacing, drying between passes top)

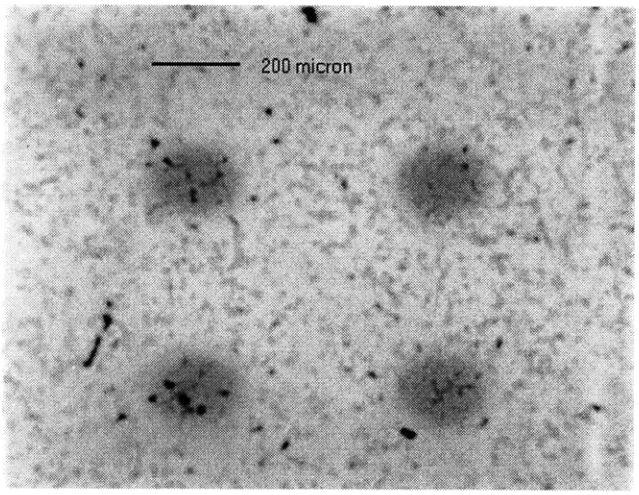

Figure 5.20: Droplet Pairs (80 μm spacing, 500 Hz, in powder bed)

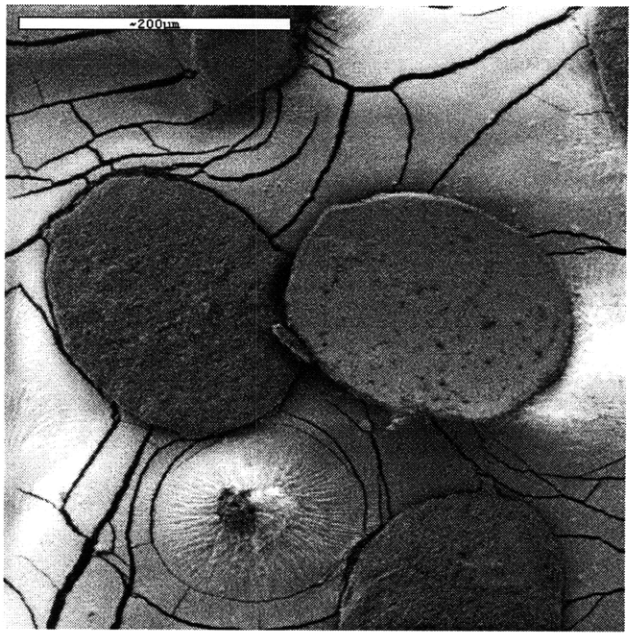

Figure 5.21: SEM of Droplet Pairs (80 μm spacing, 500 Hz, top and bottom)

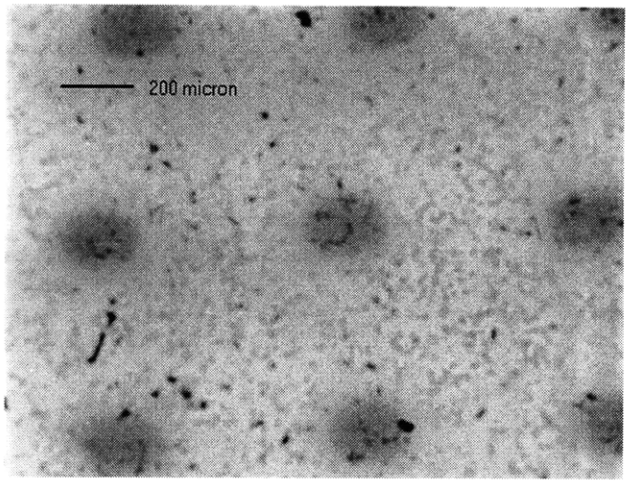

Figure 5.22: Droplet Pairs (80 μm spacing, 50 Hz, in powder bed)

Figure 5.23: SEM of Droplet Pairs (80 μm spacing, 50 Hz, bottom)

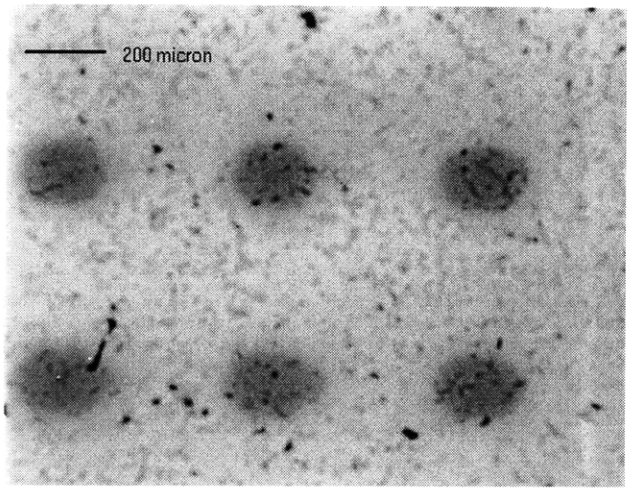

Figure 5.24: Droplet Pairs (80 μm spacing, 1 Hz, in powder bed)

Figure 5.25: SEM of Droplet Pairs (80 μm spacing, 1 Hz, top and bottom)

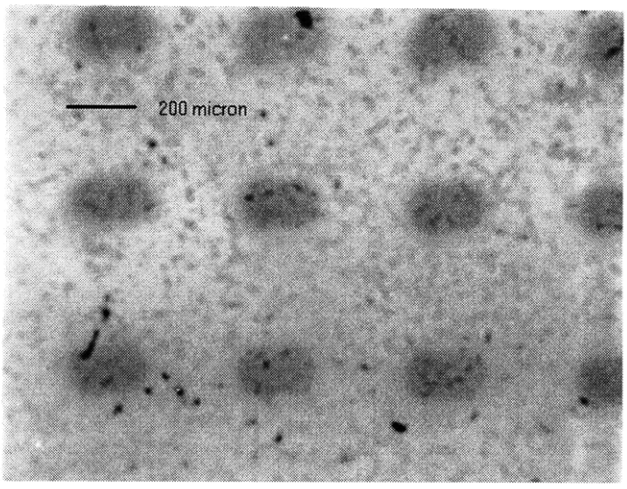

Figure 5.26: Droplet Pairs (80 μm spacing, drying after each pass, in powder bed)

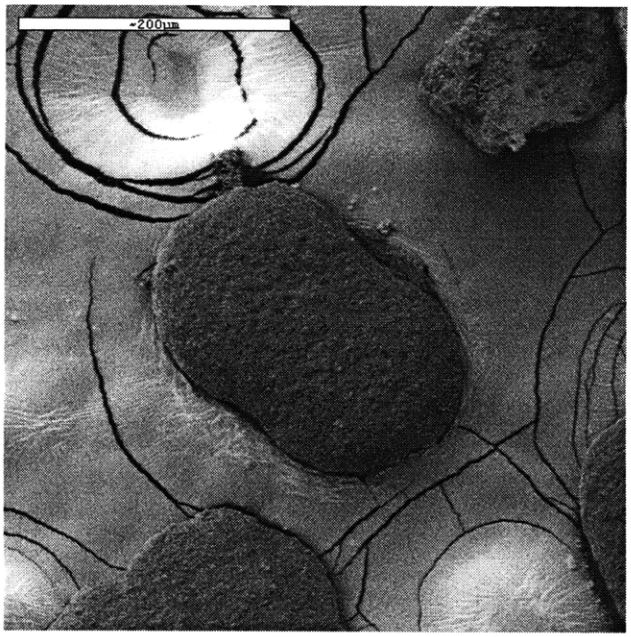

Figure 5.27: SEM of Droplet Pairs (80 μm spacing, drying after each pass, bottom)

The pictures of 40 μm spacing samples show that the higher the printing frequency, the more of a circular shape the samples assume, which was expected. Essentially the binder is pooled together into one big drop, which then absorbs into the powder bed. It can be observed that there is no difference among droplet pairs printed at 5000 Hz, 500 Hz, and 50 Hz. The resulting features are circular in shape. Only in the 50 Hz instance, can the beginning of a somewhat different infiltration process can be discerned because the droplet is starting to lose the circular shape on one side where a small protrusion can be observed.

There is a noticeable difference between 50 Hz and 1 Hz. The 1 Hz instance presents a droplet pair that is no longer circular, but rather somewhat elliptical. This indicates that the first droplet is already absorbed in the powder bed by the time the second one hits. It is not possible for the binder to form one big glob of liquid on the surface prior to infiltration, and the binder is absorbed as individual droplets. This is further pronounced in the very last case of drying the powder bed after each pass.

The same overall trend can be discerned in the 80 μm samples as well, but it is not so strikingly obvious. The reason for that is that the droplets are spaced far apart to begin with and they are never able to form one big drop.

Controls were used to monitor performance of the printhead during the course of printing for the samples where more than one pass was made in each line: 1 Hz and drying-between-passes samples. The control was a piece of ink jet transparency mounted on a small micrometer stage. After one pass was completed, the transparency would be moved by a known distance. After the second pass was printed, the droplets printed on the control medium were inspected to determine the separation between them. If that number coincided by the distance by which the stage was moved adjusted for the center-center distance, then it could be concluded that the printhead operated properly. For example, Figure 5.28 shows a control printed for 40 μm droplet pairs with drying between passes. The drops in the first pass were printed 500 μm apart. While the powder bed was cooling down, the micrometer stage was moved by 210 μm. The second pass was offset by 40 μm, so the final separation between drops on the control medium was supposed to be 250 μm. The inspection consisted of confirming that the separation between droplets in the fast axis was indeed 250 μm. Within any printed line of droplets,

the locations of droplets' center with the respect to the slow axis had to be examined as well to confirm that the printhead fired all the droplets in a straight line.

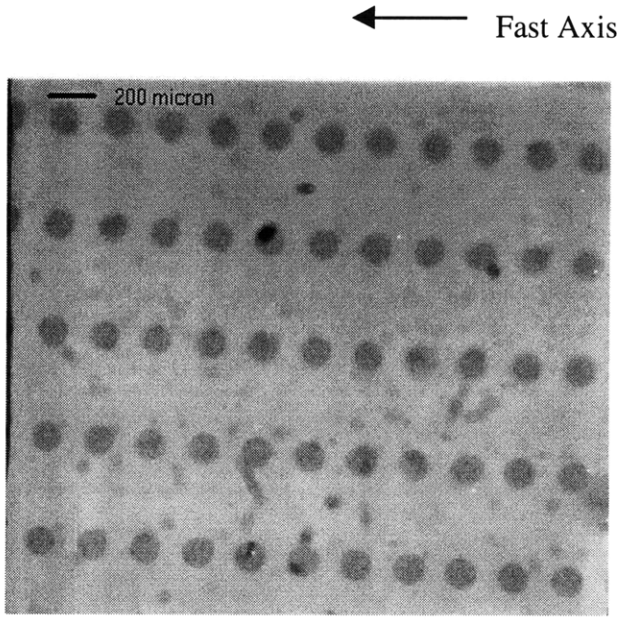

Figure 5.28: Droplet Pair (40 μm spacing, dry between passes, ink jet transparency)

5.3 Line Segments

After printing droplet pairs, the question of how these results translate when bigger structures are printed had to be answered. It was important to correlate the appearance of printed samples in powder beds and their appearance after the powder beds are redispersed. This is not possible to accomplish when printing a line that stretches for many millimeters, across the entire powder bed, because the line would inevitably break into smaller segments in the redispersion stage. However, if a short line segment consisting of a dozen or so drops is printed, it would be possible to photograph the sample while it is still in the powder bed, redisperse it, and remove the entire line segment intact to take SEM pictures. These segments had to be small enough not to break into yet smaller pieces, and still big enough that the end effects would not be noticed in its middle part. This would effectively simulate a complete line without having the associated disadvantages.

40 μm center – center droplet spacing was retained, keeping in line with the previous experiments. Each printed sample contained 30 drops, so the line segments had overall length of about 1300 μm.

Samples of 80 μm spacing were also printed. These line segments contained 20 droplets resulting in the overall length varied from 1600 to 1700 μm, depending on the print style. It was possible to redisperse and remove these samples without damaging them. The only setting missing in 80 μm samples is the setting #3 described below. It was not possible to print it because the printhead was not depositing the droplets accurately.

Different print styles were explored, similar to the droplet pairs experiments. The list of different setting is provided below:

1) Single pass at f = 500 Hz
2) Single pass at f = 50 Hz
3) Multiple pass with effective frequency of 1 Hz. N drops were deposited in N separate passes. The printhead speed v_p was always 0.495 m/s, and only one droplet was deposited in each pass. By the time the next pass arrived, one second had passed. The printhead frequency f_p was 275 and 225 Hz for 40 and 80 μm, respectively.
4) Multiple pass with effective frequency of 1 Hz, but there were more than one drop per pass. The droplets are not supposed to touch each other, so they had to be printed

sufficiently apart. The number of drops printed depended on the droplet spacing, and is indicated on each picture. The printhead speed was always 0.495 m/s, while the printhead frequency f_p was 275 and 225 Hz for 40 and 80 μm line segments.

5) Multiple pass with drying after each pass. The setting was just like in #3: each droplet in its own pass, v_p = 0.2 m/s regardless of the droplet spacing, f_p = 111 and 91 Hz for 40 and 80 μm line segments.
6) Multiple pass with drying after each pass. The setting was just like in #4: more than one droplet in one pass, v_p = 0.2 m/s regardless of the drop spacing, f_p = 111 and 91 Hz for 40 and 80 μm line segments, respectively.

The printhead rasters across the powder bed either 6 or 30 times during the multiple pass printing. It is necessary to know if the final shape of the line is due to improper functioning of the nozzles or some powder bed issues. During printing it is possible that the nozzle will become clogged, especially in those instances when the powder bed has to be heated. Cleaning it with a damp paper towel only increases chances of bumping the printhead and changing its position. Placing a piece of ink – jet transparency next to the powder bed provided the control for these issues. The binder is printed concurrently on both media. The ensuing examination of the transparency portion reveals whether or not the printhead performed satisfactorily.

The binder for these experiments was 20 wt.% PAA with amaranth, and the powder beds were created by slipcasting 30 v/o 1.0 μm alumina slurry.

Each sample also has a control that was printed simultaneously with the powder bed samples. The control medium is ink jet transparency.

All of the pictures in the following sections are oriented from right to left, following the motion of the printhead. Therefore, the first droplet of a line segment is the one most to the right of the picture.

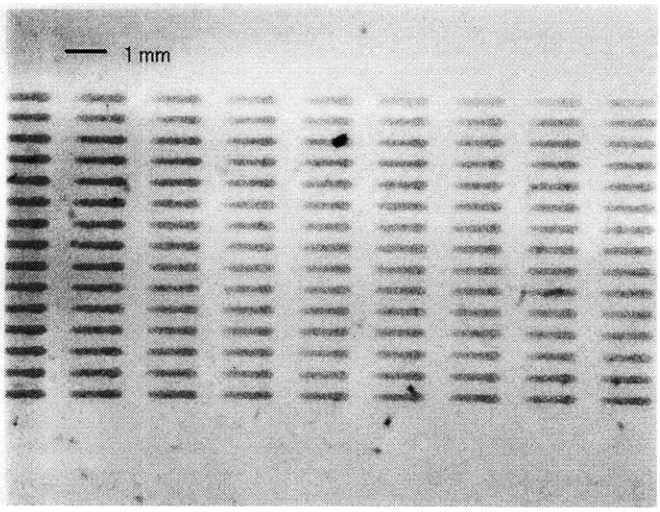

Figure 5.29: Line Segments (40 μm spacing, 500 Hz, ink jet transparency)

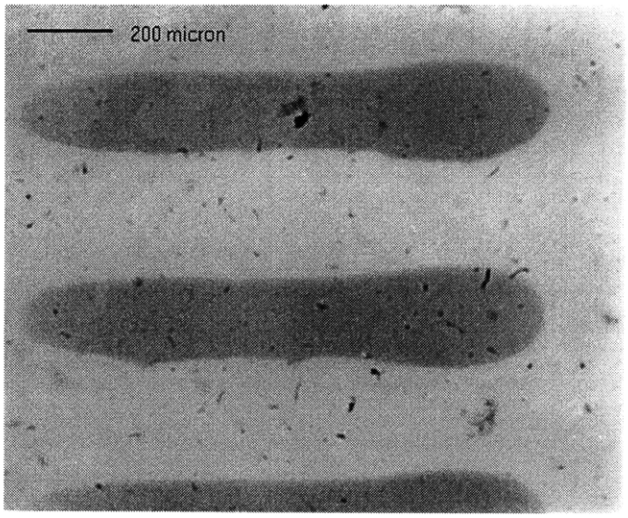

Figure 5.30: Line segments (40 μm spacing, 500 Hz, ink jet transparency)

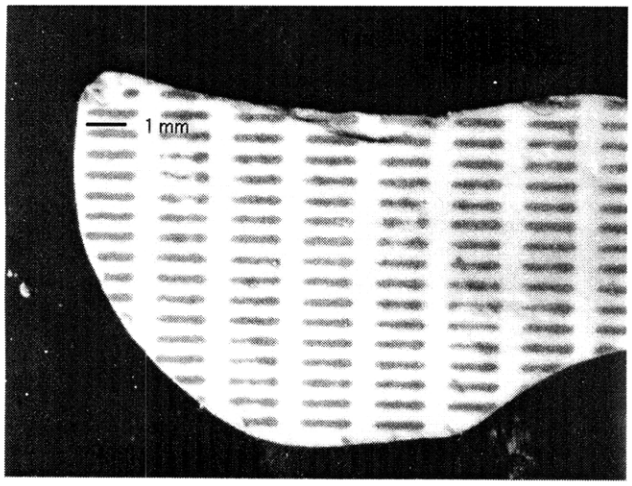

Figure 5.31: Line Segments (40 μm spacing, 500 Hz, in powder bed)

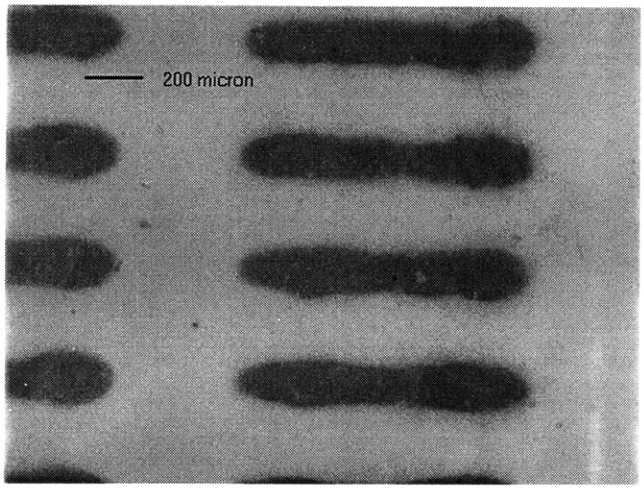

Figure 5.32: Line Segments (40 μm spacing, 500 Hz, in powder bed)

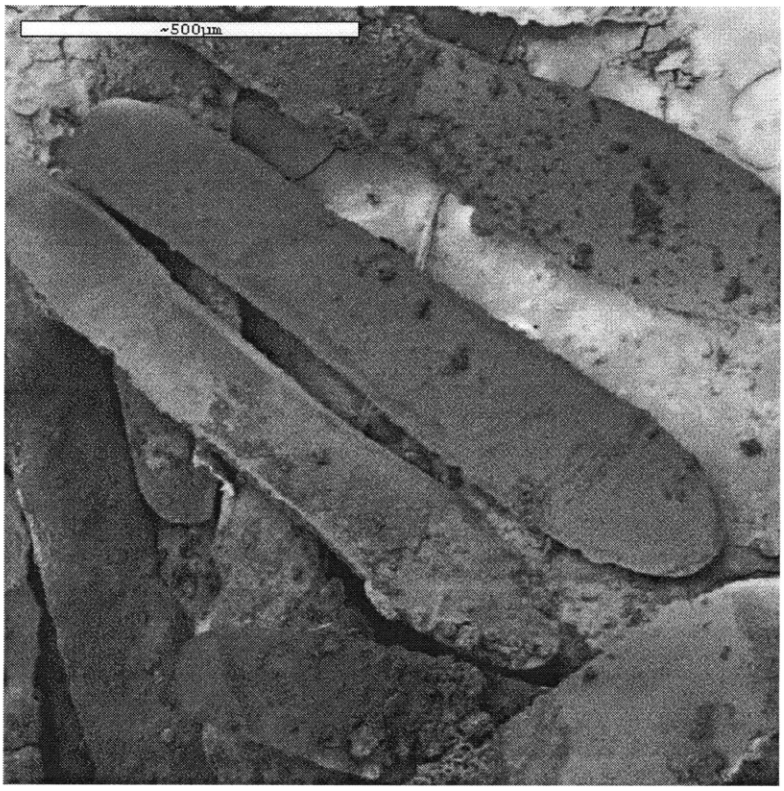

Figure 5.33: SEM of Line Segments (40 µm spacing, 500 Hz, top)

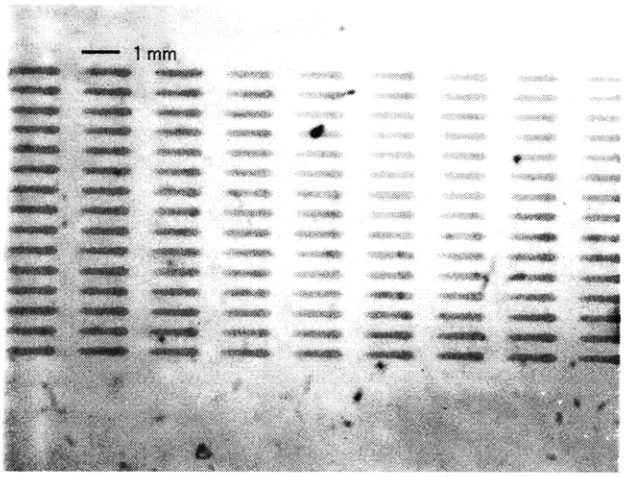

Figure 5.34: Line Segments (40 μm spacing, 50 Hz, ink jet transparency)

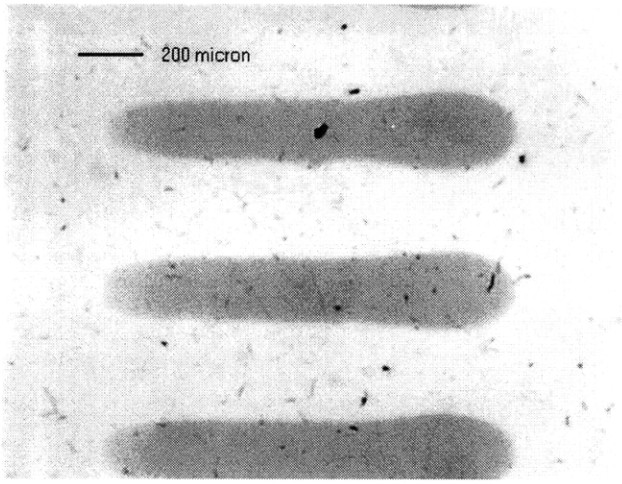

Figure 5.35: Line Segments (40 μm spacing, 50 Hz, ink jet transparency)

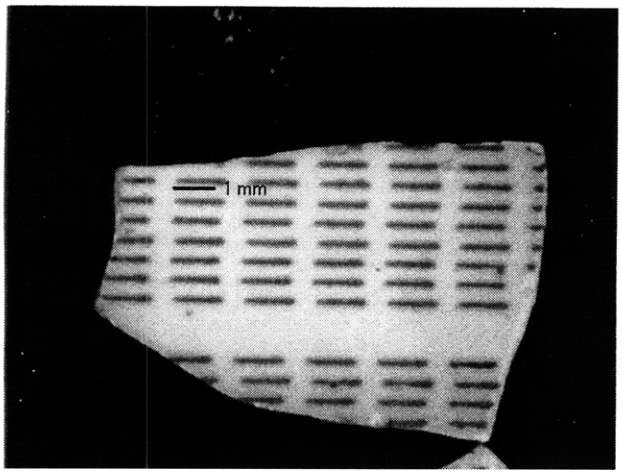

Figure 5.36: Line Segments (40 μm spacing, 50 Hz, in powder bed)

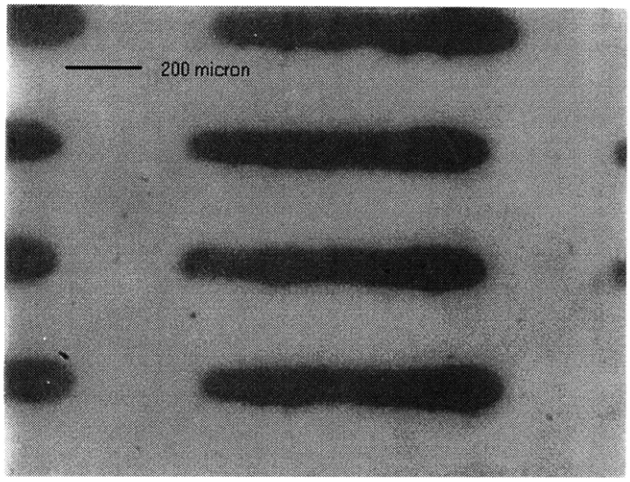

Figure 5.37: Line Segments (40 μm spacing 50 Hz, in powder bed)

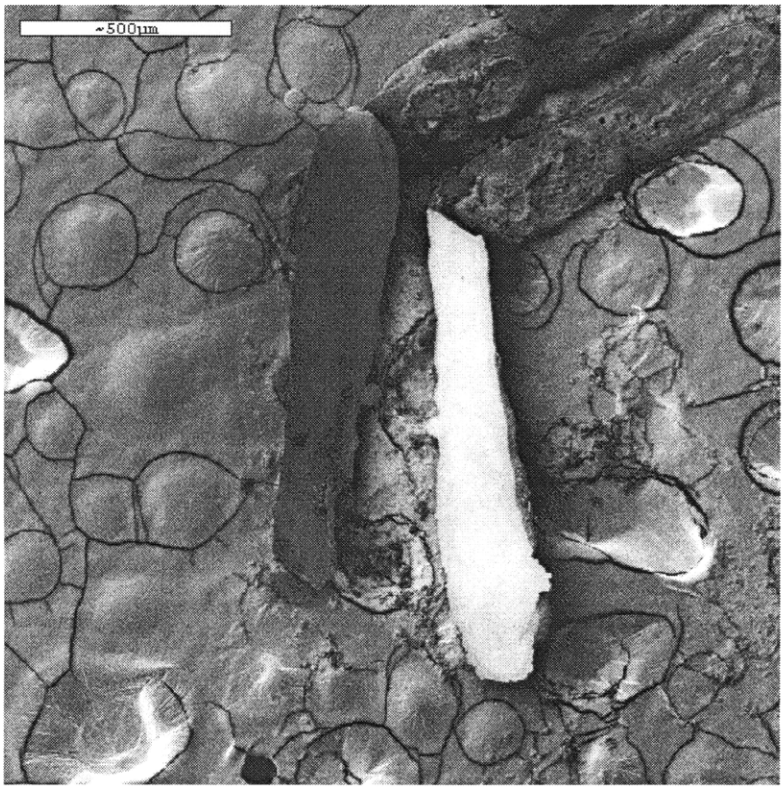

Figure 5.38: SEM of Line Segments (40 µm spacing, 50 Hz, top and bottom)

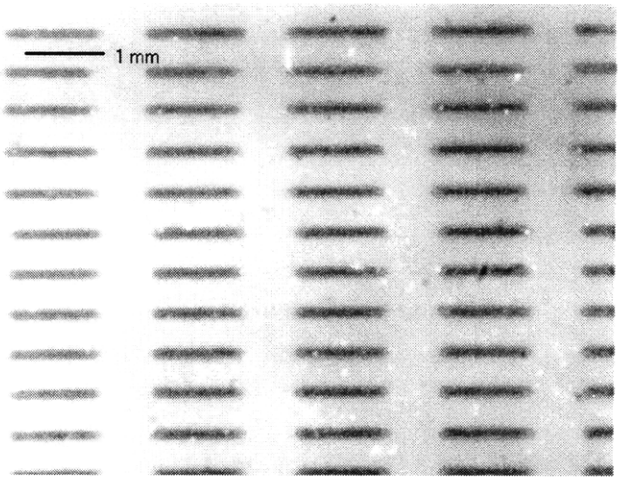

Figure 5.39: Line Segments (40 μm spacing, 1 Hz, 30 passes/line, ink jet transparency)

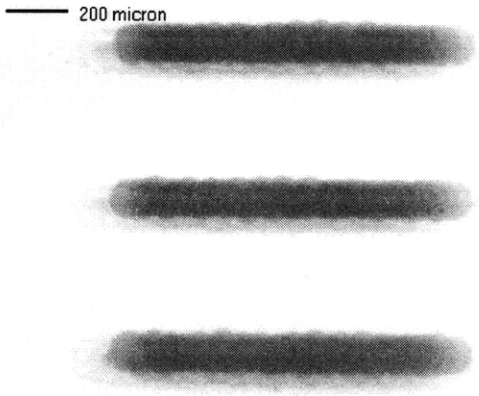

Figure 5.40: Line Segments (40 μm spacing, 1 Hz, 30 passes/line, ink jet transparency)

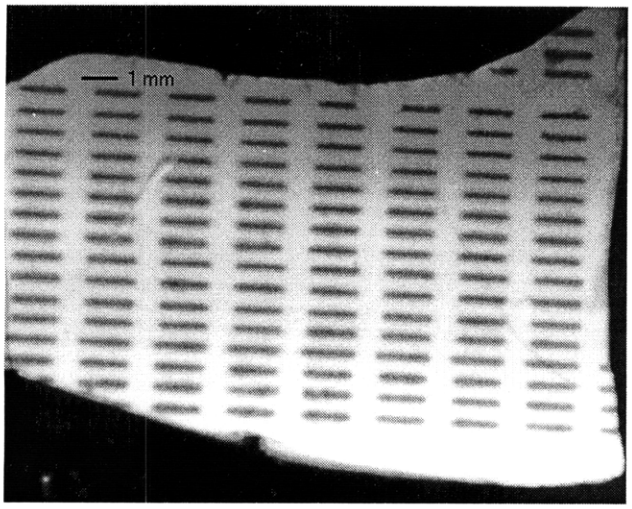

Figure 5.41: Line Segments (40 μm spacing, 1 Hz, 30 passes/line, in powder bed)

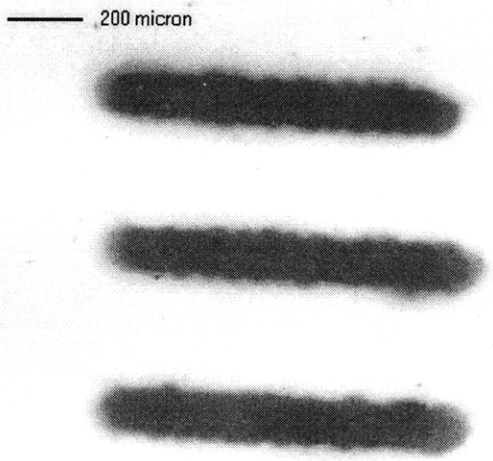

Figure 5.42: Line Segments (40 μm spacing, 1 Hz, 30 passes/line, in powder bed)

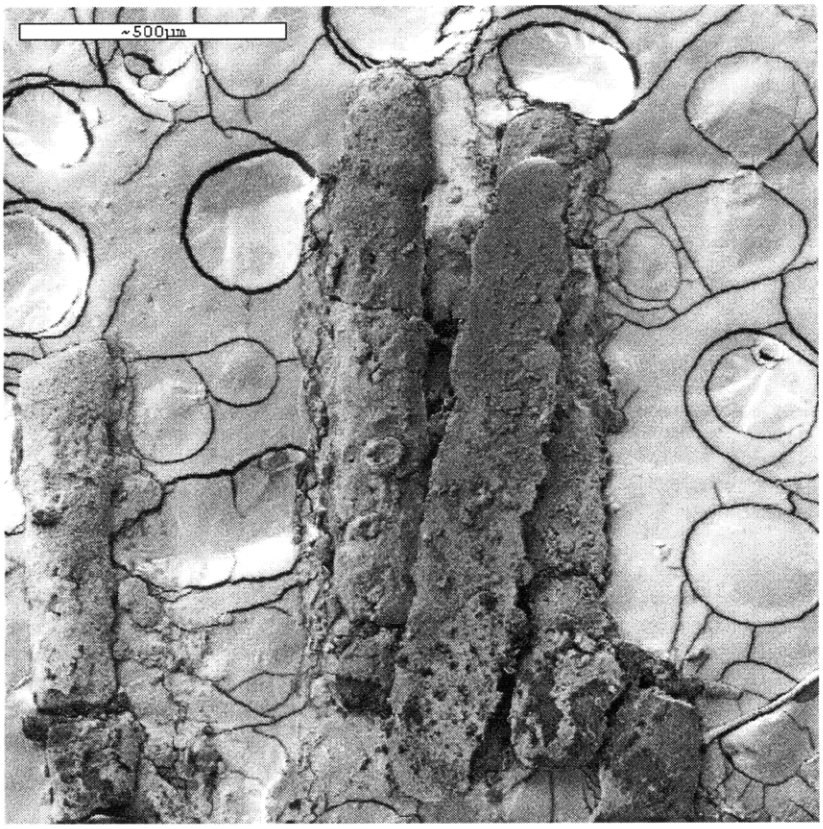

Figure 5.43: SEM of Line Segments (40 µm spacing, 1 Hz, 30 passes/line, top and bottom)

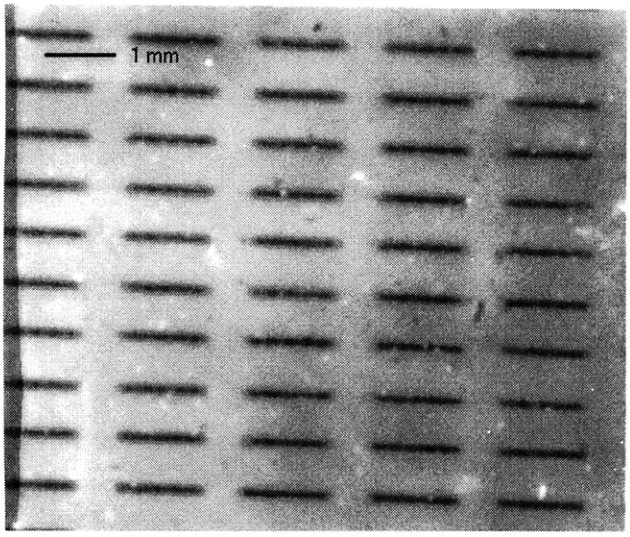

Figure 5.44: Line Segments (40 μm spacing, 1 Hz, 6 passes/line, ink jet transparency)

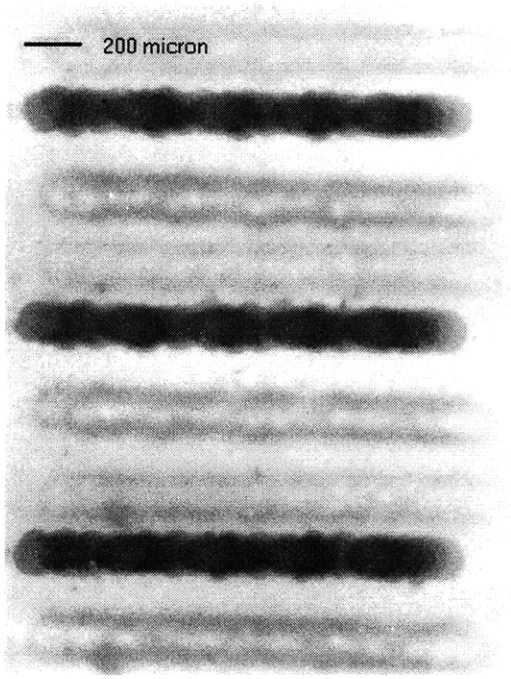

Figure 5.45: Line Segments (40 μm spacing, 1 Hz, 6 passes/line, ink jet transparency)

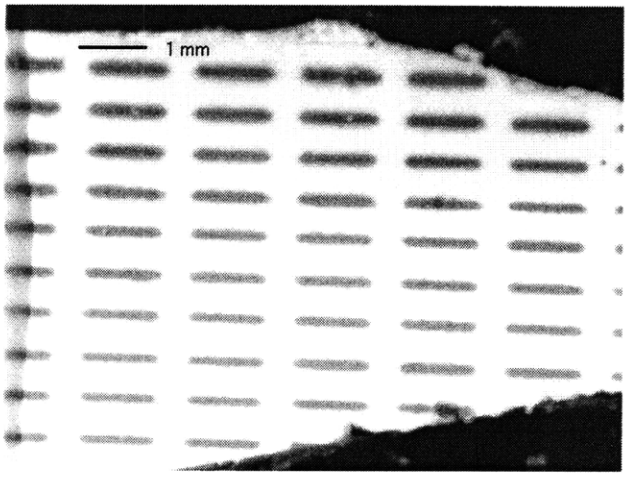

Figure 5.46: Line Segments (40 μm spacing, 1 Hz, 6 passes/line, in powder bed)

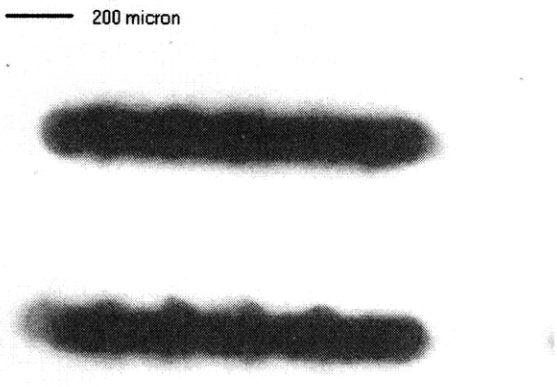

Figure 5.47: Line Segments (40 μm spacing, 1 Hz, 6 passes/line, in powder bed)

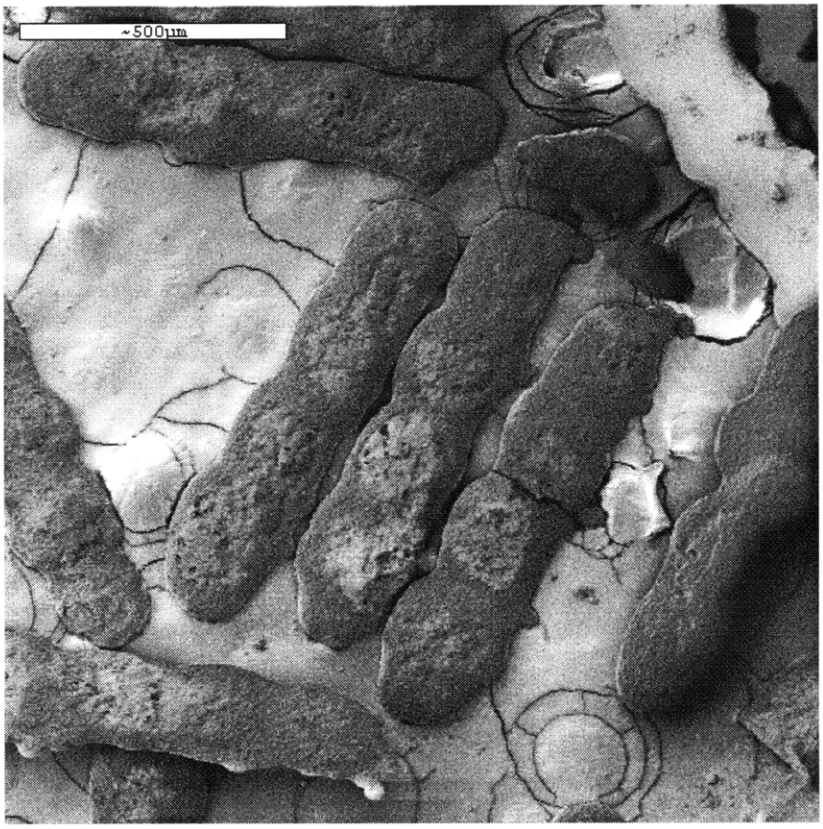

Figure 5.48: SEM of Line Segments (40 µm spacing, 1 Hz, 6 passes/line, bottom)

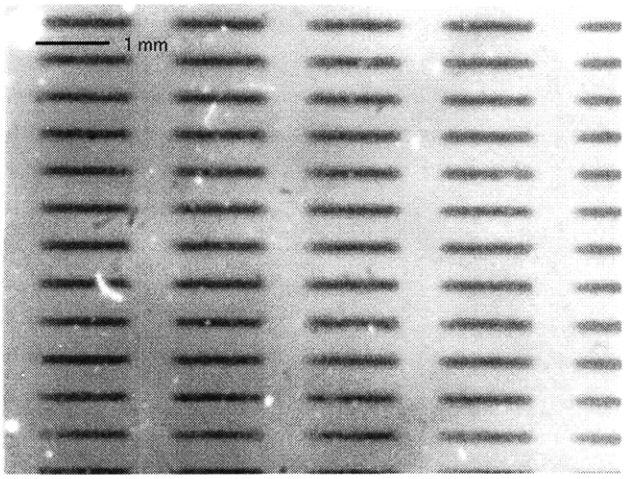

Figure 5.49: Line Segments (40 μm spacing, drying after each pass, 30 passes/line, ink jet transparency)

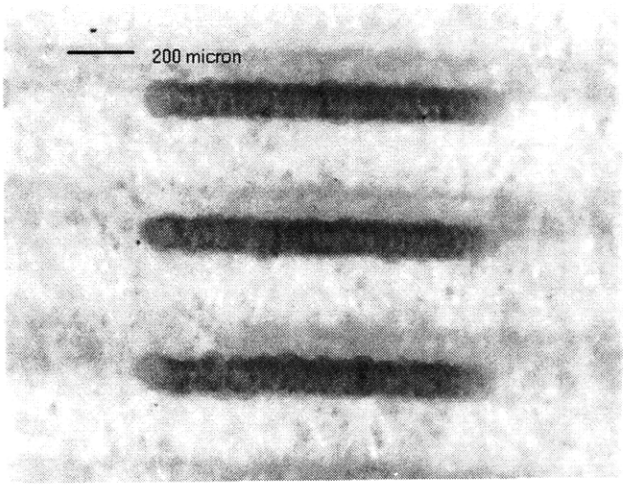

Figure 5.50: Line Segments (40 μm spacing, drying after each pass, 30 passes/line, ink jet transparency)

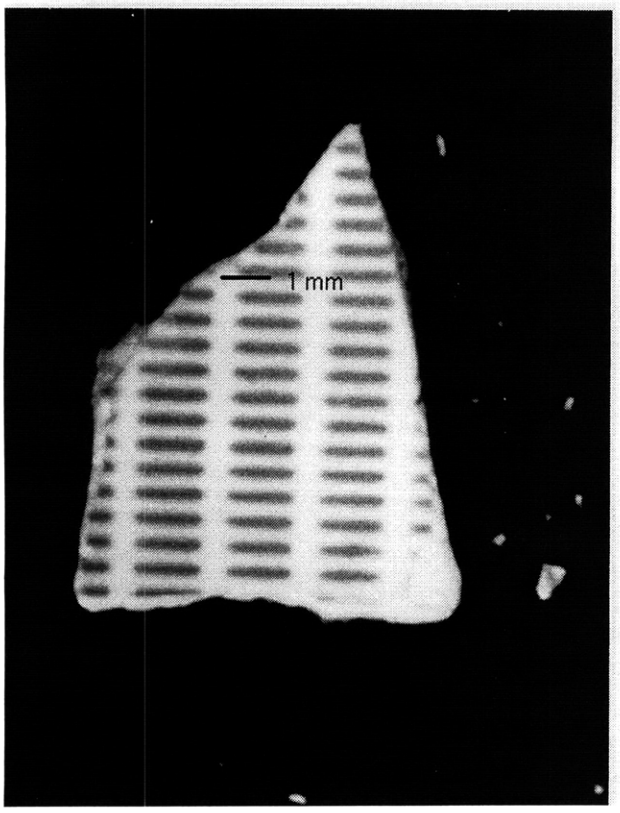

Figure 5.51: Line Segments (40 μm spacing, drying after each pass, 30 passes/line, in powder bed)

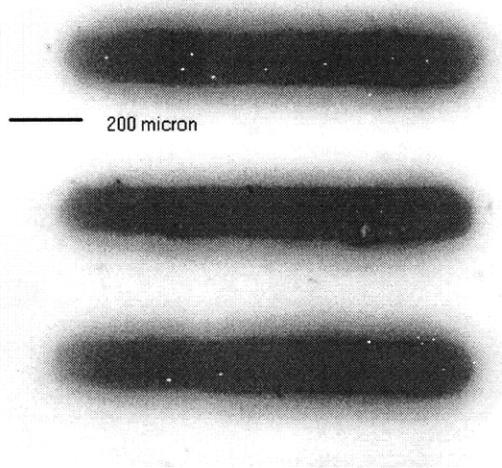

Figure 5.52: Line Segments (40 μm spacing, drying after each pass, 30 passes/line, in powder bed)

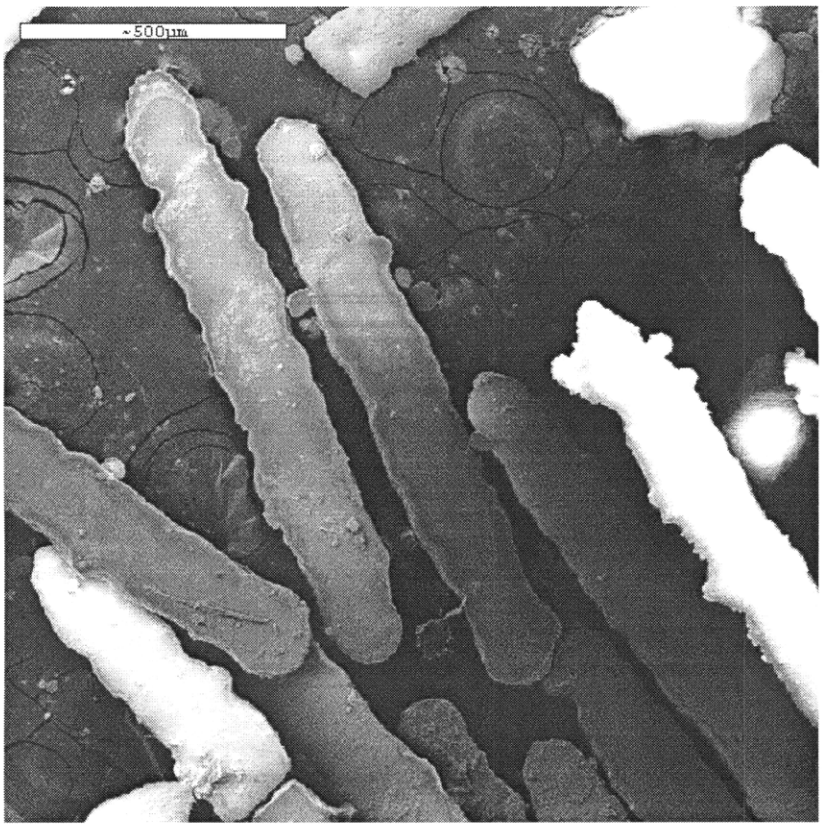

Figure 5.53: SEM of Line Segments (40 µm spacing, drying after each pass, 30 passes/line, top)

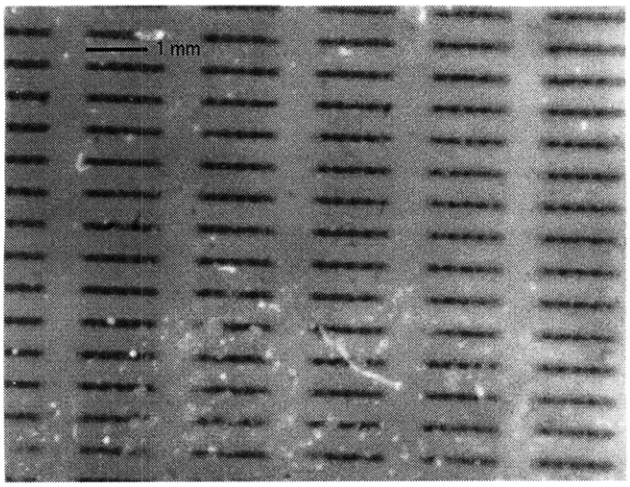

Figure 5.54: Line Segments (40 μm spacing, drying after each pass, 6 passes/line, ink jet transparency)

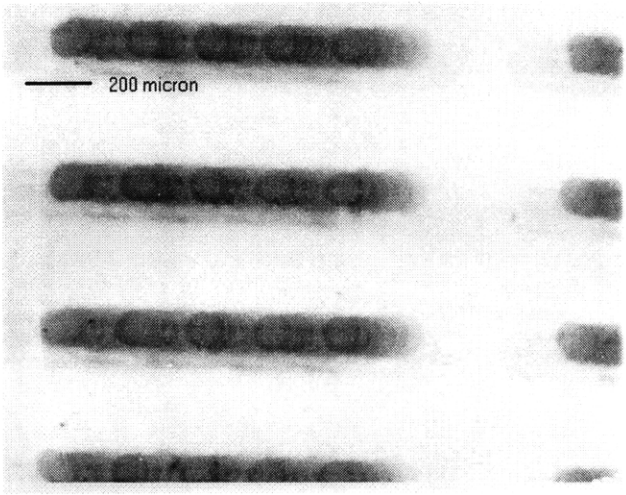

Figure 5.55: Line segments (40 μm spacing, drying after each pass, 6 passes/line, ink jet transparency)

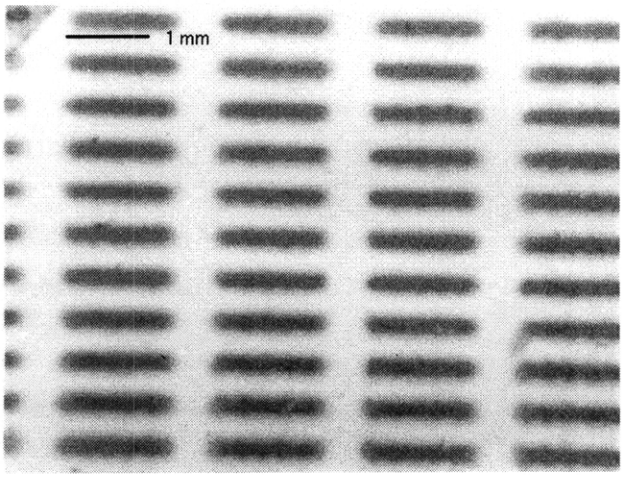

Figure 5.56: Line Segments (40 μm spacing, drying after each pass, 6 passes/line, in powder bed)

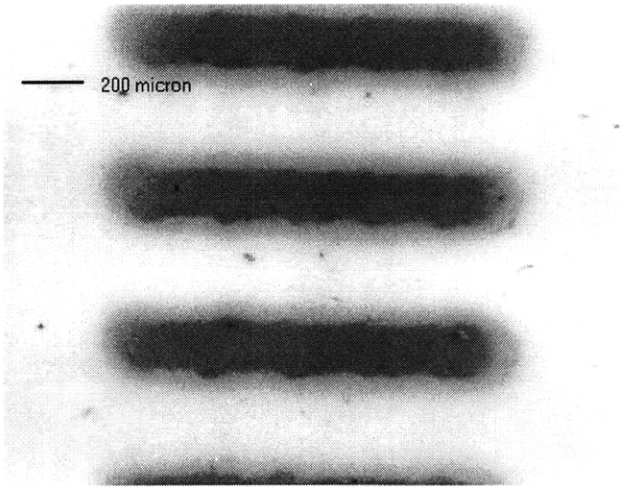

Figure 5.57: Line Segments (40 μm spacing, drying after each pass, 6 passes/line, in powder bed)

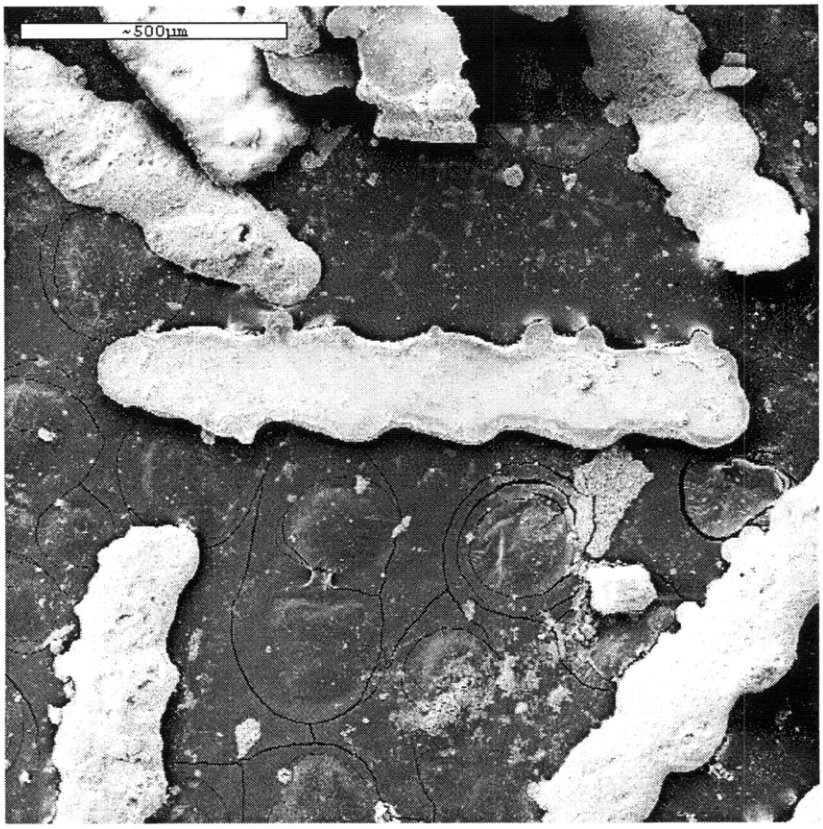

Figure 5.58: SEM of Line Segments (40 µm spacing, drying after each pass, 6 passes/line, top)

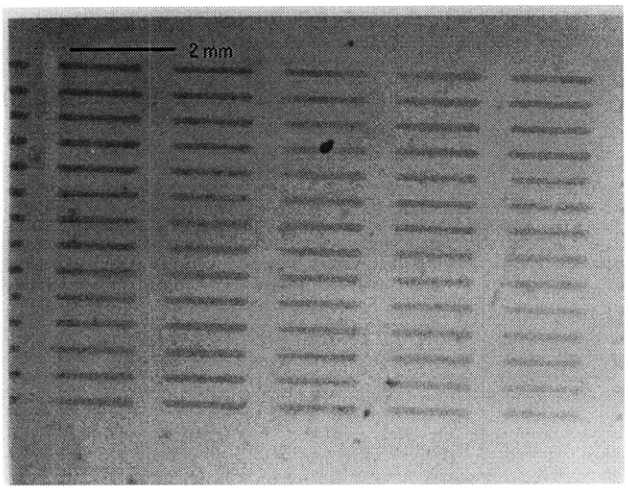

Figure 5.59: Line Segments (80 μm spacing, 500 Hz, ink jet transparency)

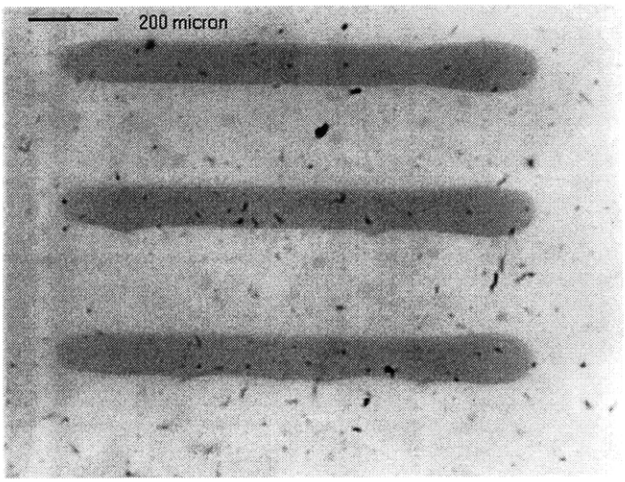

Figure 5.60: Line Segments (80 μm spacing, 500 Hz, ink jet transparency)

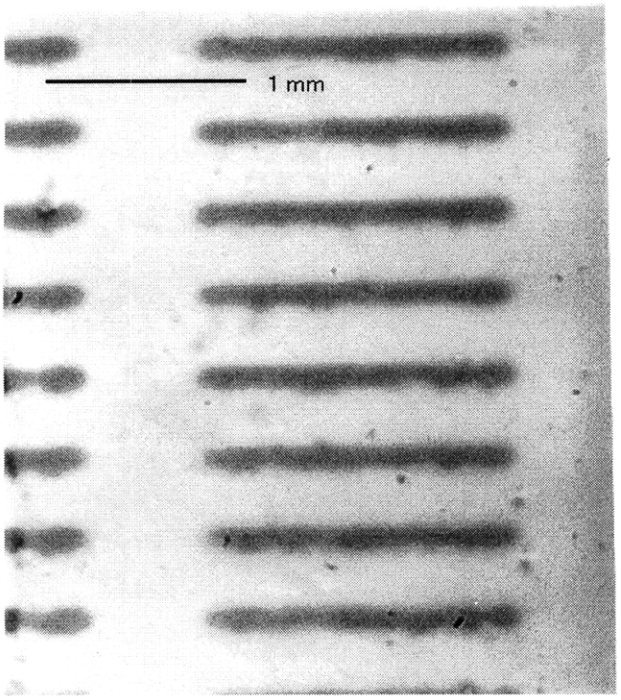

Figure 5.61: Line Segments (80 μm spacing, 500 Hz, in powder bed)

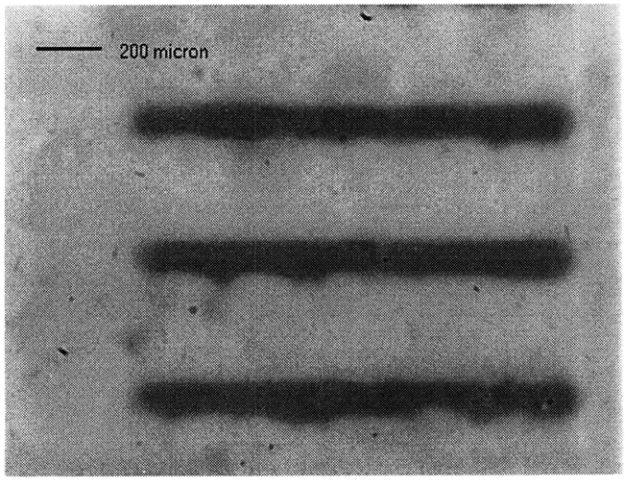

Figure 5.62: Line Segments (80 μm spacing, 500 Hz, in powder bed)

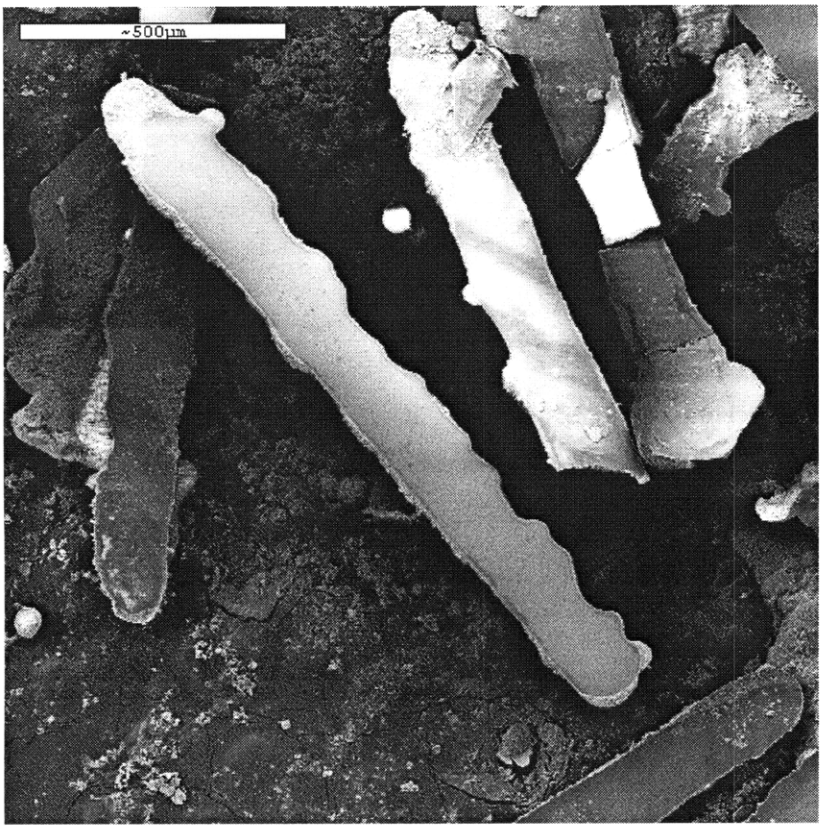

Figure 5.63: SEM of Line Segments (80 µm spacing, 500 Hz, top)

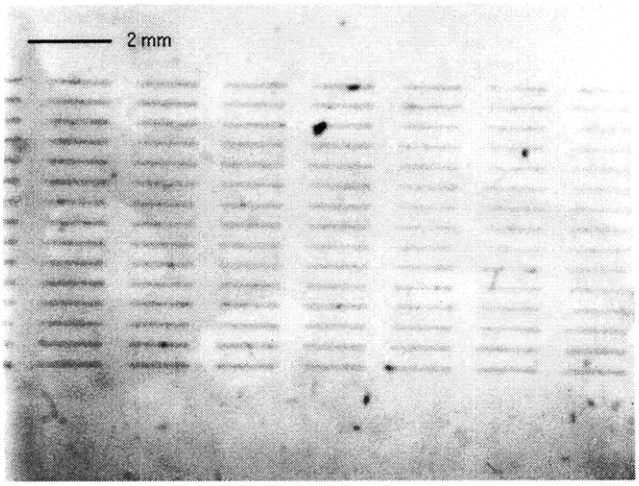

Figure 5.64: Line Segments (80 μm spacing, 50 Hz, ink jet transparency)

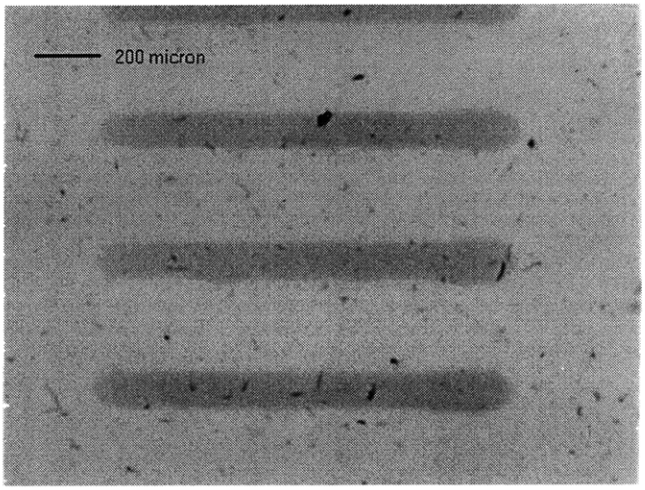

Figure 5.65: Line Segments (80 μm spacing, 50 Hz, ink jet transparency)

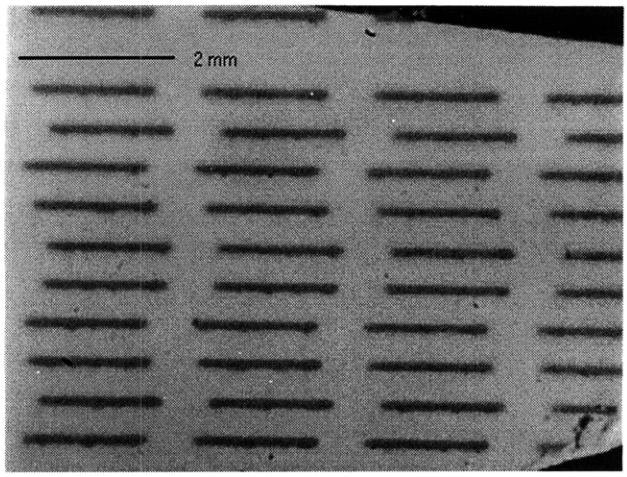

Figure 5.66: Line Segments (80 μm spacing, 50 Hz, in powder bed)

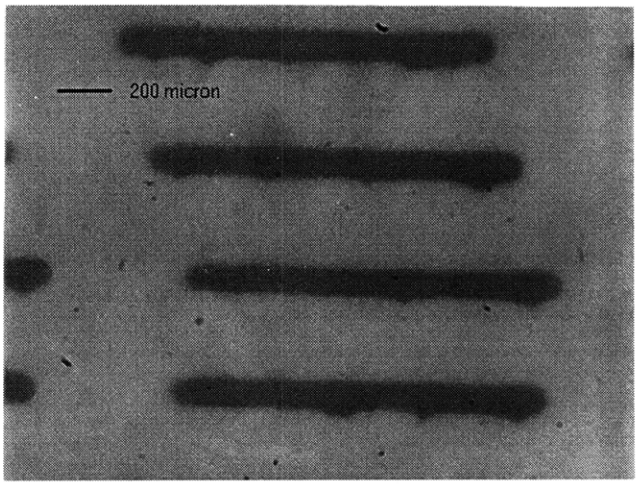

Figure 5.67: Line segments (80 μm spacing, 50 Hz, in powder bed)

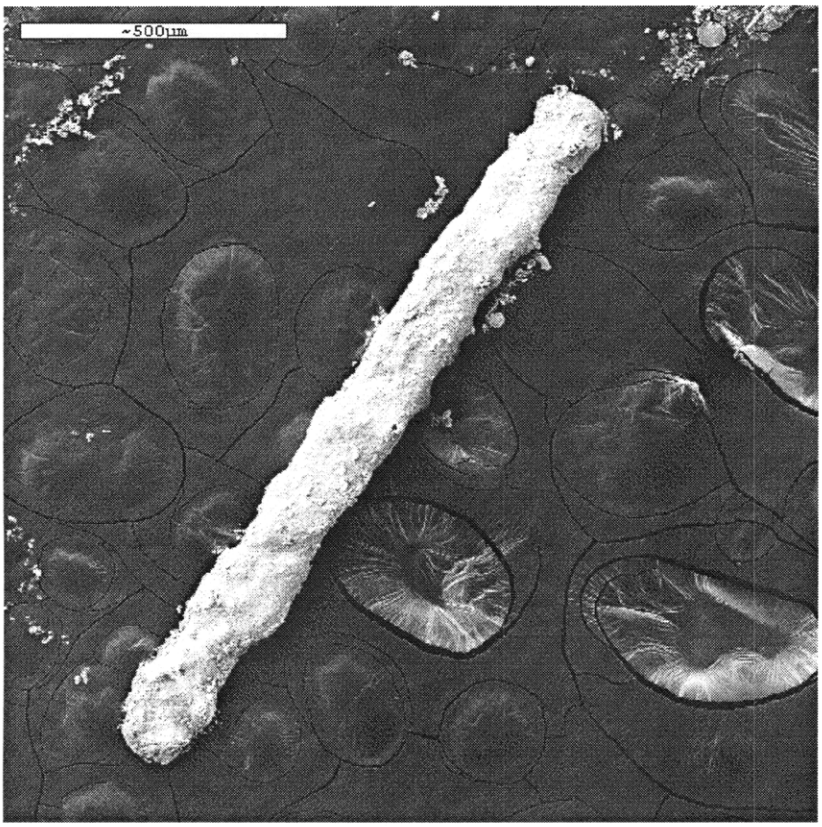

Figure 5.68: SEM of a Line Segment (80 µm spacing, 50 Hz, bottom)

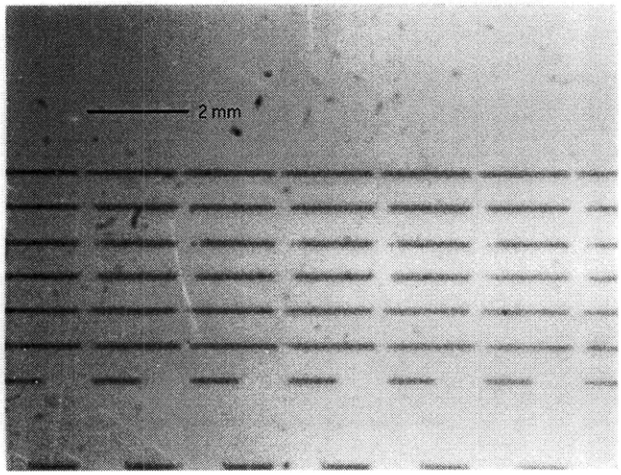

Figure 5.69: Line Segments (80 μm spacing, 1 Hz, 20 passes/line, ink jet transparency)

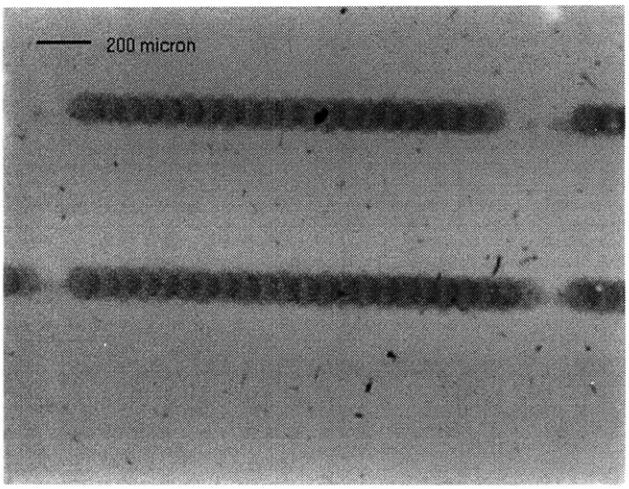

Figure 5.70: Line segments (80 μm spacing, 1 Hz, 20 passes/line, ink jet transparency)

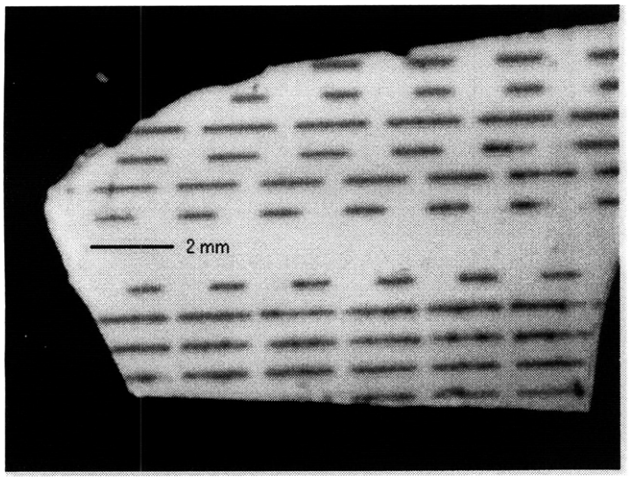

Figure 5.71: Line Segments (80 μm spacing, 1 Hz, 20 passes/line, in powder bed)

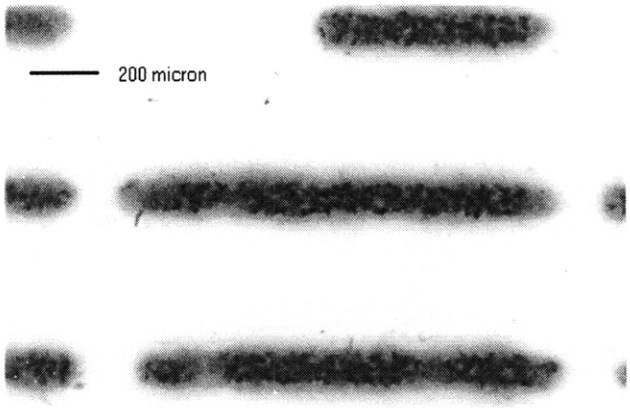

Figure 5.72: Line Segments (80 μm spacing, 1 Hz, 20 passes/line, in powder bed)

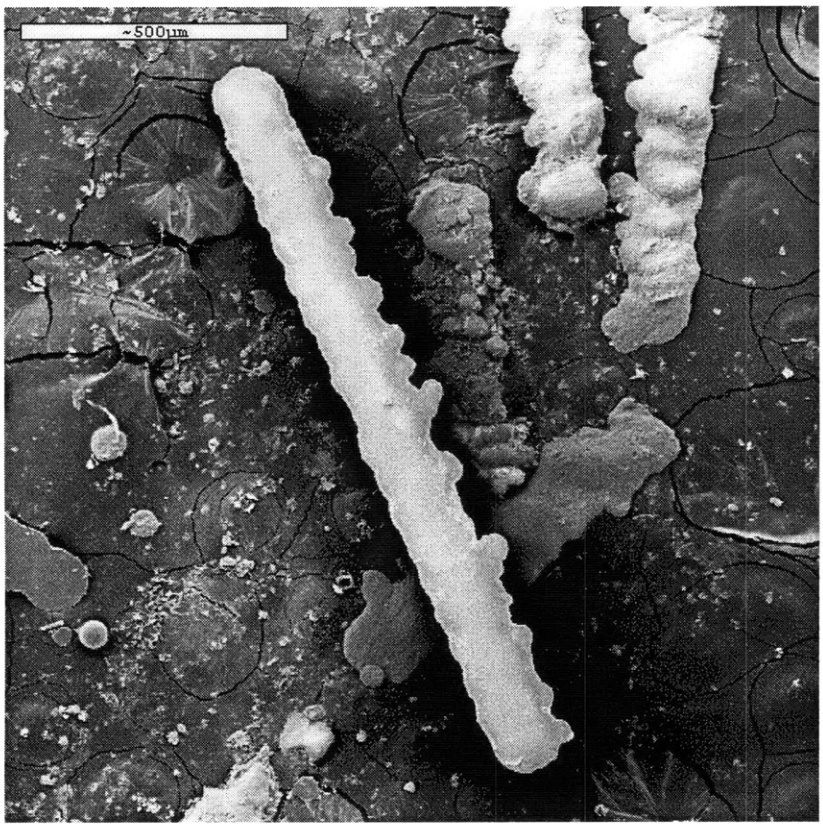

Figure 5.73: SEM of a Line Segment (80 µm spacing, 1 Hz, 20 passes/line, bottom)

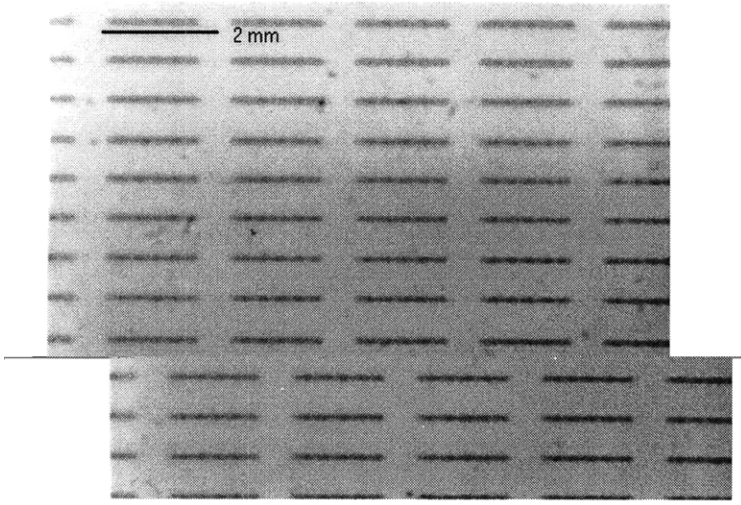

Figure 5.74: Line Segments (80 μm spacing, 1 Hz, 4 passes/line, ink jet transparency)

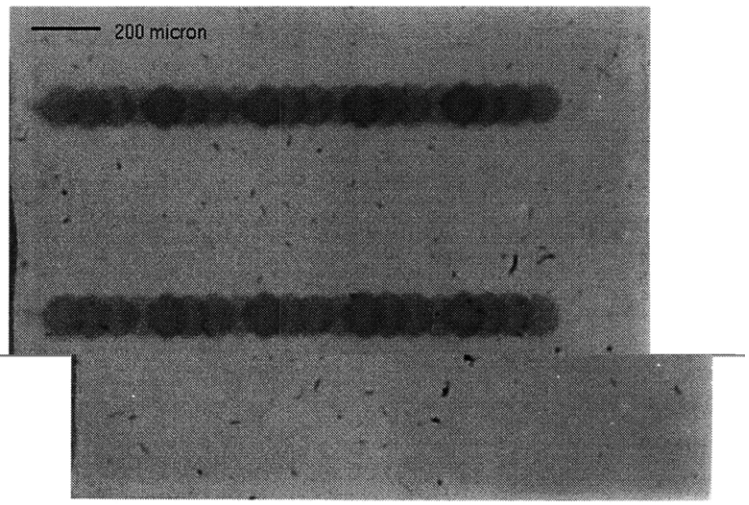

Figure 5.75: Line segments (80 μm spacing, 1 Hz, 4 passes/line, ink jet transparency)

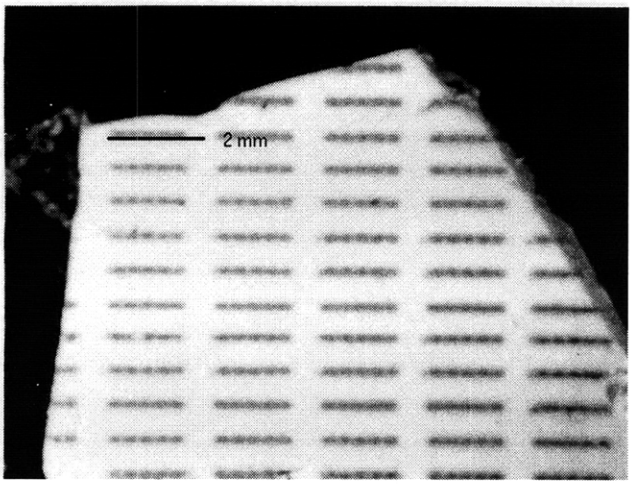

Figure 5.76: Line Segments (80 μm spacing, 1 Hz, 4 passes/line, in powder bed)

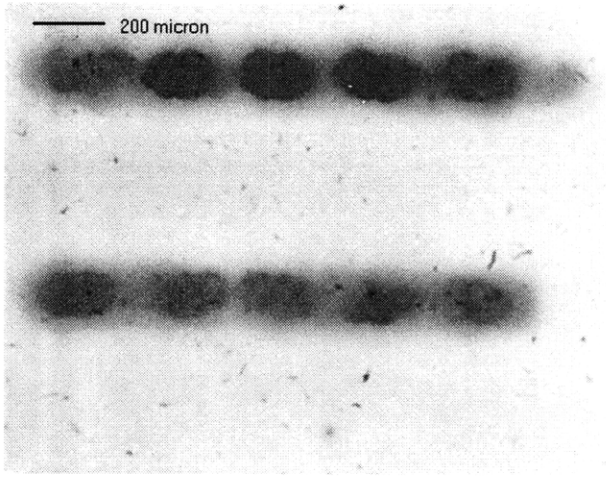

Figure 5.77: Line Segments (80 μm spacing, 1 Hz, 4 passes/line, in powder bed)

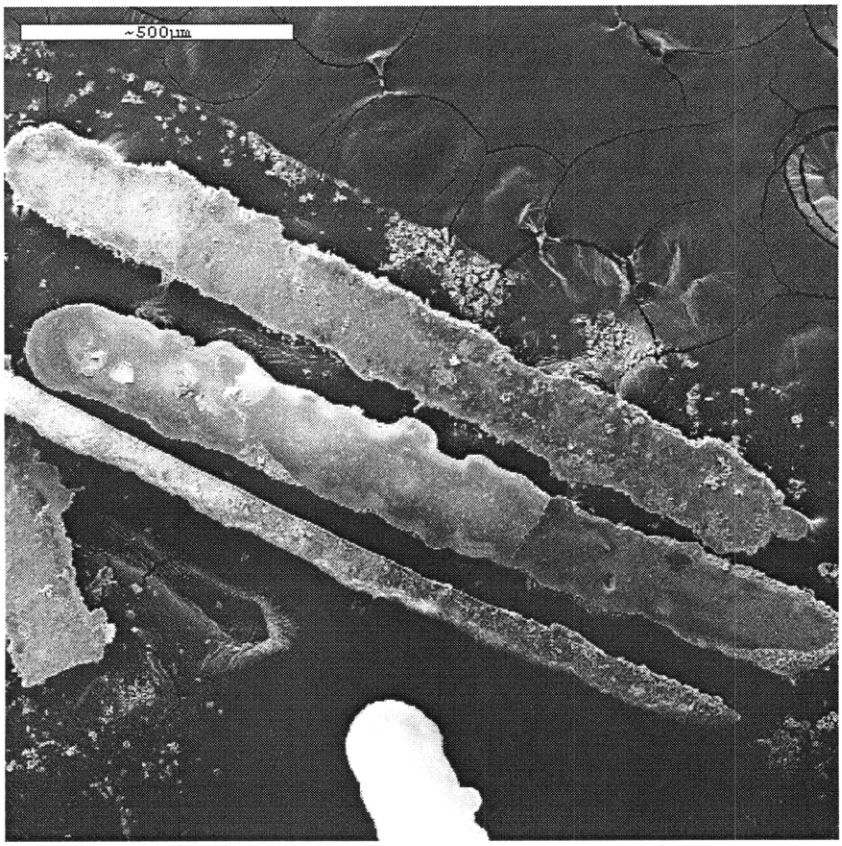

Figure 5.78: SEM of Line Segments (80 µm spacing, 1 Hz, 4 passes/line, top and laterally)

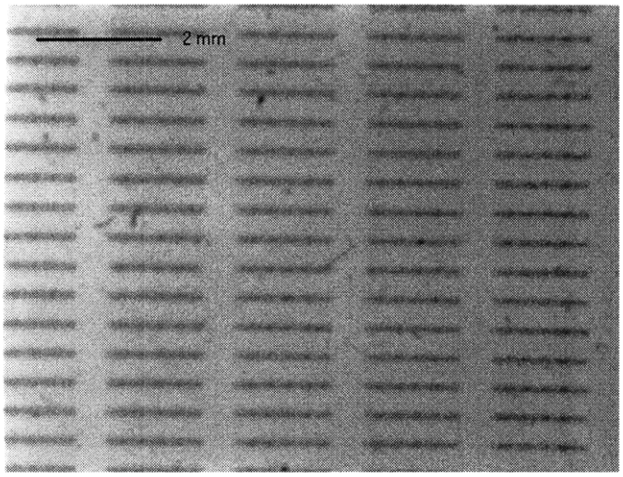

Figure 5.79: Line Segments (80 μm spacing, drying after each pass, 4 passes/line, ink jet transparency)

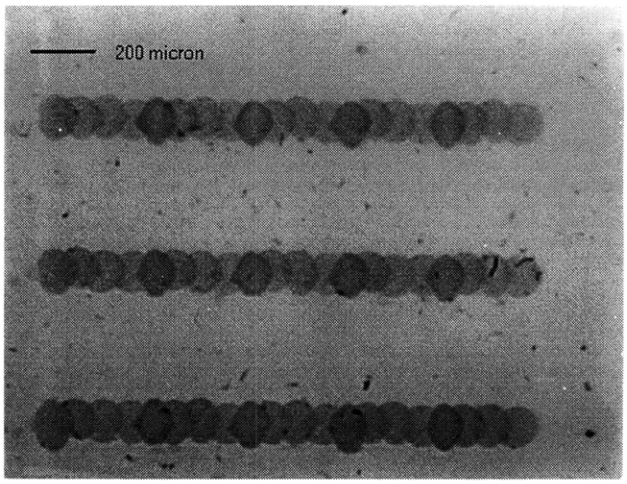

Figure 5.80: Line Segments (80 μm spacing, drying after each pass, 4 passes/line, ink jet transparency)

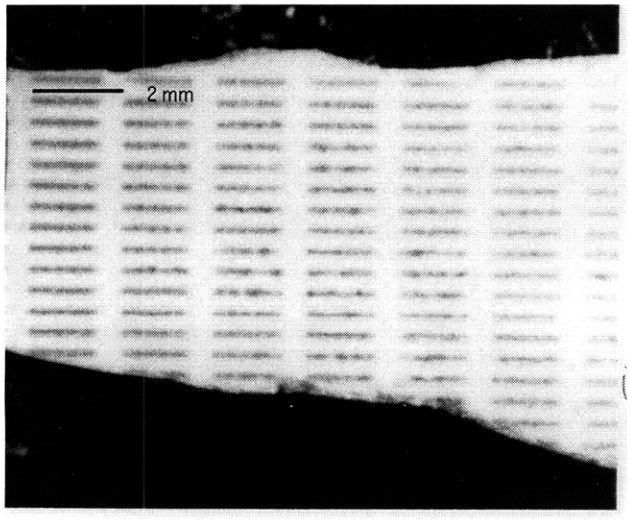

Figure 5.81: Line Segments (80 μm spacing, drying after each pass, 4 passes/line, in powder bed)

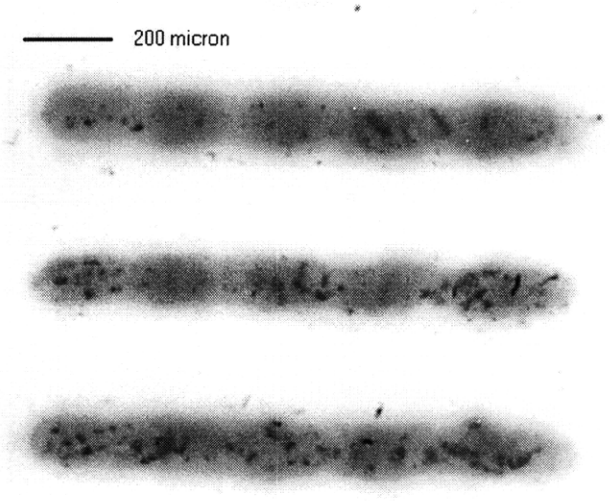

Figure 5.82: Line Segments (80 μm spacing, drying after each pass, 4 passes/line, in powder bed)

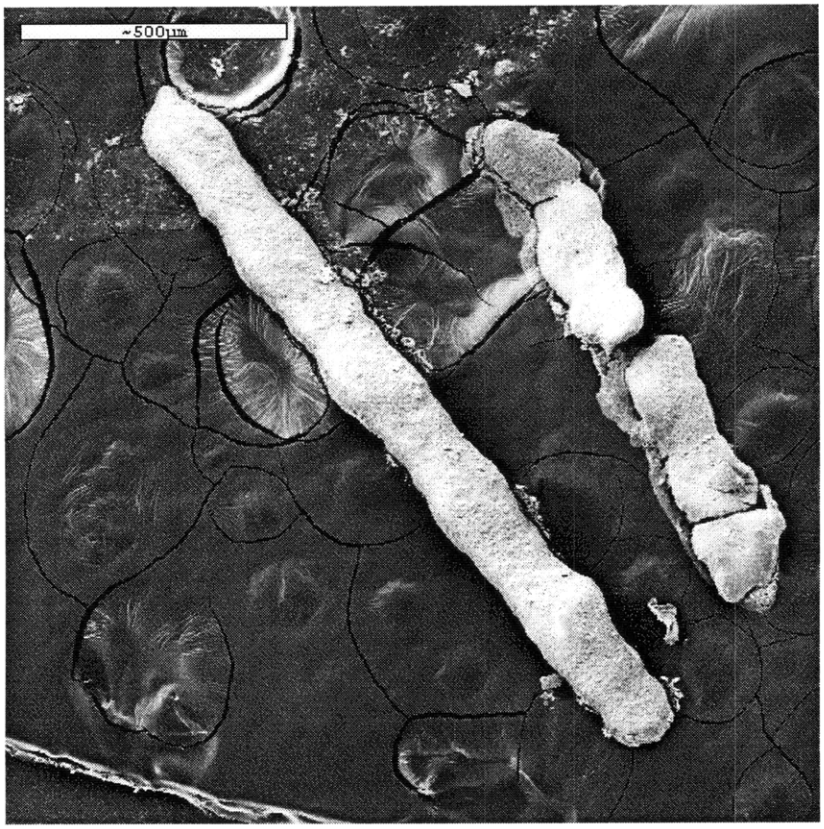

Figure 5.83: SEM of Line Segments (80 µm spacing, drying after each pass, 4 passes/line, bottom)

A number of interesting observations can be made from this collage of pictures. The first thing that can be noticed is the lack of evidence in support of the original hypothesis, which postulated that multiple pass printing, as described previously in the document, would be advantageous for improvements in the surface finish of fine ceramic parts. A brief inspection of SEM pictures shows that the best results in terms of smoothness of line edges are achieved when the entire line is deposited in just one single pass across the powder bed. Probably the best results can be seen in the 500 Hz case where the lines are rather smooth. This is slightly worse in the 50 Hz case where agglomerates can be noticed at the edges. This is due either to insufficient redispersion of the powder bed or satellite droplets.

All the other cases failed to provide the desired smoothness. It seems that each droplet impacts completely separately from the rest and fails to establish a straight edge. This is seen in both the optical micrograph photos and the SEM pictures. The lines that are created when each droplet is printed in a separate pass seem to have no noticeable pattern in roughness of their edges. However, it is clearly seen that there is periodicity in the samples where lines were created by depositing more than one drop per pass. For example, referring to the Figures 5.58, one can discern five separate regions in the line located at the center of the figure. Each of these regions measures about 250 μm in length which is a number derived by multiplying the center-center spacing among droplets (40 μm) by the number of passes per each line (6 passes/line). Clearly, there are some defects occurring at the locations where the smaller six - droplet segments combine into a bigger unit. These results seem to point that the multiple pass printing is not a good candidate for the improvement of the surface finish of fine ceramic parts.

Samples with 80 μm droplet spacing provide similar results, which dispute the hypothesis. However, unlike the 40 μm samples, the single pass specimens do not present a great advantage compared to other print styles. Furthermore, only in Figure 5.83, which shows a line printed at 4 passes/line with drying after each pass, can four separate regions be discerned. They are equally spaced along the line at distances of approximately 300μm, which corresponds to four droplets spaced 80 μm apart.

5.4 Symmetrical Line Segments

Symmetrical print style, as described in Chapter 4, was also investigated by printing 20 wt. % PAA into slipcast alumina powder beds. The results are presented in Figures 5.84 through 5.105.

There were two different spacing among droplets: 50 μm and 100 μm. It was not possible to carry over the droplet spacings of 40 μm and 80 μm that were used in the work with other line segments and droplet pairs. However, 50 μm and 100 μm are sufficient to learn about this print style and compare the results with the rest of the work on line segments. Furthermore, it was possible to print only at the frequency of 1 Hz and with drying between passes. Single pass printing by default is not symmetrical and is not included in this section. The printing variables were as follows:

1) Effective frequency of 1 Hz: v_p = 0.495 m/s, f_p = 225 and 205 Hz for 50 and 100 μm spacing line segments, respectively.
2) Drying after each pass: v_p = 0.2 m/s, f_p = 91 and 83 Hz for 50 and 100 μm spacing line segments, respectively.

The printing of 50 μm samples, regardless of the frequency, was done by first depositing droplets at the locations of 0 μm, 200 μm, 400 μm... The next pass prints drops at 100 μm, 300 μm, 500 μm... The third one is at 50 μm, 250 μm, 450 μm..., and the final one is at 150 μm, 350 μm, 550 μm... The only problem with this setting was the inability to take SEM pictures of the 50 μm line at 1 Hz because the specimens disintegrated during redispersion.

Samples with 100 μm droplet spacing required only two passes: the first one at 0, 200, 400... and the second one at 100, 300, 500...

The results are very encouraging and show lines of better finish than any other multiple print styles, regardless of the frequency or droplet spacing. Even the single pass print styles, which produced the best results, in the previous section do not have a uniform width, rather the starting end is thicker than the rest of the line. That is not the case in symmetrical printing where an entire line segment has the same width.

100 μm spacing seems to work better than the smaller spacing, which produces lines of certain unevenness as shown in Figure 5.92. The lines with the bigger spacing are

rather straight especially when the frequency is 1 Hz (Figure 5.98). Moreover, there are no or very little defects in the regions where the smaller pieces combine into a bigger feature, a problem that appears persistently in multiple pass printing.

Overall, symmetrical printing appears to be much better than single pass printing and multiple pass printing, and merits further work.

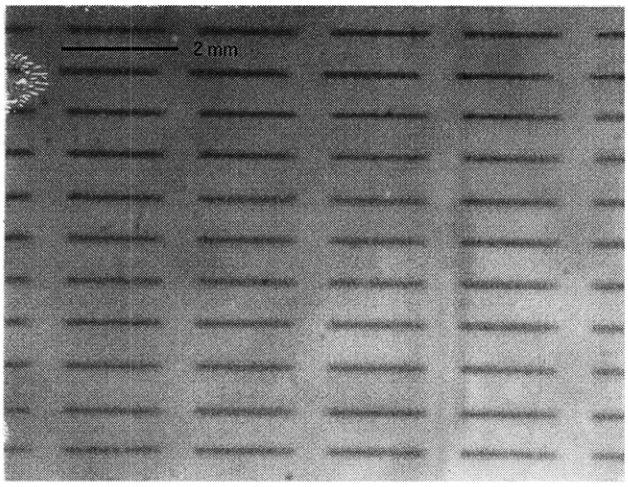

Figure 5.84: Line Segments (50 μm spacing, 1Hz, 4 passes/line, ink jet transparency)

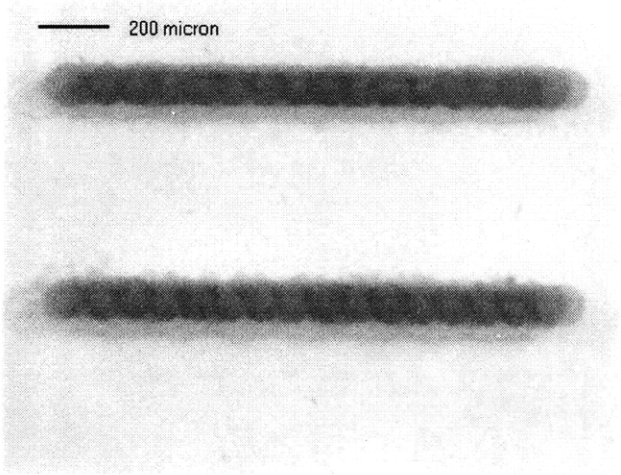

Figure 5.85: Line Segments (50 μm spacing, 4 passes/line, 1 Hz, ink jet transparency)

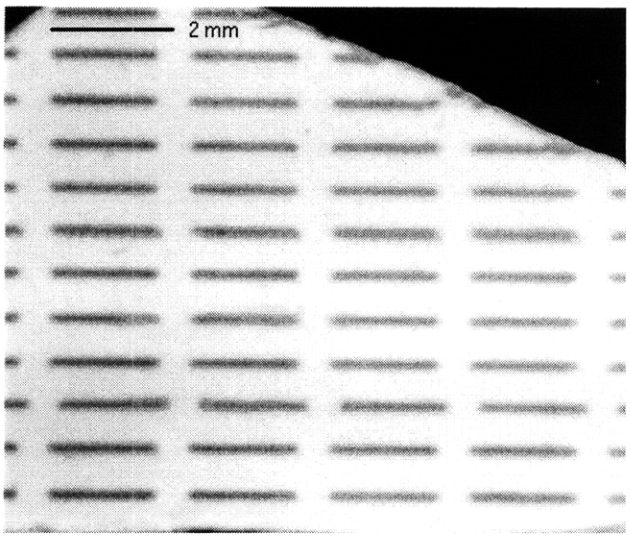

Figure 5.86: Line Segments (50 μm spacing, 1 Hz, 4 passes/line, in powder bed)

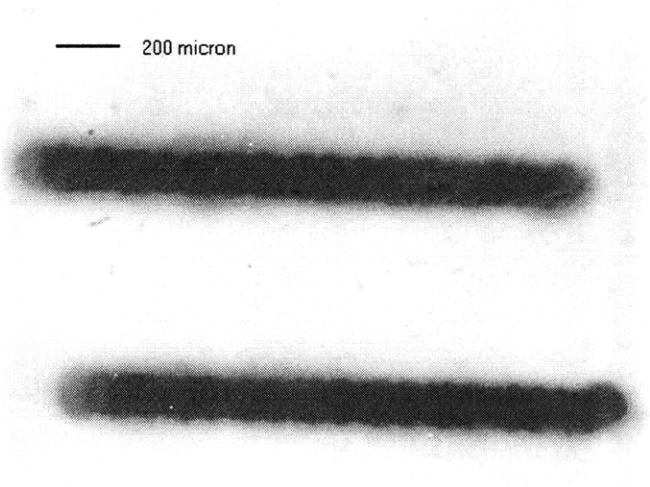

Figure 5.87: Line Segments (50 μm spacing, 4 passes/line, 1 Hz, in powder bed)

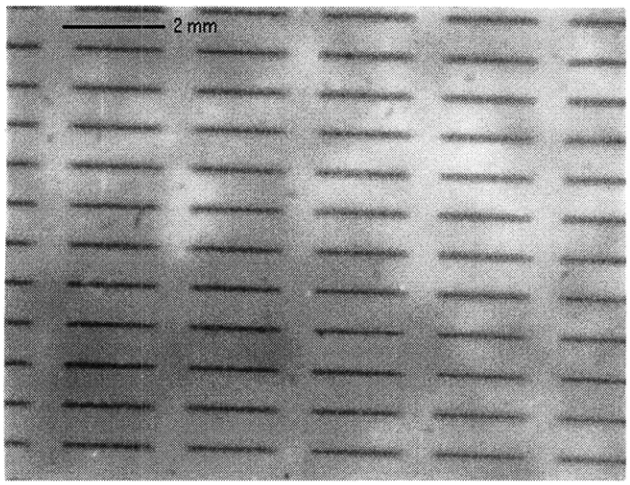

Figure 5.88: Line Segments (50 μm spacing, dry after each pass, 4 passes/line, ink jet transparency)

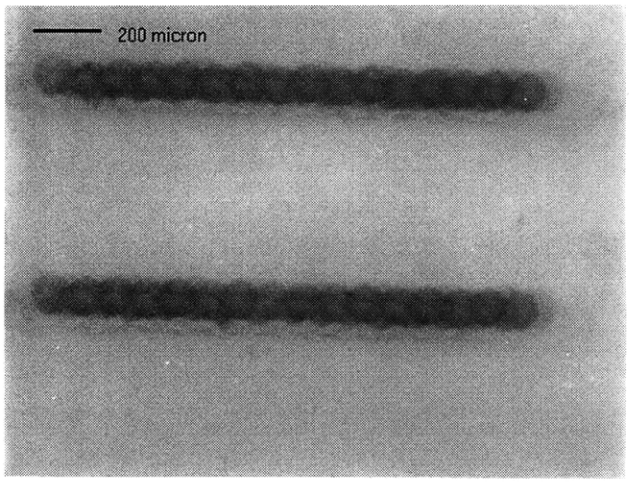

Figure 5.89: Line Segments (50 μm spacing, dry after each pass, 4 passes/line, ink jet transparency)

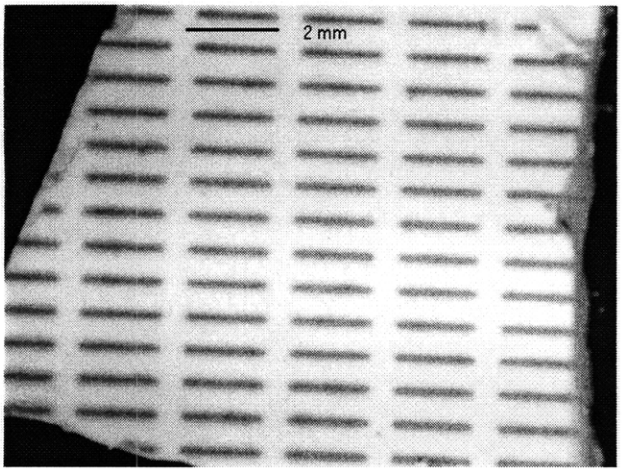

Figure 5.90: Line Segments (50 μm spacing, dry after each pass, 4 passes/line, in powder bed)

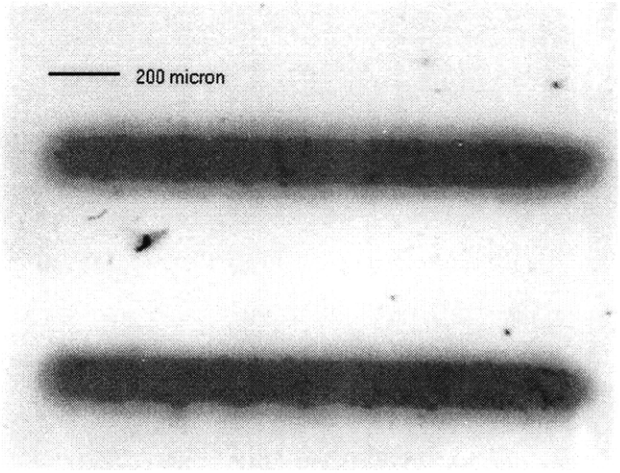

Figure 5.91: Line Segments (50 μm spacing, dry after each pass, 4 passes/line, in powder bed)

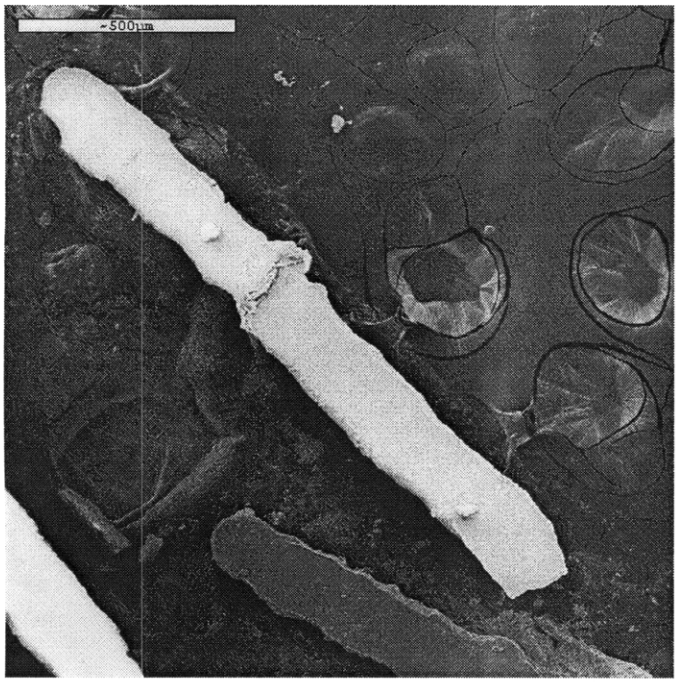

Figure 5.92: SEM of Line Segments (50 µm spacing, dry after each pass, 4 passes/line, top)

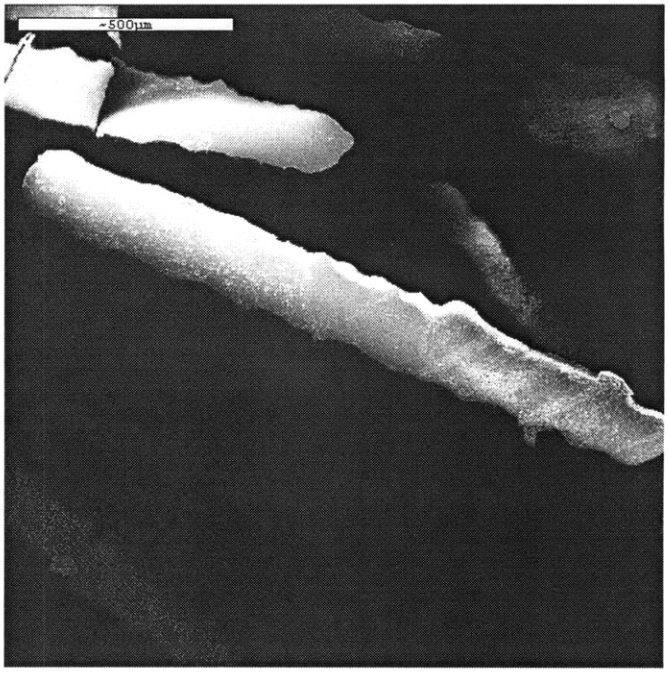

Figure 5.93: SEM of Line Segments (50 µm spacing, dry after each pass, 4 passes/line, top)

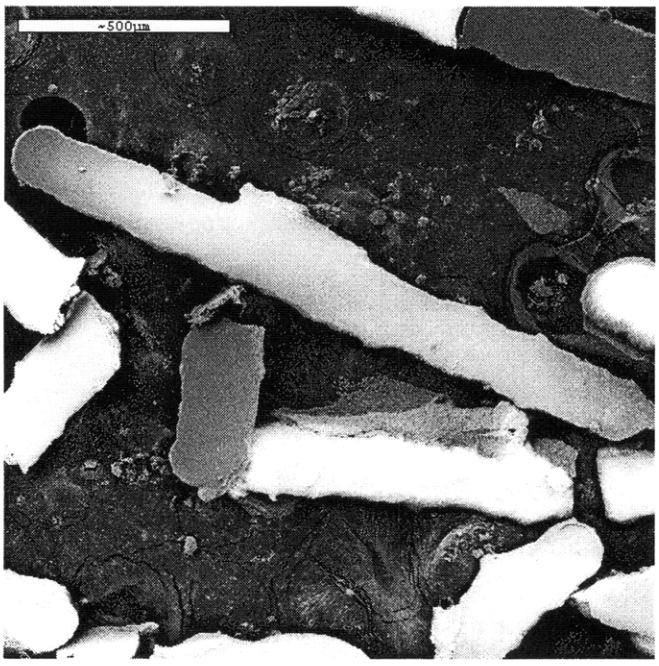

Figure 5.94: SEM of Line Segments (50 µm spacing, dry after each pass, 4 passes/line, top)

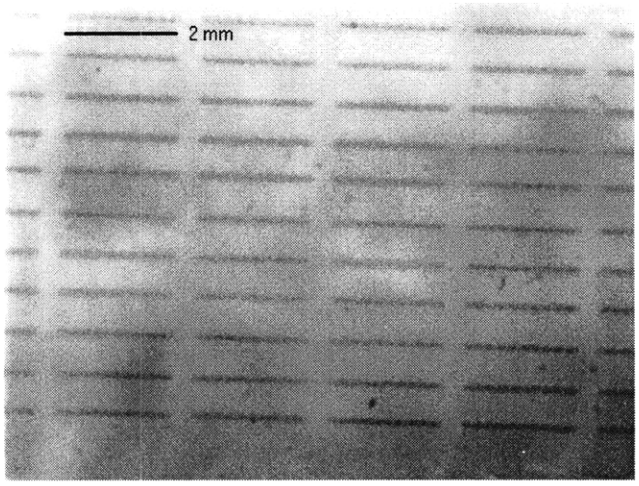

Figure 5.95: Line Segments (100 μm spacing, 1 Hz, 2 passes/line, ink jet transparency)

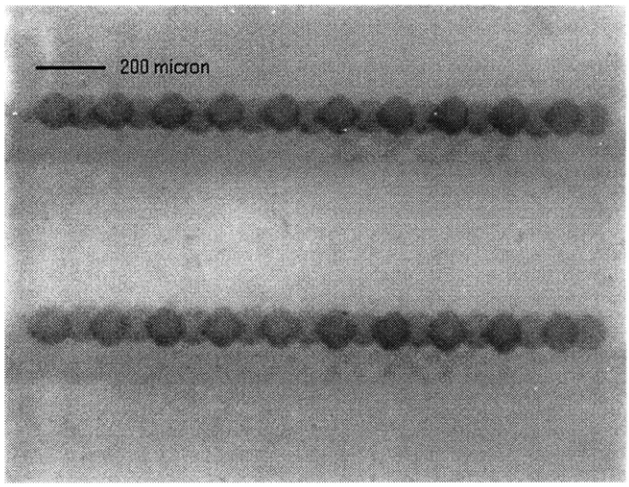

Figure 5.96: Line Segments (100 μm spacing, 1 Hz, 2 passes/line, ink jet transparency)

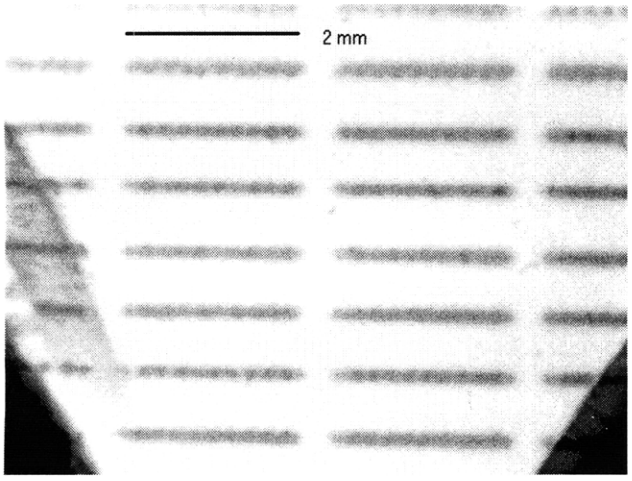

Figure 5.97: Line Segments (100 μm spacing, 1 Hz, 2 passes/line, in powder bed)

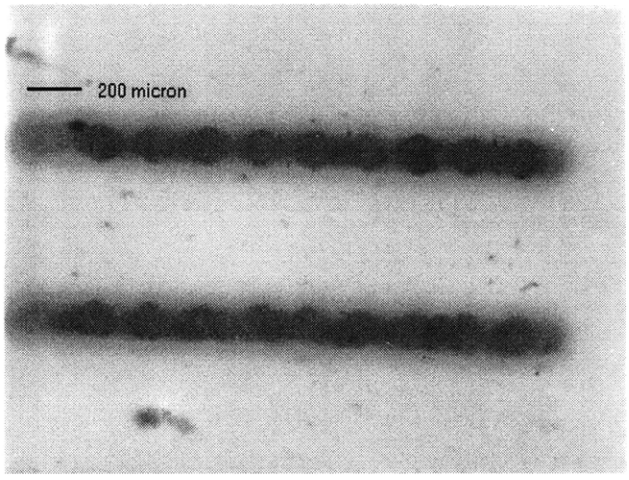

Figure 5.98: Line Segments (100 μm spacing, 1 Hz, 2 passes/line, in powder bed)

Figure 5.99: SEM of a Line Segment (100 µm spacing, 1 Hz, 2 passes/line, bottom)

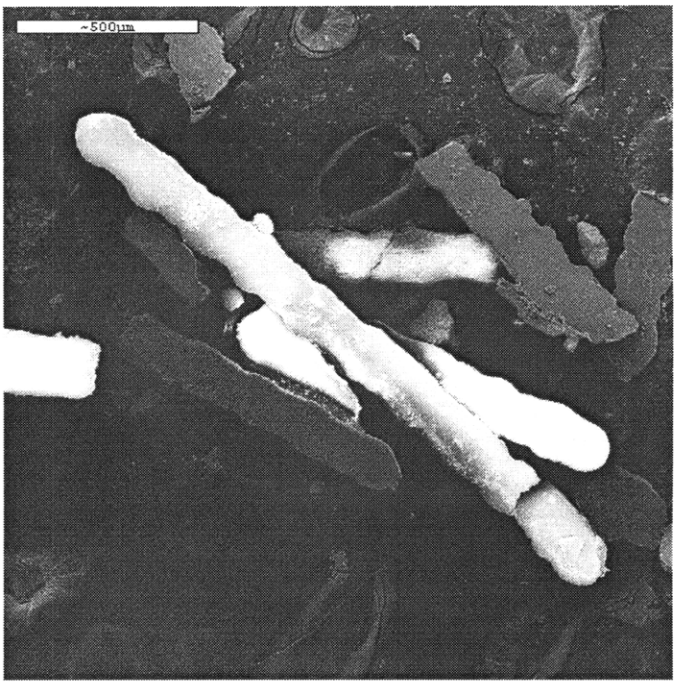

Figure 5.100: SEM of a Line Segment (100 µm spacing, 1 Hz, 2 passes/line, top)

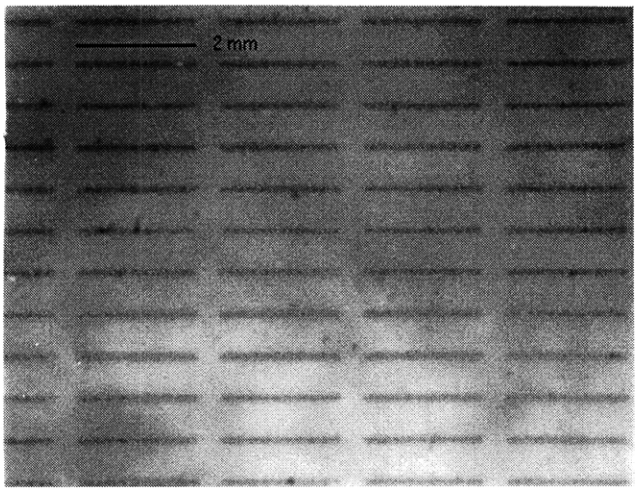

Figure 5.101: Line Segments (100 μm spacing, dry after each pass, 2 passes/line, ink jet transparency)

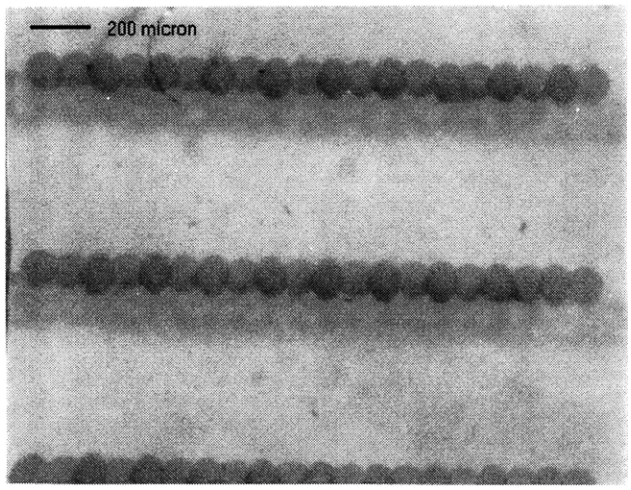

Figure 5.102: Line Segments (100 μm spacing, dry after each pass, 2 passes/line, ink jet transparency)

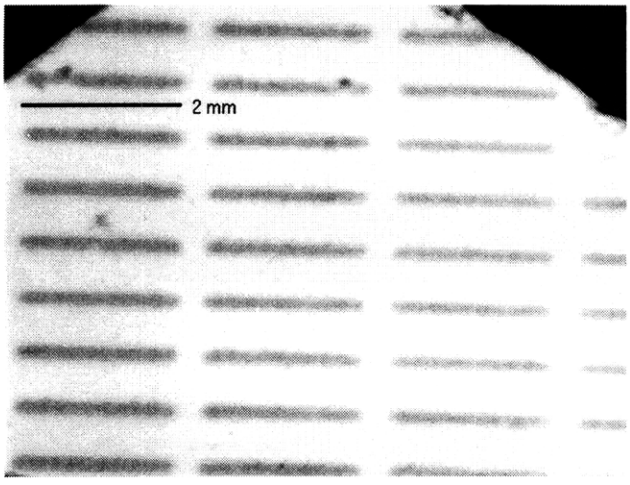

Figure 5.103: Line Segments (100 μm spacing, dry after each pass, 2 passes/line, in powder bed)

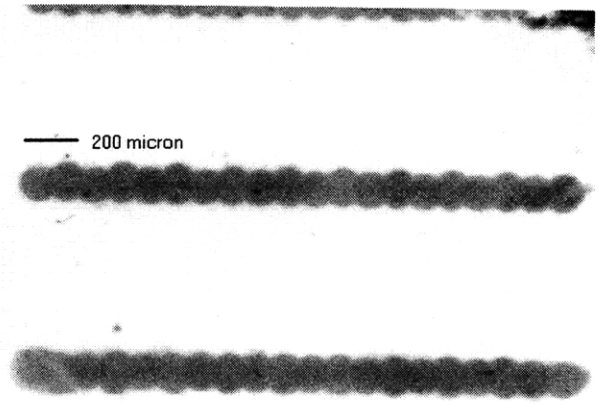

Figure 5.104: Line Segments (100 μm spacing, dry after each pass. 2 passes/line, in powder bed)

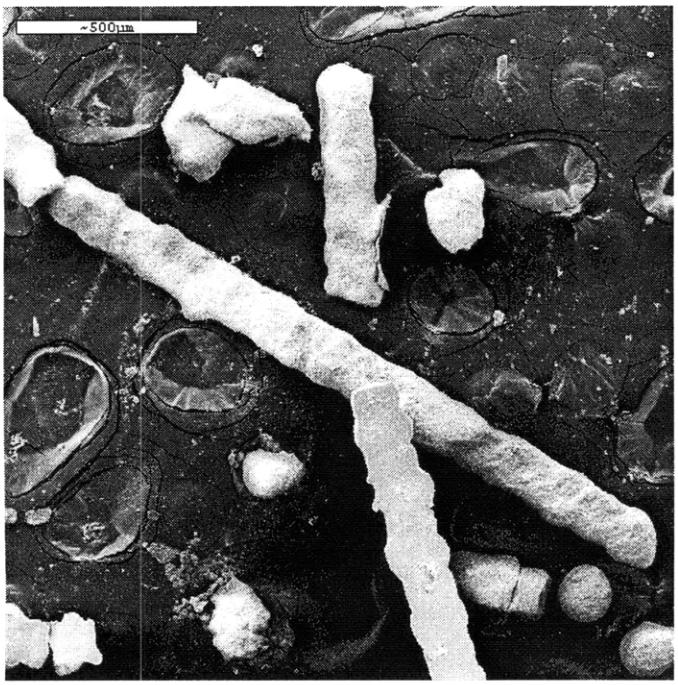

Figure 5.105: SEM of a Line Segment (100 µm spacing, dry after each pass, 2 passes/line, bottom)

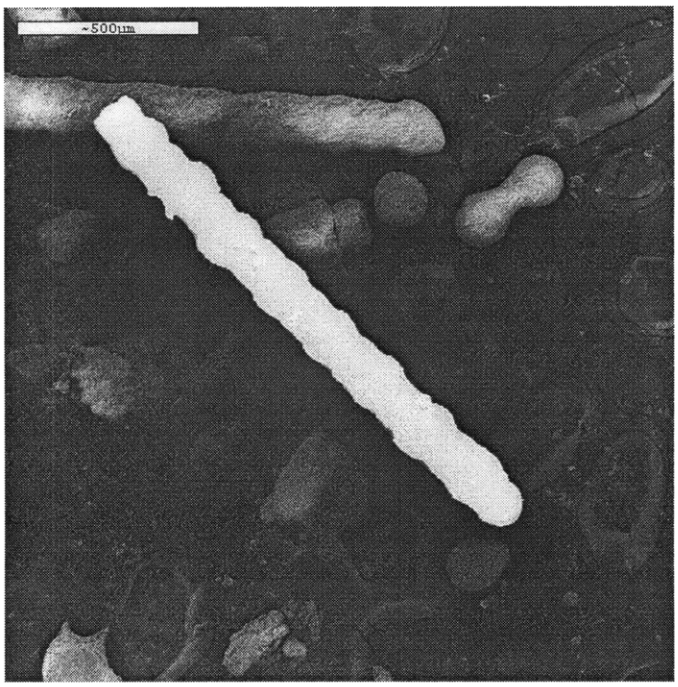

Figure 5.106: SEM of a Line Segment (100 µm spacing, dry after each pass, 2 passes/line, top)

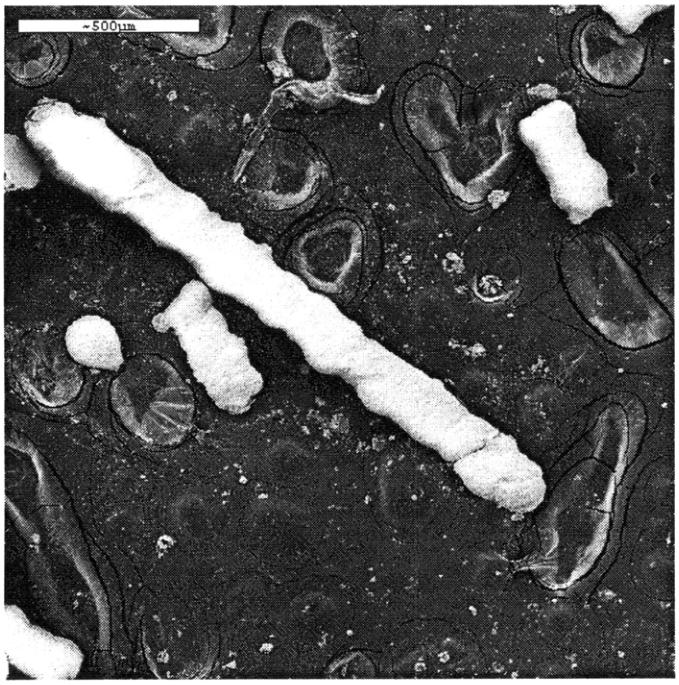

Figure 5.107: SEM of a Line Segment (100 µm spacing, dry after each pass, 2 passes/line, bottom)

5.5 Effect of Print Style on Line Width

The study of line segments has shown that print styles influence the quality of lines. Moreover, it is clear from the optical micrographs and SEM pictures that different print styles produce lines with markedly different line widths.

To explore the effect of different print styles on the line width, single continuous lines were printed using HP DOD printhead under a variety of conditions. The binder was 10 wt. % PAA with amaranth, and substrates were slipcast powder beds made out of 35 v/o HPA Ceralox 1.0 μm alumina powder slurry. Lines were printed with just a single pass in each line at different frequencies (40, 2500, and 5000 Hz) and with multiple pass printing (40 and 833 Hz). The results are presented in Figure 5.108.

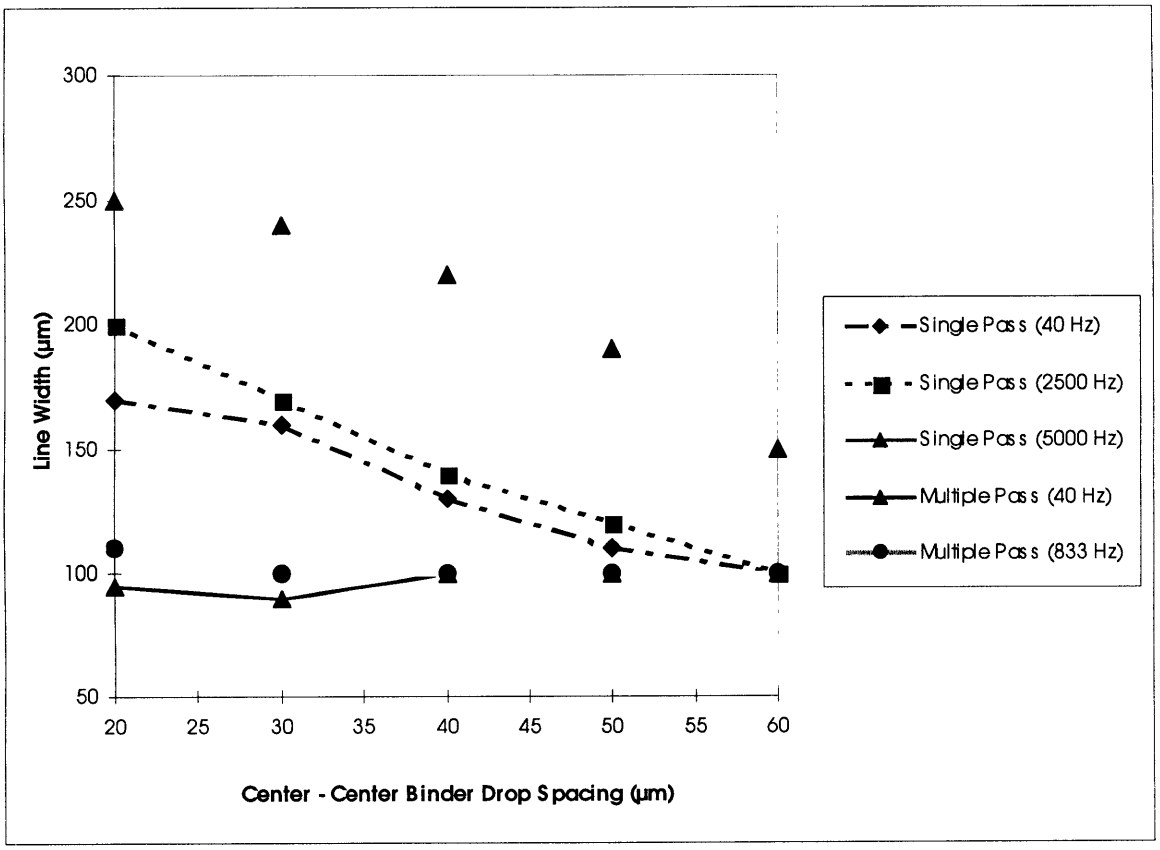

Figure 5.108: Line Width in powder bed vs. Center – Center Binder Drop Spacing for different print styles

The study shows that the higher the frequency at which a line is printed, the wider the impact area of the drop, and consequently the line, is going to be. Single pass lines start off with different line widths for a given center – center spacing, but the widths converge as the spacing increases and the effective binder dose decreases.

Multiple pass lines do not change in width very much but stay somewhere around 100 – 110 μm. That figure is also the point of convergence for single pass lines, with the exception of 5000 Hz lines which also converge but not a strongly. It can be assumed that this is the impact area of a single DOD droplet.

[Arthur] studied the dependence of line width upon the binder dose. Arthur used continuous jet printhead printing 10 wt. % PAA binder into slipcast powder beds. The comparison of continuous jet results vs. DOD results is presented in Figure 5.109.

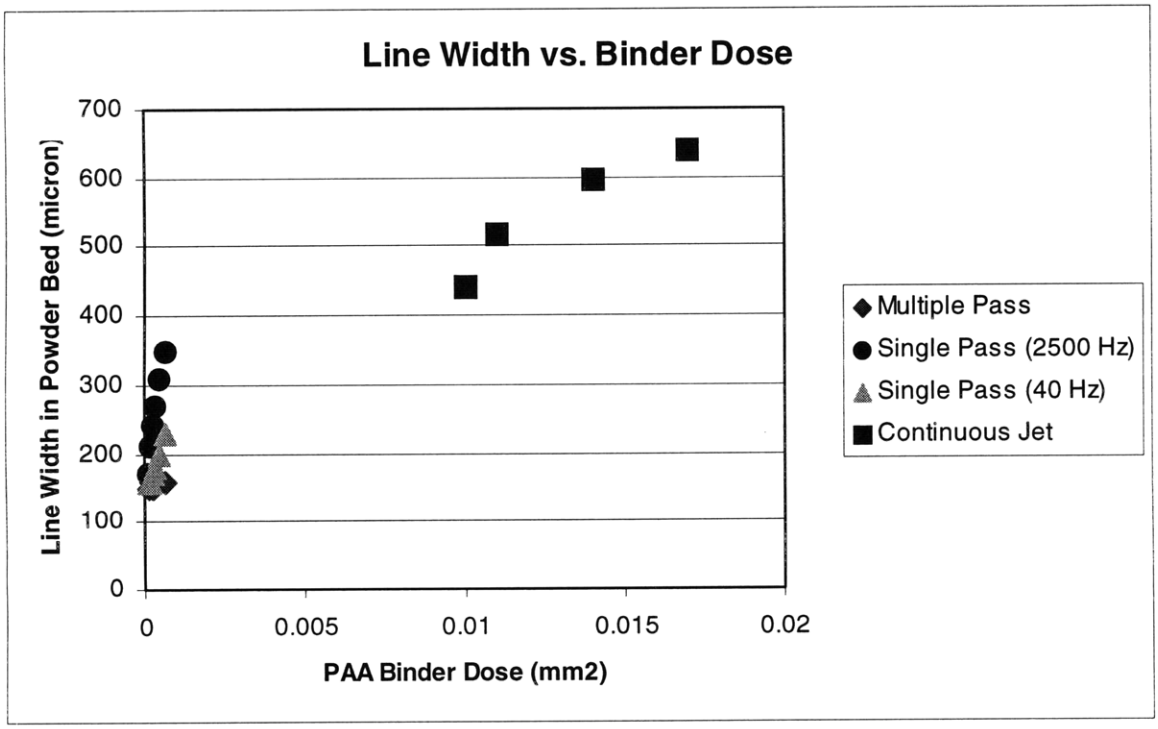

Figure 5.109: Line Width in Powder Bed vs. Binder Dose

Chapter 6: Conclusions and Future Work

6.1 Introduction

The interaction of droplets with powder is the key set of phenomena that determine many aspects of Three Dimensional Printing (3DP) including dimensional control and surface finish of the printed part. In the creation of structural ceramic parts by 3D printing, fine powders on the order of 1 μm in size must be used. Such small size powders enable production of parts with high green density. These powders can not be spread by using a counter – rotating rod, which is a standard form of spreading new layers of a powder bed in 3DP. They have to be deposited as slurry and then dried to form a fairly hard cohesive powder bed, either through slipcasting or tapecasting.

The purpose of this work was to understand the interaction of binder droplets with such cohesive powder beds, the integration of droplets with previously printed droplets, and to explore print styles which improve the dimensional control and surface finish.

6.2 Summary of Results

The binder used in this study was aqueous PAA solution with a molecular weight of 5000. PAA was used as 10 and 20 wt. % solution in water. A red dye, amaranth, was also added to the binder so that printed features could be visualized. The binder was deposited via Drop – on – demand (DOD) printhead. The advantages of this approach were smaller droplets as compared with the continuous jet printing, usability over a wide range of frequencies, and the possibility of easy interfacing with the existing hardware on the Alpha Machine for study of different print styles.

Evaluation of print styles and other printing variables was done by printing a variety of features: single primitives created by the impact of a single drop of binder into a powder bed, pairs of droplets for study of different time domains, and line segments.

Single drop primitives were printed and removed from the slipcast powder bed. They were found to resemble discs with a flat top and a rounded bottom with a typical diameter of 180 μm and a thickness of 40 μm. It was not possible to redisperse tapecast

powder bed and remove the primitives. However, when observed in the powder bed, they were larger in diameter, about 170 μm, than primitives in slipcast powder beds whose diameter was 140 μm.

A number of different time domains are defined based on the interaction of droplets with cohesive powder beds. Critical times in defining these domains are: 1) the amount of time it takes for a droplet to splat and spread on the powder bed, 2) the amount of time it takes for the droplet to absorb into a powder bed, and 3) the amount of time it takes for an absorbed droplet to dry. Although it was not possible to directly measure these times, the experiments were designed based on simple assumptions. Based on these time domains, doublets composed of two printhead droplets spaced 40 and 80 μm apart were printed at different interarrival times. At short interarrival times, the doublet appeared to be roughly equivalent to a single drop primitive but slightly larger. As the interarrival time increased the doublet became increasingly oblong. This trend was particularly evident in the 40 μm droplet pairs. 80 μm pairs also exhibited similar behavior but it was not so pronounced due to the larger droplet spacing.

When printing continuous line segments high rate printing requires that droplets be placed as rapidly as possible. Line segments with varying drop deposition styles were investigated. In one style, droplets are deposited one after the other at high rate such that droplets are arriving before the previous droplets are absorbed into the powder bed. Such line segments show evidence of binder rearrangement due to capillary effects on the surface of the powder bed.

Two fundamental alternative styles were investigated where droplets are printed far enough apart that they interact with the powder bed and not with liquid on the surface of the powder bed. The basics of the first approach consisted of printing a line by depositing a drop of binder in the first pass and offsetting the subsequent passes by a certain amount. All the lines created with this print style, including all of its variations, fail to achieve the desired results and show periodicity in the regions where different regions of binder are joined together. In the more successful of these styles, so called symmetrical printing, a line segment is created in either 2 or 4 passes of the printhead depending on the final droplet spacing, and droplets are always deposited in a symmetrical configuration with respect to previously deposited droplets. For example, in

a first pass, droplets are deposited 200 microns apart and in a second pass droplets are once again deposited 200 microns apart but at a position intermediate to the droplets deposited on the previous pass. Such line segments showed straighter edges and narrower widths than those printed with single pass high frequency printing.

6.3 Recommendations for Future Work

This study focused on printing basic building blocks of 3DP parts in one dimension. The natural extension of the work would be to continue the work in 2D and 3D. The next step would be to study how lines of binder printed via different print styles interact with each other, what is the surface finish of these structures, and what kind of defects, if any, are present in regions where the binder is stitched together. This can be easily accomplished by printing a single layer of binder into an alumina powder bed.

The study of different print styles can be carried still further into 3D by printing simple parts which would be designed to answer simple question such as is it possible to reduce stair-stepping effect etc.

On the other hand, still more work should be done to continue droplet pair work and enhance the understanding of binder – powder interaction. This will be tremendously facilitated by use of Droplet Observation Station, which could allow one to directly observe the formation of 3DP features as they are being printed.

BIBLIOGRAPHY

Arthur, Tara L. Factors Limiting the Surface Finish of Three Dimensional Printed Parts, MS Thesis, MIT, June 1996.

Baker, Jr. Peter Three Dimensional Printing with Fine Metal Powders, MS Thesis, MIT, June 1997.

Caradonna, Michael Anthony The Fabrication of High Packing Density Ceramic Powder Beds for the Three Dimensional Printing Process, MS Thesis, MIT, June 1997.

Khanuja, Satbir Singh Origin and Control of Anisotropy in Three Dimensional Printing of Structural Ceramics, Ph.D. Thesis, MIT, February 1996.

Fan, Tailin Droplet – Powder Impact Interaction in Three Dimensional Printing, Ph.D. Thesis, MIT, September 1995.

MIT Alpha Machine Electronics – Documentation

Barnes, H., Holbrook, S. (1993) High Concentration suspensions: preparation and properties. In P. Shamlou (Ed.), Processing of Solid-Liquid Suspensions (pp. 231-245). London: Butterworth-Heinemann Ltd.

Appendix A: Epson DOD Printhead

A.1 Introduction

Unlike Hewlett Packard DeskJet line of printers, the kind that was used in this research, where the printhead works on the principle of thermal ejection of droplets through the nozzle, Epson Stylus line of printers has a printhead where a piezo electric element (PZT) causes a droplet to be discharged. This is a potentially much better printhead for 3D printing because it is no longer required to pay much attention to the thermal properties of the binder. Some binder can not be used with the HP DOD printhead because they are either volatile or they leave a residue in the chamber after the discharge.

Furthermore, the droplet velocity should be lower in piezo jets than in bubble jets, 8 m/s and 10 m/s, respectively. The lower velocity might be very helpful in reducing splashing [Baker].

Epson Color Stylus 400, a color printer, was the printer used in this research for testing the usefulness of PZT based jets (Figure A.1). The droplet is printed when the print signal from the main board is sent to the driver board and then to printhead unit and to the PZT. The PZT pushes the ink – containing cavity, which discharges the ink from the nozzle in the nozzle plate (Figure A.2).

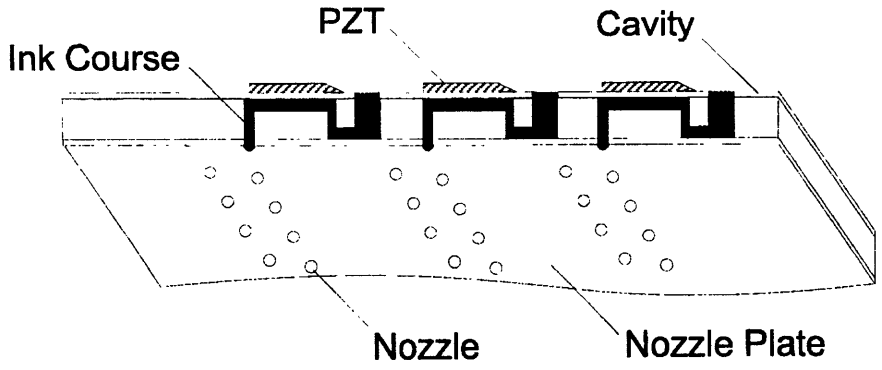

Figure A.1: Printhead in Normal State

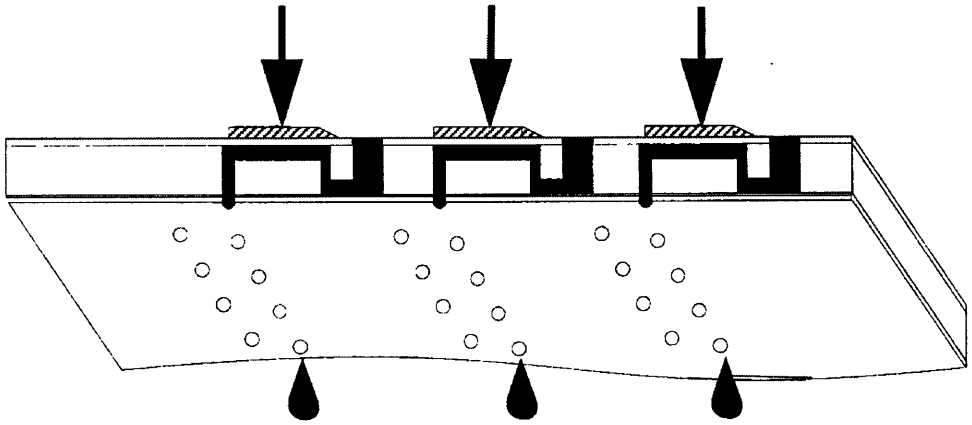

Figure A.2: Printhead in Ejecting State

A.2 Driving the printhead

The printhead of the Epson Color Stylus 400 printer contains black and color (Cyan, Magenta, Yellow or CMY) nozzles operating at the head drive frequency of 14.4 kHz (Figure A.3). There are 64 black nozzles placed in a staggered configuration of 32 nozzles in 2 columns. The distance among nozzles in one column is 90 dpi. The other column is offset vertically with respect to the first one by 180 dpi. Therefore, this effectively gives 64 nozzles where the nozzle – nozzle spacing is 180 dpi. Other colors (CMY) each have 21 nozzles configured in such a way that each color has its own column. The nozzles are separated by 90 dpi within a column. The overall resolution of the printer is 720 * 720 DPI, which translates into the spacing of 35 μm.

HP DOD nozzles were directly accessible, and feeding the signal of correct amplitude and frequency to the printhead could fire droplets. This is not possible with the Epson printhead because the printer contains analog and digital circuits that interpret the signals and fire a combination of nozzles correspondingly. It was deemed that an attempt to decipher the signals and build the circuits for droplet discharge was not effective.

An alternative approach required the use of Corel PHOTO – PAINT! 4.0 software package (Corel Corporation). The software can be used to create black and white images that will be reproduced on paper. If the black ink cartridge is filled with a binder such as

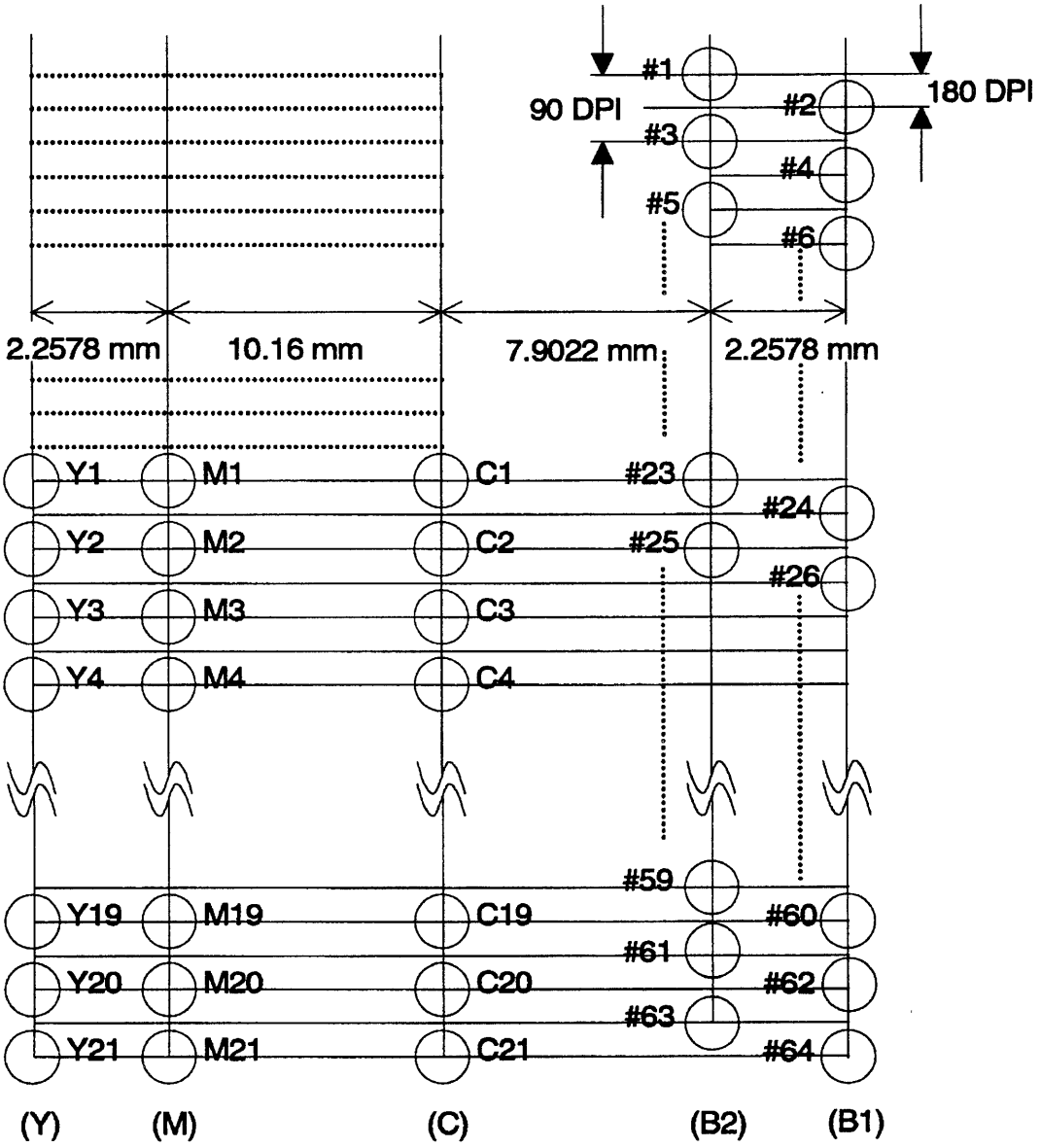

Figure A.3: Nozzle Arrangement

PAA and a ceramics powder bed used instead of paper as a printing medium, then it is possible to create simple features such as lines and analyze them.

Corel PHOTO – PAINT! allows a user to create a black and white images and specify their resolution. The Zoom feature at the setting of 1600% enables the user to draw the image pixel by pixel at the time with the hope that during printing each of these

pixels will be translated into a fired binder droplet. The Epson printer is programmed in such a way that in the 720 * 720 DPI mode one ink drop is fired for each pixel, while in the 360 * 360 DPI mode it prints 2 ink droplets per each pixel, so called "dual firing". The latter is not very practical for two reasons: it creates larger primitives, which translates into less detailed texture and their shape are not circular but vary, which indicates that a great deal of splashing is present.

However, the printhead is not perfect and each color pixel does not become an ink droplet. Moreover, sometimes 2 drops are fired per pixel. Therefore it was crucial to determine what kind of an image pattern would translate accurately into the printed image. Grids of pixels of different spacing were printed (Figure A.4). Grids of different spacing were printed: both A and B were varied from 2 to 4 for a total of nine different combination. It was ascertained that the most accurate setting was A = 3 and B = 2 where about 97% of pixels were correctly represented on the paper.

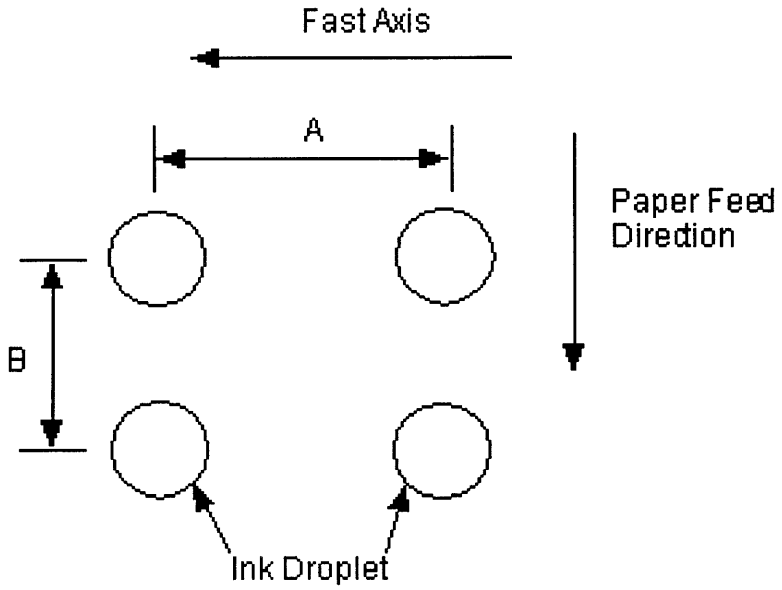

Figure A.4: Grid Pattern

Figure A.5 shows the optimal pattern (A=3, B=2) printed on the Epson printer with the black ink on the high quality ink – jet paper. The picture clearly shows that the droplet alignment is not perfect and there is some waviness in the lines.

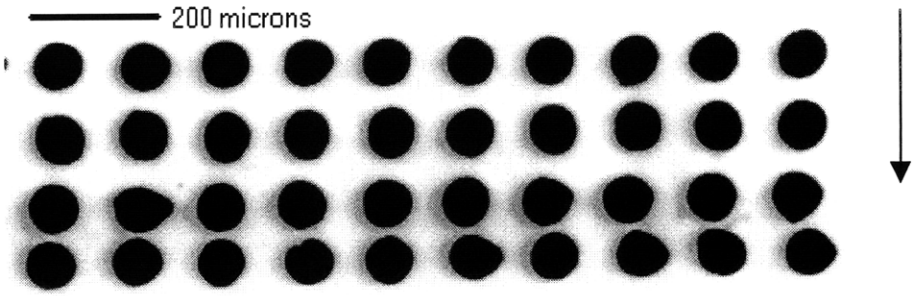

Figure A.5: Epson optimal pattern

A.3 Measurement of the droplet size

Binder dose is one of the variables that have a tremendous impact on the surface finish of 3DP parts. Too much of it causes binder bleeding, while a too low binder dose produces a green part whose strength is insufficient for post – processing steps. Binder dose is determined in the file preparation by adjusting the printhead frequency and the droplet spacing. Therefore, it is important to determine the droplet size discharged by a jet.

The droplet size of the Epson printhead could not be found in the literature so it had to be measured experimentally. The measurement was done with the original Epson black ink. The method is described below:

1) A small ceramic or glass container is carefully weighed before and after adding a known volume of the black ink. The liquid is left to evaporate by heating it gently overnight at the temperature of 50°C. When all of the liquid is evaporated, the container is weighed again. The difference between the final and starting mass determines the ink solid content.

   1.28 mL of the black ink was placed into a glass container. After evaporation in a heat oven, the solid content of the ink was measured to be 0.26542gm or 0.206gm/mL.

   The experiment required the use of a Mettler AT20 balance whose resolution is 10 micrograms.

2) A black and white image is created in Corel software at the resolution of 720 DPI. The image is a grid whose size is 2.75" * 2.75" with the optimum spacing as described in the previous section. The image is constructed in such a way that a total number of black pixels is well known, about 307,000 pixels.

   This image is printed dozens of times by Epson on a high quality ink jet paper, whose mass is carefully recorded before the printing. The high number of printing repetitions is required so that appreciable ink mass can be deposited on paper. The mass of the paper is recorded again after the ink dries. The difference in the mass of paper gives the ink solid content for a known number of drops, within some margin of error as reported in the previous section.

   The paper weighed 11.03473gm prior to the printing and 11.14385gm after printing the image, described previously, 54 times. The solid ink content of 54*307,000=16.5 million drops was 0.10912gm.

3) Relating the measurements from steps 1 and 2, it is possible to establish the relationship between the known number of drops and the total ink volume. It is a straightforward matter then to calculate a volume of a single drop, and then its radius.
4) The experiment lasted 2 days so it was necessary to have a control to determine if its mass would change on a day to day basis. A sheet of the high quality ink jet paper was used for this purpose.

The experimental data suggest that the droplet volume is 32 pL and the corresponding radius 19.5 μm. The diameter of a splat that a droplet creates when printed in the powder bed is 90 μm, while its diameter when printed on the high quality ink – jet paper is 70 μm. This is much smaller than the HP DOD system where droplet volume is about 50 pL, which makes it possible to print smaller features.

A.4 Printing lines

Lines were printed by drawing the corresponding images in the Corel software and then printing into a powder bed. The binder was 10 wt. % PAA with amaranth, and the substrate was a slipcast powder bed made of 35 v/o Ceralox HPA 1.0 μm Al_2O_3 with MgO, 0.05M HNO_3, 2 wt. % PEG_{400} slurry dispersed in deionized water. The spacing between consecutive drops was 35 μm. Lines were printed in a single pass of the printhead.

The Epson Color Stylus 400 printer had to be slightly modified to allow for powder bed printing. A piece of the front paper guide, which is a part of the printer carriage mechanism, had to be removed by cutting a 2"*¾" hole. The stacker assembly of the printer was also disassembled and removed. The entire printer was mounted and fastened to a ½" aluminum board to minimize vibrations. A small z-axis micrometer stage was fixed to the aluminum board and placed directly under the previously cut hole. Pieces of powder beds were placed on top of the stage prior to the printing. The appropriate files were run and the binder printed as the printhead rastered across the powder bed.

The width of a printed line while still in the powder bed was 140 μm. SEM pictures revealed that the true width is about 190 μm (Figure A.6) and the thickness about 40-50 μm (Figure A.7).

Discharging two droplets of binder for one pixel probably caused the small appendage in the lower right corner. It is also interesting to note that the line is straight despite that it was printed under less than ideal conditions. This indicates that if this printhead is to be adopted for 3D printing, a better control over the spacing and frequency of printing must be achieved.

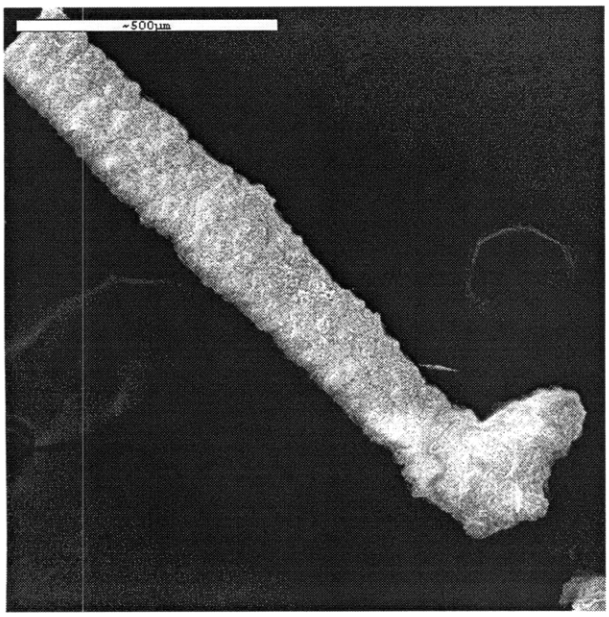

Figure A.6: Single line printed by the Epson printhead

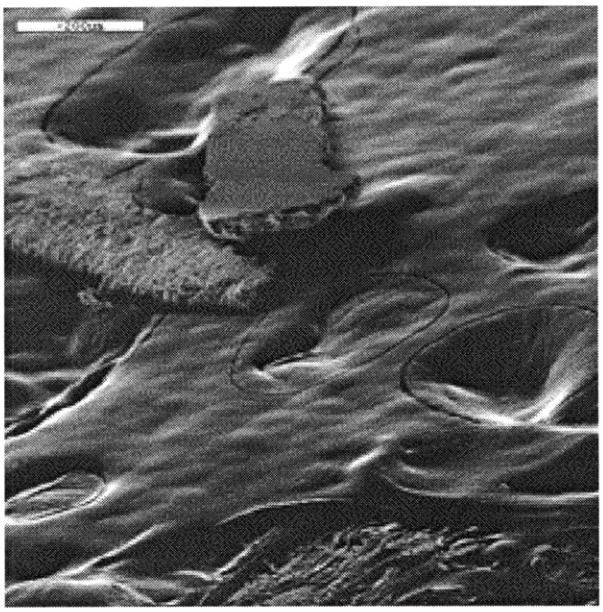

Figure A.7: Cross – section of a single line

The setup described in this appendix was adequate for the printing of single lines and measuring the droplet size. The lack of control over driving this printhead prevents further study of the effect of different printing variables on the surface finish as was possible to accomplish with the HP DOD setup and the study was terminated at this point. Still, it is possible to achieve some progress even with this setup by simulating single pass line printing at different frequencies.

Varying the frequency of printing can be accomplished by dismantling the Epson Color Stylus 400 printer and mounting the printhead with the corresponding parts required for driving it, onto the carriage of the Alpha Machine. The fast axis velocity of the carriage can be easily controlled via LabVIEW programs. The Epson printhead would still be controlled independently by Corel PHOTO – PAINT! files run on a PC computer. The difference in this case is that the files would contain patterns that would fire 1 droplet for every N pixels. If the fast axis speed is adjusted so that the droplets deposited onto the powder bed have sufficient overlap to create a continuous line, the end effect would be a

reduction in the original frequency of 14.4 kHz by the factor of N. The drawback of this method is that the motion of the printhead down the fast axis and the firing of the droplets are not synchronous.

The use of PZT based printheads has its benefits for 3DP, namely the possibility of printing with different binders and a smaller feature size compared with the existing DOD setup. However, a far better control over driving the printhead is necessary before any further serious studies can be undertaken with this printhead.

Appendix B: LabVIEW Software

B.1 Introduction

All of the samples presented in this thesis were printed on the Alpha Machine. Important parts of the overall experimental apparatus are different LabVIEW virtual instruments (VIs), that is, computer programs used to control how the samples are printed. The signals generated by VIs are then fed from the Alpha Machine into the analog/digital circuit that is presented in Chapter 3. After the signal is given the right amplitude and duration, it is finally passed on to a DOD cartridge, and droplets are fired.

There are several LabVIEW VIs that were used to print a variety of features such as single primitives, droplet pairs, line segments, with different print styles. The following sections will describe their structure and user interface. They share many common features so only one VI will be described in details, while others will contain descriptions of those features that are specific to that program. All VIs have been programmed in such a way that the units are always microns and seconds.

The VIs described in this appendix are located on the Alpha Machine Mac computer in the folder: Desktop → Alpha Controller → Students – under develop. → Vedran.

B.2 Vedran DOD VI

Each LabVIEW VI has two components: 1) user interface or panel where a user inputs new values for variables, reads the output etc., and 2) diagram window where programming of the VI is done so that all the variables, controls, and other elements of the program run together.

B.2.1 Vedran DOD Panel

These variables are present on the panel window of the Vedran DOD LabVIEW VI:

1) Number of lines to be printed

2) Increment between lines: the separation between lines in the slow axis.

3) Slow – axis start position: the location along the slow axis where the printhead begins to move.

4) Start printing location: the location along the fast axis where the printhead begins to fire drops.

5) Stop printing location: the location along the fast axis where the printhead stops firing drops.

6) Initial spacing between drops: the spacing between consecutive drops along the fast axis, in only one pass along the line.

7) Center – to – center spacing between drops: the spacing by which the location where the printing commences will be offset with regard to the previous pass along that same line.

8) Left target: the location along the fast axis where the printhead stops traversing and returns to the start location.

9) Right target: the location along the fast axis where the printhead start traversing.

10) Velocity: printhead velocity

It is worth noting that the slow and fast axes refer to the Alpha Machine, and that the printhead traverses from right to left. Furthermore, the term "lines" applies to primitives, droplet pairs, line segments, and single lines.

B.2.2 Vedran DOD Diagram

Vedran DOD VI contains a number of different structures such as FOR loops, sequences etc. so the most convenient way to describe it is to relate what actions take place inside the biggest loop in the program. It was used to print primitives, although other VIs are also well capable of doing the same, and single lines.

The entire program is contained within the outermost FOR loop that determines the number of lines that will be printed. Inside the FOR loop is a sequence structure with a number of frames. The program can be described frame by frame:

FRAME 0: Re-zeros the printhead.

FRAME 1: Moves the printhead along the slow axis.

FRAME 2: Completes one line. This frame contains a smaller sequence whose frames hold the following actions: 0) NuLogic x and y positions get ready, 1) RAM is cleared and initialized, 2) Data where the droplets will be printed are generated and downloaded, 3) target positions are read, 4) the printhead traverses to the left printing the droplets, 5) NuLogic x and y position get ready for the return pass, 6) the printhead returns to the starting location.

FRAME 3: The printhead goes to home position.

All of the actions (FRAME 0 through FRAME 3) within this loop will be repeated until all of the lines are printed.

B.3 Vedran DOD – 2 drops VI

Vedran DOD – 2 drops program is used to print droplet pairs of different spacing, but can do it only at 1 pass/line. The relevant controls are:

1) Spacing between droplet pairs: distance between droplet pairs along the fast axis.

2) Center – to – center spacing between drops: refers to the drops of the same pair.

B.4 Vedran DOD – modified 3 VI

Vedran DOD – modified 3 VI has almost the same set of controls as the Vedran DOD VI. The only addition is the "Delay time" control that allows the user to specify the time interval during which the printhead will be idle at home position, if so desired. Some line segments where the powder bed was dried after each pass were printed using this program. The time interval was set to 150 seconds, which was enough to dry the powder bed (30 seconds) and allow it to cool down to the ambient temperature (120 seconds). To shorten the printing time, the Vedran DOD – modified 3 was programmed to print n^{th} drop of each line segment across the entire powder bed before returning the printhead to the home position, rather then to print line by line which would take much more time.

B.5 Vedran DOD – B VI

This VI makes it possible to print line segments of variable overall length, different droplet spacing, and variable frequencies. It does it at only 1 pass/line. The new controls are:

1) Spacing between line segments: refers to their spacing along the fast axis.
2) Number of drops per line segment
3) Center – to – center spacing between drops: refers to the drop spacing within one line segment.

B.6 Vedran DOD – C VI

This VI was used to print those line segments in which there was more than one drop printed per each pass. Such line segments were printed at 2 different settings: frequency of 1 Hz, and drying after each pass of the printhead. Vedran DOD – C was suited for this because of the "Delay time" control. Other controls that need to be described are:

1) Initial spacing between drops: refers to the spacing between droplets in one line segment that are deposited in the same pass. For example, in 80 μm line segments this was 320 μm.
2) Number of passes in one line: the number of times the printhead will traverse along the same line i.e. in 80 μm line segments there were 4 passes/line.
3) Number of drops per pass (per segment): the number of droplets the printhead is going to fire for one line segment in just one pass. For 80 μm line segments, there were 5 drops/pass and 4 passes/line, so that the complete line segment was comprised of 20 binder droplets.
4) Spacing between segments: refers to their spacing along the fast axis.

B.7 Vedran DOD – D VI

Vedran DOD – D VI was used to print symmetrical line segments of variable droplets spacing. The only new control is "Offset of each new pass" that allows the user

to determine the distance by which the location where the printhead begins to fire droplets will be offset in regard to the previous pass along that same line.